

# **Design of Passive SIW Components for Microwave and Millimeterwave Applications**

**Thesis submitted**

**by**

**Souma Guha Mallick**

**Doctor of Philosophy (Engineering)**

**Department of Electronics and Telecommunication Engineering  
Faculty Council of Engineering & Technology  
Jadavpur University  
Kolkata, India  
2023**

# **Design of Passive SIW Components for Microwave and Millimeterwave Applications**

**Thesis submitted in partial fulfillment of the requirement for  
the degree of**

**Doctor of Philosophy (Ph.D.)**

**In Engineering**

**by**

**Souma Guha Mallick**

**Department of Electronics and Telecommunication Engineering  
Faculty Council of Engineering & Technology  
Jadavpur University  
Kolkata, India  
2023**

# **JADAVPUR UNIVERSITY**

**KOKATA – 700032, INDIA**

**INDEX NO. 42/16/E**

1. **Name of the Thesis:** Design of Passive SIW Components for Microwave and Millimeterwave Applications

2. **Name, Designation & Institution of the Supervisors:**

**Dr. Sayan Chatterjee**, Professor, Dept. of Electronics and Telecommunication Engineering, Jadavpur University, Kolkata – 700032, West Bengal, India

**Dr. D. R. Poddar**, Ex-Professor, Dept. of Electronics and Telecommunication Engineering, Jadavpur University, Kolkata – 700032, West Bengal, India

**Dr. Gande Arun Kumar**, Assistant Professor, Dept. of Electronics and Communication Engineering, National Institute of Technology, Warangal – 506004, Telangana, India

3. **List of Publications:** Kindly refer to **Appendix I**

4. **List of Patents:** NIL

5. **List of Presentations in National/International/Conferences/Workshops:**

[1] **S. G. Mallick**, G. A. Kumar, S. Chatterjee, B. Biswas and D. R. Poddar, “Transitions from SIW to Various Transmission Lines for Substrate Integrated Circuits,” *2019 URSI Asia-Pacific Radio Science Conference (AP-RASC)*, New Delhi, India, 2019, pp. 1-4.

[2] **S. G. Mallick**, B. Biswas, S. Chatterjee, G. A. Kumar and D. R. Poddar, “A Multilayered Transition between SIW and ESIW,” *2020 IEEE Calcutta Conference (CALCON)*, Kolkata, India, 2020, pp. 181-183.

## STATEMENT OF ORIGINALITY

I, **Souma Guha Mallick**, registered on **02/11/2016** do hereby declare that this thesis entitled “**Design of Passive SIW Components for Microwave and Millimeterwave Applications**” contains literature survey and original research work done by the undersigned candidate as part of Doctoral studies.

All information in this thesis have been obtained and presented in accordance with existing academic rules and ethical conduct. I declare that, as required by these rules and conduct, I have fully cited and referred all materials and results that are not original to this work.

I also declare that I have checked this thesis as per the “Policy on Anti Plagiarism, Jadavpur University, 2019”, and the level of similarity as checked by iThenticate software is 6%.



Signature of Candidate

Date: **04.10.2023**

Certified by Supervisor(s):




Dr. Sayan Chatterjee  
Professor  
Electronics & Telecomm. Engg. Dept.,  
Jadavpur University, Kolkata - 700032.

Dr. Sayan Chatterjee  
Professor, Dept. of ETCE  
Jadavpur University, Kolkata – 700032



Dr. D. R. Poddar  
Ex-Professor, Dept. of ETCE  
Jadavpur University, Kolkata – 700032



Dr. GANDE ARUN KUMAR  
Assistant Professor  
Department of Electronics & Communication Engg.  
NATIONAL INSTITUTE OF TECHNOLOGY  
Warangal-506004 (T.S.)

Dr. Gande Arun Kumar  
Assistant Professor, Dept. of ECE  
National Institute of Technology, Warangal – 506004

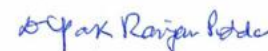


## CERTIFICATE FROM THE SUPERVISORS


This is to certify that the thesis entitled “**Design of Passive SIW Components for Microwave and Millimeterwave Applications**” submitted by **Shri Souma Guha Mallick**, who got his name registered on **02/11/2016** for the award of Ph. D. (Engg.) degree of Jadavpur University is absolutely based upon his own work under the supervisions of **Prof. (Dr.) Sayan Chatterjee**, and, **Ex-Professor (Dr.) D. R. Poddar**, Dept. of Electronics and Telecommunication Engineering, Jadavpur University, Kolkata – 700032, West Bengal, India, and, **Dr. Gande Arun Kumar**, Assistant Professor, Dept. of Electronics and Communication Engineering, National Institute of Technology, Warangal – 506004, Telangana, India, and, that neither his thesis nor any part of the thesis has been submitted for any degree/diploma or any other academic award anywhere before.

  
**Dr. Sayan Chatterjee**  
Professor  
Electronics & Telecomm. Engg. Dept.,  
Jadavpur University, Kolkata - 700032.

**Dr. Sayan Chatterjee**  
Professor, Dept. of ETCE  
Jadavpur University, Kolkata – 700032



**Dr. D. R. Poddar**  
Ex-Professor, Dept. of ETCE  
Jadavpur University, Kolkata – 700032

  
**Dr. GANDE ARUN KUMAR**  
Assistant Professor  
Department of Electronics & Communication Engg.  
NATIONAL INSTITUTE OF TECHNOLOGY  
Warangal-506004 (T.S.)

**Dr. Gande Arun Kumar**  
Assistant Professor, Dept. of ECE  
National Institute of Technology, Warangal – 506004

# Acknowledgements

---

I want to seize this moment to convey my profound and heartfelt appreciation to my supervisor, **ex-Professor Dipak Ranjan Poddar**, from the Department of Electronics and Telecommunication Engineering at Jadavpur University. I extend my gratitude to Professor Poddar for his continuous enthusiasm and encouragement, as this work would not have reached its conclusion without his unwavering support.

Acknowledging everyone who contributed to my journey and the creation of this dissertation is an impossible task, but I would like to begin by expressing my heartfelt gratitude to my supervisors. **Dr. Sayan Chatterjee**, a Professor in the Department of Electronics and Telecommunication Engineering at Jadavpur University, and **Dr. Gande Arun Kumar**, an Assistant Professor in the Department of Electronics and Communication Engineering at the National Institute of Technology, Warangal, have been my guiding lights. Every discussion we had, every topic we explored together, and every setback I encountered, their presence provided me with a gentle illumination, greatly enhancing my technical knowledge. They reminded me of the boundless power of knowledge and inspired me to forge ahead with renewed determination and energy as I navigated through my doctoral research.

I am also indebted to **Mr. Bijit Biswas**, Scientist D, SAMEER, MeitY, Govt. of India for the many knowledge and guidance provided along with his effort in helping me in the experimental work.

I must thank **Mr. Sumit Kumar Varshney**, Asst. Professor at Supreme Knowledge Foundation Group of Institutions for helping me in organizing the thesis and for helping me in building the theoretical concepts related to my work.

During my tenure at this department where I worked, I had the privilege to have **Dr. Manotosh Biswas**, and **Dr. Sheli Sinha Chaudhuri (2018-2020)** as the Heads of the Department – each of whom personally assisted me in every problem I came across during their times in office. I would like to thank personally each of them as their assistance made my journey comfortable, easier to take and indeed an experience to cherish for the years to come. I would also like to thank all the administrative staff members, officers of the University, at the Research Section or at the Faculty office, on in any other department – whose active assistance I received at all the times.

Further I must thank **Mr. Arijit Majumder**, Scientist E, SAMEER, MeitY, Govt. of India and OIC – SAMEER – Kolkata for several support provided during the journey. I would also like to thank **Mr. Aritra Banerjee**, Scientist D, SAMEER, MeitY, Govt. of India and **Mr. Dhruba Das**, Scientist D, SAMEER, MeitY, Govt. of India for their cooperation and encouragement, and, today I reminisce the moments of enrichment, when we discussed technical problems or talked about how to handle a new machine or instrument beyond the official lab hours – the moments I wish to remember a lifetime.

I take this opportunity to acknowledge my fellow research members – **Dr. Amartya Banerjee and Ms. Baisakhi Bandyopadhyay** with whom I had little time to interact but I sincerely hope to have more opportunities to work with them in the coming future.

Apart from these, I would like to thank **Dr. B N Basu, ex- Professor and Head**, Electronics Engineering Department, IIT-BHU, and distinguished Adjunct Professor at Supreme Knowledge Foundation Group of Institutions and **Dr. B. N. Biswas**, Emeritus Professor, Chairman - Education Division, Supreme Knowledge Foundation, Hooghly, West Bengal, India who paved my journey towards the world of research in RF and microwave technologies.

Without a family, one cannot strive for greatness – but before I formally acknowledge my parents, I would like to recall the names of my maternal grandparents **Late Narendranath Bose** and **Late Ila Bose**, who believed in my abilities and above all paved me the way to be a good humanitarian. Their unwavering love, encouragement, and sacrifices have been my greatest source of strength. I thank my parents, **Mr. Bijoy Guha Mallick** and **Mrs. Ratna Guha Mallick**, for whom no words are enough for their patience and what they have went through and bore with through these years of my Ph.D. I am immensely thankful to my wonderful wife **Debeshi** for her continuous support and encouragement in all these years during this work. Special mention goes to my parents in law **Mr. Dipankar Basu** and **Mrs. Indra Basu** and the dearest **Mrs. Chhanda Mitra** (Debeshi's grandmother) for thier blessings and love.

Lastly, as a closing note – I would like to thank all the members at **SUPREME KNOWLEDGE FOUNDATION** and **SUPREME GROUP** as all of them took the pain of providing continued service to the society, which **SUPREME GROUP** aims at, while I was pursuing my research.

**SOUMA GUHA MALLICK**

Dated: 04 / 10 / 2023, Kolkata

# Contents

---

Acknowledgement	i
Contents	iii
List of Figures	v
List of Tables	ix
<b>CHAPTER 1: INTRODUCTION</b>	<b>1</b>
1.1 Substrate Integrated Circuits (SIC)	1
1.2 Substrate Integrated Waveguide (SIW)	2
1.3 Application of SIW in power division and combining	3
1.4 Motivation of the research	4
1.5 Outline of the chapters	5
References	7
<b>CHAPTER 2: LITERATURE REVIEW</b>	<b>11</b>
2.1 Review on Substrate Integrated Waveguide as a promising SIC technology	11
2.2 Review on various forms of SIW Transitions to planar and non planar guides	16
2.3 Review on various SIW power dividers and couplers	22
References	39
<b>CHAPTER 3: SIW THEORETICAL CONCEPTS AND TRANSITIONS</b>	<b>49</b>
3.1 Objective	49
3.2 Introduction to SIW	49
3.3 Construction of an SIW	52
3.3.1 Basic Geometry of an SIW	52
3.3.2 Construction Parameters of an SIW	54
3.3.3 Design Procedures of an SIW	55
3.4 Field Configuration of an SIW	56
3.5 Losses in an SIW	58
3.6 Miniaturization of SIW	62
3.6.1 Basic Requirement of Miniaturization	62
3.6.2 Half-Mode Substrate Integrated Waveguide	63
3.6.3 Quarter-Mode Substrate Integrated Waveguide	64
3.6.4 Folded Substrate Integrated Waveguide	65
3.6.5 Empty Substrate Integrated Waveguide	66

3.7 Simulation Study of Basic SIW	67
3.7.1 Simulated Parametric Analysis of SIW	67
3.7.2 Simulated Parametric Analysis of SIW	74
3.8 Transition	76
3.8.1 SIW to Microstrip	77
3.8.2 SIW to Waveguide	81
3.8.3 SIW to ESIW	87
3.9 Conclusion	90
References	92

## **CHAPTER 4: A COMPACT, BROADBAND THREE-WAY SIW RIBLET COUPLER** **97**

4.1 Objective	97
4.2 Introduction	97
4.3 Ribet Coupler	99
4.4 Three-way SIW Riblet Coupler	102
4.5 Conclusion	113
References	113

## **CHAPTER 5: COMPACT, BROADBAND AND MULTIBAND SIW RADIAL POWER DIVIDER** **117**

5.1 Objective	117
5.2 Introduction	117
5.3 Multiway SIW radial power dividers	121
5.3.1 Layout	121
5.3.2 Equivalent Circuit	122
5.3.3 Eight Way Radial SIW Power Dividers (Single Band)	127
5.3.4 Eight Way Radial SIW Power Dividers (Multi Band)	135
5.4 Conclusion	146
References	148

## **CHAPTER 6: CONCLUSION AND FUTURE SCOPE OF WORK** **151**

6.1 Conclusion	151
6.2 Future Scope of Work	155

## **APPENDIX I** **I**

# List of Figures

---

Fig. 3.1: SIW power dividers: (a) 2-way dual band [20], (b) 4-way [21], (c) 4-way broadband [22].	52
Fig. 3.2: (a) Top View of an SIW, (b) Side View of an SIW, (c) Front View of an SIW	53
Fig. 3.3: $TE_{10}$ mode surface current distribution on an SIW.	57
The metalized via holes are replaced with narrow slot openings on the side wall [24].	
Fig. 3.4: Top view of HMSIW.	63
Fig. 3.5: Top view of QMSIW.	64
Fig. 3.6: Cross-sectional view of FSIW showing dominant $TE_{10}$ type mode [31].	65
Fig. 3.7: Layout of ESIW [34].	66
Fig. 3.8: Simulated S11 and S21 for SIW having $a = 13.35$ mm, $p = 1.5$ mm and $d = 1$ mm.	68
Fig. 3.9: Simulated S11 for SIW having $a$ (in mm) = 13, 13.35, 15, 17, 17.5, 18, $p = 1.5$ mm and $d = 1$ mm.	69
Fig. 3.10: Simulated S21 for SIW having $a$ (in mm) = 13, 13.35, 15, 17, 17.5, 18, $p = 1.5$ mm and $d = 1$ mm.	70
Fig. 3.11: Simulated S11 for SIW having $p$ (in mm) = 1, 1.2, 1.4, 1.5, $a = 17.5$ mm and $d = 1$ mm.	71
Fig. 3.12: Simulated S11 for SIW having $d$ (in mm) = 0.8, 0.9, 1, 1.1, 1.2, $a = 17.5$ mm and $p = 1$ mm.	72
Fig. 3.13: Simulated S11 and S21 for SIW having $a = 17.5$ mm, $d = 1$ mm and $p = 1$ mm.	73
Fig. 3.14: Simulated S11 and S21 for ESIW having $a = 18.75$ mm.	74
Fig. 3.15: Simulated S11 and S21 for ESIW having $a$ (mm) = 18, 20, 22.86, 24.	75
Fig. 3.16: Simulated S11 and S21 for ESIW having $a = 20$ mm.	76
Fig. 3.17: Basic layout of the proposed microstrip-SIW transition.	78
Fig. 3.18: Design parameters of the proposed microstrip-SIW transition.	79
Fig. 3.19: HFSS simulation result of the proposed microstrip-SIW transition.	80
Fig. 3.20: Basic layout of the proposed transition between SIW and waveguide with dual slot configuration.	82
Fig. 3.21: Design parameters of the proposed single band transition between SIW and waveguide.	83
Fig. 3.22: HFSS Simulation of the proposed single band transition between SIW and waveguide.	84
Fig. 3.23: Design parameters of the proposed dual band transition between SIW and waveguide.	85
Fig. 3.24: HFSS Simulation of the proposed dual band transition between SIW and waveguide.	86
Fig. 3.25: Basic structure of the proposed transition between SIW and ESIW.	88
Fig. 3.26: Design parameters of the proposed multilayered SIW-ESIW transition structure in top view.	88
Fig. 3.27: HFSS simulation result of the proposed multilayered SIW-ESIW transition.	89
Fig. 3.28: HFSS E-Field plot of the proposed multilayered SIW-ESIW transition.	90
Fig. 4.1: Ansys HFSS E-field plot in an SIW channel for (a) $TE_{10}$ and (b) $TE_{30}$ modes.	101
Fig. 4.2: The proposed structure of the three-way SIW Riblet Coupler	102
Fig. 4.3: Design parameters of the three-way SIW Riblet Coupler.	104
Fig. 4.4: Simulated reflection coefficient with variations in the coupler structure.	106
The optimized structure consists of unequal SIW channels, input, and output posts.	

Fig. 4.5: Simulated isolation coefficient with variations in the coupler structure.	106
The optimized structure consists of unequal SIW channels, input, and output posts.	
Fig. 4.6: Field distribution of the three-way SIW riblet coupler at the centre frequency with excitation at port 1. (a) Electric field distribution (b) Magnetic field distribution.	108
Fig. 4.7: The fabricated prototype of three-way SIW Riblet Coupler.	109
Fig. 4.8: Simulated and measured power division at three output ports of the three-way SIW riblet coupler.	110
Fig. 4.9: Simulated and measured reflection and isolation coefficient between the ports of the three-way SIW riblet coupler.	111
Fig. 4.10: Measured transmission phase of output ports of the three-way SIW riblet coupler.	111
Fig. 5.1: Layout of an eight way substrate integrated waveguide radial power divider. (a) Top view. b) Bottom view.	122
Fig. 5.2: Extraction of the equivalent circuit from the N-way radial SIW power divider of a single sector.	123
Fig. 5.3: Equivalent circuit from the 8-way radial SIW power divider.	123
Fig. 5.4: Simulated input return loss (S11) and insertion loss (S12, S13) of ADS equivalent circuit model of 2-way SIW radial power divider.	125
Fig. 5.5: Simulated input return loss (S11) and insertion loss (S12, S13, S14, S15) of ADS equivalent circuit model of 4-way radial SIW power divider.	126
Fig. 5.6: Dependence of the input return loss on (a) L1 and (b) L2 for an 8-way radial SIW power divider.	127
Fig. 5.7: Dependence of the input return loss on (a) C1 and (b) C4 for an 8-way SIW power divider	128
Fig. 5.8: Simulation structure of the proposed eight way radial SIW power divider; Port 1: Input, Port 2-9: Output.	129
Fig. 5.9: Design parameters of the proposed eight-way radial SIW power divider (a) Top view, (b) Bottom view.	130
Fig. 5.10: Simulated input return loss (S11) and average insertion loss (IL) of HFSS 3D model of 8-way radial SIW power divider.	131
Fig. 5.11: Simulated input return loss (S11) and average insertion loss (IL) of ADS equivalent circuit and HFSS 3D model of the eight-way radial SIW power divider.	132
Fig. 5.12: Fabricated power divider (a) Top view and machined SMA connector (inset), (b) Bottom view	132
Fig. 5.13: Simulated & measured transmission and reflection parameters of the power divider for port 2-5	133
Fig. 5.14: Measured transmission phase of the power divider from port 2 to port 5.	133
Fig. 5.15: Simulated and measured isolation of the power divider between output port 2 and output ports 3, 4, 5, 6.	134
Fig. 5.16: Layout of a dual-band eight-way radial SIW power divider. (a) Top view. b) Bottom view.	136
Fig. 5.17: Simulation structure of the dual-band eight-way radial SIW power divider; Port 1: Input, Port 2-9: Output.	138
Fig. 5.18: Design parameters of the dual-band eight-way radial SIW power divider (a) Top view, (b) Bottom view.	138
Fig. 5.19: Ansys HFSS simulated field propagation at the stopband centre frequency of 5.5 GHz.	140

Fig. 5.20: Layout of the dual-band eight-way substrate integrated waveguide radial power divider with four CSRRs (Top view).	141
Fig. 5.21: Simulated input return loss (S11) and average insertion loss (IL) of Ansys HFSS 3D model of the proposed power divider using four and eight CSRRs.	141
Fig. 5.22: Simulated isolation of Ansys HFSS 3D model of the proposed power divider between port 2 and port 3 (adjacent ports), and, between port 2 and port 6 (farthest ports), with four and eight SRRs.	142
Fig. 5.23: Photograph of the fabricated dual band eight-way radial SIW power divider.	143
Fig. 5.24: Simulated and measured transmission and reflection parameters of the dual band eight-way radial SIW power divider.	143
Fig. 5.25: Simulated and measured isolation of the dual band eight-way radial SIW power divider between port 2 and port 3 (adjacent ports), and, between port 2 and port 6 (farthest ports).	144
Fig. 5.26: Simulated and measured transmission phase of the dual band eight-way radial SIW power divider between port 2 and port 6 (farthest ports).	144
Fig. 5.27: Measured amplitude balance between output ports 2 and 6 of the dual band eight-way radial SIW power divider.	145
Fig. 5.28: Measured phase balance between output ports 2 and 6 of the dual band eight-way radial SIW power divider	145





# List of Tables

---

Table 3.1: Comparison of Losses in Planar Transmission Lines	62
Table 3.2: Dimensions of the Proposed Microstrip to SIW Transition	79
Table 3.3: Comparison of Microstrip Taper Transitions in <i>Ref</i> [36] and This Work for Return Loss more than 20dB and Return Loss more than 15 dB	80
Table 3.4: Dimensions of the proposed single band SIW to waveguide transition	83
Table 3.5: Dimensions of the proposed dual band SIW to waveguide transition	85
Table 3.6: Dimensions of proposed transition (Unit: millimeters)	89
Table 4.1: Optimized Dimensions of the Three-Way SIW Riblet Coupler (Unit: Millimeters)	105
Table 4.2: Comparison of performances with other reported structures	112
Table 5.1: Optimized Dimensions of Narrow Band Eight-Way Radial SIW Power Divider (Unit: Millimeters)	130
Table 5.2: Optimized Dimensions of Broadband Eight-Way Radial SIW Power Divider (Unit: Millimeters)	131
Table 5.3: Comparison of Fabricated Planar Multi-Way Power Dividers	135
Table 5.4: Optimized Dimensions of Dual-band Eight-Way radial SIW Power Divider (Unit: millimeters)	142



## *INTRODUCTION*

---

### **1.1 Substrate Integrated Circuits (SIC)**

There has been immense development in wireless technologies in the last few decades. It is mainly due to the introduction of cellular technology and the emergence of multiple services that requires continuous research on the better functioning of microwave systems, which includes lower loss, lighter weight systems, and effectiveness. In conjunction with these, researchers are striving for low power, minimum interference, and low radiation options for the current and future wireless applications. A microwave system is usually a combination of various fundamental microwave components, such as antennas [1], active [2] and passive [3] devices. Out of which passive devices, such as couplers, power divider/combiners, filters, etc., and the transmission lines occupy the major fabrication area and also play an important role as the overall performance of the complete system is determined to a great extent by the transition lines and passive devices. Several passive devices are reported in both planar and non-planar forms of transmission media, such as waveguide [4], coaxial waveguide [5], stripline [6], and microstrip [7].

However, the upcoming compact systems and technologies involve a large number of hardware, and hence the components should be compact, low loss, economical, and can be easily integrated. With the Substrate Integrated Circuit (SIC) concept, an entire system is realized within a single substrate by developing the non-planar circuits in a planar form and

## INTRODUCTION

---

integrating them with the existing planar circuits of the system on the same substrate [8]. Not only antennas, but SIC is also used to implement active and passive circuits as well. Unlike waveguides and coaxial lines, where broadband impedance matching and packaging between the guides is difficult, SIC can embed devices on the same substrate. It also allows interconnection between various transmission lines.

In order to facilitate proper SIC systems, the designer should aim at the following characteristics:

- To reduce the systems' bulkiness and avoid non-planar transmission lines, like waveguides, and planar alternatives are explored.
- The SIC components, mainly the passive devices, should have lower losses, which planar transmission medias are usually not known for.
- Proper transition between the SIC components should be developed.

### 1.2 Substrate Integrated Waveguide

Substrate Integrated Waveguide (SIW) is an emerging SIC technology [9][10]. It is realized on a substrate and acts as the planar form of the waveguide. SIW structure promotes integration with other planar and non-planar structures and hence finds useful even in dense packaging systems. SIW, thus, acts as a very important transmission line to design components, including passive devices. The advantages of SIW are its lightweight, lower losses, the common mode of transmission with the waveguide, and cost-effective, which would meet the needs of the emerging industry trends [11]-[17].

## INTRODUCTION

---

As discussed, a microwave system consists of various subsystems and devices, these subsystems and devices are not necessarily of the same transmission media, and it can be formed as a combination of various non-planar and planar lines. To successfully integrate these planar and non-planar devices, a special passive device must be designed to transfer and transform the fields from one form of transmission line to another. Such devices are known as transitions. Transitions maintain the system's bandwidth, center frequency, and impedance between the two devices [18],[19]. A well-designed transition may avoid many problems related to power consumption, signal integrity, thermal dissipation, and bandwidth can be solved. Being an alternative form of waveguide, SIW can also be used to design transitions. Not only transitions between planar technologies but between bulky non-planar technologies, as well. Already a lot of advancements in various forms of transitions of SIW into other transmission lines have been achieved. However, there is scope for multiband transitions and other forms of SIC devices.

### **1.3 Application of SIW in power division and combining**

In a microwave and millimeter wave system, power divider plays a very important role as a passive component. The recent challenge in the communication industry is that the electromagnetic spectrum is becoming more crowded with wireless signals. The future generation of wireless communication systems along with other industrial electronic applications would demand critical spectral channelization of coexisting bandwidths, which might be already in use for other applications. Researchers are also getting ready to introduce multiple-input multiple-output (MIMO) techniques in the above mentioned systems and applications. It is hence evident that to support these techniques, power dividers with more than

# INTRODUCTION

---

two ways of division i.e. multiway power dividers/combiners are immensely required. Several multiway power dividers are reported in both planar and non-planar forms of transmission media [20]-[23]. However, the upcoming systems and technologies including MIMO involve a large number of hardware and hence the components should be compact, low loss, economical which can be easily integrated. SIW, thus, may act as a very important transmission line to design couplers and power dividers, including multiway power divisions, which would meet the needs of the emerging industry trends. The advancement of 5G and satellite communications technologies push for wider bandwidth hence there is huge requirement for multi-band passive devices, components and transitions.

## 1.4 Motivation of the research

Thus, this thesis is being presented with this motivation, which explores various SIW passive devices and transitions that would cater to the concept of SIC along with multi-band and multi-way capabilities for 5G and satellite communications and beyond communication applications. The thesis proposes the following designs and analysis:

- To workout/design novel planar configurations of riblet couplers in SIW, which would be compact, broadband with improved isolation and achieve three-way power division
- To develop compact broadband, eight-way SIW-based radial power divider.
- To explore dual band capability of the radial eight-way SIW power divider by realizing it in dual-band configurations.
- To investigate the transition capabilities of the SIW transitions with various planar and non-planar guides and achieve multi-band capabilities out of it.

## 1.5 Outline of the chapters

The investigations studied and reported in this thesis are organized into the following chapters:

**Chapter 2** is a review on the substrate integrated waveguide (SIW) since the time it was first proposed in 1998. Based on the earlier works, SIW have been studied and analyzed. The evolution of SIW into various applications from its initial developmental phase is also discussed. Transitions of the fields of an SIW to other various planar and non-planar guides are also appraised. Special emphasis on the power division applications of an SIW is investigated as well along with their advantages and disadvantages.

**Chapter 3** addresses the fundamental principles of Substrate Integrated Waveguide (SIW) theory and analyzes the design of a functional SIW that operates effectively within circuits. In addition, the research involves an exploration of various transitions between SIW and alternative technologies. Through simulation-based investigations, the focus is on creating compact transitions that facilitate seamless connections between SIW and microstrip, waveguide, and empty substrate integrated waveguide (ESIW). The key challenge is to ensure efficient power transfer between transmission lines by achieving appropriate impedance and field matching. These methodologies hold significance within the context of substrate integrated circuit (SIC) technology, paving the way for enhanced integration and performance.

**Chapter 4** provides a space-efficient three-way power divider using Substrate Integrated Waveguide (SIW) technology, operating in the X-band frequency range. This design is based



## INTRODUCTION

---

on a Riblet configuration. The power coupling among the three output ports is achieved through the inclusion of short openings in the narrow walls of the central SIW channel. To further enhance the performance in terms of return loss and isolation between ports, matching posts are strategically placed. These posts are positioned at both the input and output ends of the coupling region. It's worth noting that this specific SIW three-way power divider design is distinct in that it demonstrates non-adjacent port isolation, which sets it apart from other six-port couplers.

**Chapter 5** presents a study on compact multi-way power divider using Substrate Integrated Waveguide (SIW) technology. The designs mentioned are intended to serve both broadband and dual-band applications. The approach involves the incorporation of a planar impedance transformer, which includes an annular slot and a circular patch at the input and output feed locations. Through an analysis of the equivalent circuit, the optimization of these elements on the substrate is carried out, resulting in the attainment of a broadband operational bandwidth. Furthermore, by utilizing complementary split ring resonator (CSRR) metamaterial, the design achieves dual-band capabilities.

**Chapter 6** furnishes a comprehensive summary of all the preceding chapters. It offers an overview and synthesis of the key points, findings, and insights presented in each individual chapter. It serves as a condensed reference that allows readers to not only grasp the main contributions, outcomes, and implications of the entire body of work behind SIW's multiway and multiband usage, especially in the power division and combining applications but also paves way into the future evolutions of SIW applications and its integration with other technologies.

## References:

- [1] B. N. Kim, S. O. Park, Y. S. Yoon, J. K. Oh, K. J. Lee and G. Y. Koo, "Hexaband Planar Inverted-F Antenna With Novel Feed Structure for Wireless Terminals," *IEEE Antennas and Wireless Propagation Letters*, vol. 6, pp. 66-69, Mar. 2007.
- [2] Y. S. Lin, C. W. Hsu, C. L. Lu and Y. H. Wang, "A Low-Power Quadrature Local Oscillator Using Current-Mode-Logic Ring Oscillator and Frequency Triplers," *IEEE Microwave and Wireless Components Letters*, vol. 23, no. 12, pp. 650-652, Dec. 2013.
- [3] C. W. Tang and M. G. Chen, "A Microstrip Ultra-Wideband Bandpass Filter With Cascaded Broadband Bandpass and Bandstop Filters," *IEEE Transactions on Microwave Theory and Techniques*, vol. 55, no. 11, pp. 2412-2418, Nov. 2007.
- [4] J. Deng, P. Burasa and K. Wu, "Waveguide Coupler With Polarized Rotation Characteristics for Terahertz Applications," in *IEEE Transactions on Microwave Theory and Techniques*, vol. 71, no. 5, pp. 2091-2103, May 2023.
- [5] K. Song and Q. Xue, "Planar Probe Coaxial-Waveguide Power Combiner/Divider," *IEEE Transactions on Microwave Theory and Techniques*, vol. 57, no. 11, pp. 2761-2767, Nov. 2009.
- [6] Y. Zhu and Y. Dong, "Stripline Resonator Loaded Compact SIW Filters With Wide Suppression and Flexible Response," *IEEE Microwave and Wireless Components Letters*, vol. 30, no. 5, pp. 465-468, May 2020.
- [7] R. Gomez-Garcia, M. Sanchez-Renedo, B. Jarry, J. Lintignat and B. Barelaud, "A Class of Microwave Transversal Signal-Interference Dual-Passband Planar Filters," *IEEE Microwave and Wireless Components Letters*, vol. 19, no. 3, pp. 158-160, Mar. 2009.
- [8] K. Wu, D. Deslandes, and Y. Cassivi, "The Substrate Integrated Circuits—A New Concept for High-Frequency Electronics and Optoelectronics," *Telecommun. Modern Satellite, Cable, Broadcast. Service*, vol. 1, pp. P-III–P-X, Oct. 2003.
- [9] J. Hirokawa and M. Ando, "Single-Layer Feed Waveguide Consisting of Posts for Plane TEM Wave Excitation in Parallel Plates," *IEEE Trans. Ant. Propag.*, vol. 46, no. 5, pp. 625-630, May 1998.
- [10] H. Uchimura, T. Takenoshita, M. Fujii, "Development of a Laminated Waveguide," *IEEE Trans. Microw. Theory Tech.*, vol. 46, no. 12, pp. 2438-2443, Dec. 1998.

# INTRODUCTION

---

- [11] J. Hirokawa and M. Ando, "Efficiency of 76 GHz Post-Wall Waveguide-Fed Parallel Plate Slot Arrays," in *Proc. 29<sup>th</sup> Eur. Microw. Conf. (EuMC)*, Munich, pp. 271-274, Oct. 1999.
- [12] A. Zeid and H. Baudrand, "Electromagnetic Scattering by Metallic Holes and its Applications in Microwave Circuit Design," *IEEE Trans. Microw. Theory Tech.*, vol. 50, no. 4, pp. 1198-1206, Apr. 2002.
- [13] A. Suntives and R. Abhari, "Characterizations of Interconnects Formed in Electromagnetic Bandgap Substrates," in *Proc. 9th IEEE Workshop Signal Propagation Interconnects (SPI)*, Garmisch-Partenkirchen, Germany, May 10-13, 2005, pp. 75-78.
- [14] A. Suntives and R. Abhari, "Design and Characterization of the EBG Waveguide-Based Interconnects," *IEEE Trans. Adv. Packag.*, vol. 30, no. 2, pp. 163-170, May 2007.
- [15] D. Deslandes and K. Wu, "Design Considerations and Performance Analysis of Substrate Integrated Waveguide Components," in *Eur. Microw. Conf.*, pp. 881-884, Sep. 2002.
- [16] Y. Cassivi, L. Perregrini, K. Wu, and G. Concinauro, "Low-Cost and High-Q Millimeter-Wave Resonator Using Substrate Integrated Waveguide Technique," in *Proc. 32nd Eur. Microwave Conf.*, vol. 2, Milan, Italy, Sep. 23-27, 2002, pp. 737-740.
- [17] D. Deslandes and K. Wu, "Single-Substrate Integration Technique of Planar Circuits and Waveguide Filters," *IEEE Trans. Microw. Theory Tech.*, vol. 51, no. 2, pp. 593-596, Apr. 2003.
- [18] K. H. Kloke, J. Joubert and J. W. Odendaal, "Coaxial End-Launched and Microstrip to Partial H-Plane Waveguide Transitions," *IEEE Transactions on Microwave Theory and Techniques*, vol. 63, no. 10, pp. 3103-3108, Oct. 2015.
- [19] A. M. E. Safwat, K. A. Zaki, W. Johnson and C. H. Lee, "Novel transition between different configurations of planar transmission lines," *IEEE Microwave and Wireless Components Letters*, vol. 12, no. 4, pp. 128-130, Apr. 2002.
- [20] J. Zhou, K. A. Morris and M. J. Lancaster, "General Design of Multiway Multisection Power Dividers by Interconnecting Two-Way Dividers," in *IEEE Transactions on Microwave Theory and Techniques*, vol. 55, no. 10, pp. 2208-2215, Oct. 2007.
- [21] Y. Xu and R. G. Bosisio, "Design of Multiway Power Divider by Using Stepped-Impedance Transformers," in *IEEE Transactions on Microwave Theory and Techniques*, vol. 60, no. 9, pp. 2781-2790, Sept. 2012.
- [22] T. Yu and J. Tsai, "Design of multiway power dividers including all connecting lines," in *IET Microwaves, Antennas & Propagation*, vol. 12, no. 8, pp. 1367-1374, 2018.

## INTRODUCTION

---

- [23] C. Sun and J. Li, "Design of planar multi-way differential power division network using double-sided parallel stripline," in *Electronics Letters*, vol. 53, no. 20, pp. 1364-1366, 2017.

## INTRODUCTION

---

## ***LITERATURE REVIEW***

---

### **2.1 Review on Substrate Integrated Waveguide as a promising SIC technology**

Transmission lines are used to transport signal from one point to the other and twin-wire transmission lines were reportedly widely used at low frequency range. But as the frequency range increases, they present large radiation losses. To overcome this loss, a shielded coaxial line was used. But here again ohmic losses were huge at higher frequency region due to the central conductor. Hence the central conductor was removed giving circular and rectangular waveguides which had only one loss as dielectric loss which was negligible and hence they were used for long. But they were bulky and occupied larger space. Hence the designers opted for planar lines like microstrip, stripline, SIW. Till now various high performance microwave and millimeter wave components in various technologies such as waveguides, microstrip, stripline, coaxial line, coplanar waveguides, etc have been developed. Technologies, such as waveguides, even though proved to be useful in high performance systems, were however bulky, complex and expensive to build. Whereas, traditional planar circuitry proves to be either lossy or difficult in integrating with other non-planar structures. In the last decade a lot of research has been carried out in developing components in a technology known as the Substrate integrated circuit (SIC) which doesn't come up with the problems mentioned above. The concept of SIC is based on the foundation of realizing an entire system and hence all the circuits in a single substrate or multilayered platforms. The scheme includes the unified

## LITERATURE REVIEW

---

integration of various planar and non-planar components in a single substrate by the realisation of various non-planar components into their planar forms and is interconnected to each other through proper transitions, designed on the same dielectric substrate. One such popular SIC technology is the Substrate Integrated Waveguide (SIW).

Initially introduced as post wall waveguide [1] and laminated waveguides [2] Substrate Integrated Waveguides are the planar realization of the air filled rectangular waveguides, that can be easily fabricated using common printed circuit board (PCB) fabrication methods. In [1] the technique to excite TEM waves in a parallel plate waveguide was proposed using a dense array of posts on the same layer of the parallel plate as the feed structure. For feeding a line, microstrip lines produce radiation losses at discontinuities. Coplanar lines are worse than microstrip and also produce radiation losses. Triplate line however doesn't radiate at bends, but parallel plate modes occur at the feeding point. Waveguide has the best transmission characteristics but their large sizes prevent them from being embedded into circuit boards or packages. Also since the waveguides have vertical sidewalls, it can't be manufactured using lamination techniques. Post-wall waveguides can be built in circuit boards and are also smaller in size, but allow current flow only in the vertical direction. Though it reflects the vertical component of the electric field, it cannot reflect the horizontal component, hence electromagnetic waves will leak at these points. An application of the post wall waveguide was presented by developing a parallel plate slot array antenna which is fed using the post wall waveguide [3]. A gain of 35.3 dB with 39.3% efficiency has been measured at 77.0 GHz for a size of 104 mm x 100 mm. A waveguide of new structure has been introduced, the laminated waveguides [2]. These guides have their sidewalls made up of arrays of via-holes, and can be manufactured using lamination techniques. Through electromagnetic simulation, it is found

## LITERATURE REVIEW

---

that electromagnetic waves do not leak from the waveguide of a via-hole pitch smaller than a quarter wavelength. Samples are designed and fabricated. Results show that they have low loss and also have a good isolation between two lines. Basic bends, branches, and dividers also showed good performances. The laminated waveguides are suitable for feed lines of a small size array antenna.

The common form of SIW is synthesized by placing two rows of periodic metallized via-holes in the substrate. The cut-off frequency is only related to the width of the integrated waveguide. But, the width should always be greater than the substrate thickness. The diameter and radius of the holes are set such that the radiation loss and the return loss are minimized [4]. The metallic posts are laser drilled on the substrate and then the metal, usually copper, is deposited on the inner walls of the drilled holes. In [5], close analysis on period arrangement of metallic holes showed that this arrangement could be used for new guiding microwave structures. The structures having an array of periodically arranged metallic holes, which result in the formation of stop bands in the microwave frequency range, are known as electromagnetic band gap (EBG) structures. The EM waves scattered by the materials act as secondary sources which destructively interfere at certain frequency ranges. SIW should be designed at frequency ranges where there is no bandgap effect [6]-[7]. In [6], the concept of EBG has been applied to design SIW interconnects with a systematic approach to the placement of side-wall vias. Any interconnect based out of SIW can provide way better efficiency in a bend geometry than microstrip. Multiple connects, when investigated, showed minimal far-end and near-end couplings [7]. SIW is a better choice for high frequency compact routine networks. The design and performance analysis of SIW has been discussed in [8]. The authors have also reported a few basic structures like H-plane step at 37 GHz, post resonator at



## LITERATURE REVIEW

---

30 GHz, and a wideband 90° curve having a 15 dB return loss from 25 GHz to 38 GHz. In 2002, the first cavity using SIW was designed along with mathematical equations required to design the SIW cavity [9]. Subsequently, to prove its usefulness an SIW cavity based filter was developed by the authors at 20 GHz. The filter measurements reported a bandwidth of 260 MHz with an insertion loss of 2.4 dB. In [10], another study has been conducted to substantiate the complete integration of planar circuits. It also showcases a Chebyshev filter at 28 GHz. The inductive posts are designed using drilled metallic vias which are aligned in an offset arrangement with the same dimensions, instead of centred posts with various diameters. A 1 GHz bandwidth is obtained with a return loss more than 15 dB. To validate the guided-wave characteristics of SIW, which is similar to that of a conventional waveguide, the dispersion properties of SIW was obtained using the BI-RME method combined with Floquet's theorem [11]. An algorithm using finite difference frequency domain (FDFD) method was also suggested for SIW in [12]. Both the simulated and experimental results show the similarity in the behaviour of SIW and standard waveguides. In [13], the authors have used the approach of method of lines along with Z-transform for the absorbing boundary conditions to propose propagation constants of SIW. The authors have also presented a frequency independent empirical equation to calculate the adjusted attenuation constant for qualitatively understanding the leakage loss property. A new method of analysis for determining the complex propagation constants has been documented in [14] which further demonstrate the wave guiding mechanisms, basic SIW characteristics, leakage losses, design, bandgap effects. The paper also presents steps to choose the dimensions of the via hole diameter and its periodicity which are a function of the cutoff frequency. It also explains that the modes that will be excited in an SIW are  $TE_{m0}$ , only. Further investigations on the propagation of only  $TE_{m0}$  modes in an SIW shows that the dispersion characteristics match with that of a waveguide for the same  $TE_{m0}$

## LITERATURE REVIEW

---

mode [15]. Improved design equations are also suggested by the authors and they proposed smaller vias and lesser gaps between the vias are beneficial to prevent leakage loss. In an SIW, the conductor and the dielectric significantly contribute to the losses than the radiation loss and all the three types of losses are modelled in [16] using the BI-RME method, which also allows easy derivation of the equivalent circuitry for the SIW lossy discontinuities. In [17], the unloaded quality factor of an SIW is studied. It was studied that though the unloaded quality factor of an SIW resonator is lower than that of the waveguide, but at higher frequencies it is much higher than that of a microstrip. The paper also suggested that thicker substrates are preferred in narrowband applications where the insertion loss greatly matters. To understand the similarity between an SIW and the conventional waveguide, research has been carried out in [18] where it has been found out that a waveguide has its sidewalls replaced by vertical conducting cylinders, it behaves similar to an SIW. The analytical equivalence between an SIW and a rectangular waveguide has also been proposed [19]. It was carried out by comparing the surface impedance of both the side walls of an SIW and the waveguide by an analytical continuity.

Integrated waveguide techniques, which were filed as a patent way back in 1994 [20], gained popularity with the SIW scheme from 2000. Till now SIW has been applied in the design of filters [21], couplers [22], oscillators [23], power amplifiers [24], slot array[25] and leaky antennas [26], circulators [27], mixers [28] and many more [29].

With the advancement of SIW technology, several modified forms of SIW have also been discovered. If the SIW is bisected along the longitudinal axis, it results in an Half Mode SIW (HMSIW), which not only retains the features of SIW, but reduces the entire size by half [30].

## LITERATURE REVIEW

---

A directional filter at 12 GHz has been reported in HMSIW in [31]. The bandwidth is reported to be 250 MHz with less than 3.2 dB. Quarter-Mode SIW or QMSIW is the quadrant structure of a square SIW resonator [32]. The first two cavity modes of QMSIW are  $TE_{101}^{QM}$  and  $TE_{202}^{QM}$ . It finds huge applications in antenna designs with lesser footprint [33]. The concept of folded waveguide can also be realised in planar form using a dual layer substrate, which reduces the waveguide width, and is called Substrate Integrated Folded Waveguides (SIFW) [34]. Filter fabricated in SIFW technology showed good results at 7 GHz with a bandwidth of 5.71% [35]. If the dielectric part of an SIW is removed and metallic-via array sidewalls are replaced by continuous metallic wall, an empty SIW (ESIW) is formed [36]. The losses in the ESIW are less and the quality factor is more than SIW. Filters designed in ESIW, by the authors, have 4.5 times more quality factor than SIW. High-performance millimeter wave ESIW passive components such as a 90° hybrid coupler and a T-junction over Ka-band have been proposed in [37]. A combination of HMSIW and SIFW technology was also introduced as a folded half-mode substrate integrated waveguide (FHMSIW) in 2008 to design a 3dB coupler of a further reduced size [38].

### 2.2 Review on various forms of SIW Transitions to planar and non planar guides

Even though the new scheme, Substrate Integrated Circuit (SIC), was proposed to eliminate the drawbacks of the planar and non-planar circuits by synthesizing the entire system within a single substrate [39], the wireless systems may be made up of several other microwave or millimeter wave components and they need not necessarily be constructed using the same technology. In fact it might so happen that at least one component is a non-planar device. It is

## LITERATURE REVIEW

---

thus very important to have a near to perfect impedance matching and mode matching between the ports of the transition and the technologies. The transitions available between different planar and non planar structures such as waveguide, coaxial, microstrip, etc are bulky and the mechanical fabrication involved in it makes it expensive and complex [40]. Due to its planar construction and conformability, SIC technology allows interconnection of different transmission lines through simple transitions. Over the past few years, as the SIW is gaining popularity as an emerging technology in SIC microwave and millimeter-wave systems [41], [42], researchers are looking forward to realizing SIW transitions as well. SIW inherits the lower loss and higher quality factor properties from the waveguide due to the construction of the sidewalls and thus can handle power at higher frequencies. SIW being compact and inexpensive [42], the transition between SIW and other structures becomes easier. It can be integrated with other planar and non-planar structures in higher degree of integration and dense packaging systems [41]. Various transitions between SIW and other technologies like waveguide, coaxial, microstrip and CPW along with their advantages and disadvantages [43]-[71] have been discussed in this section. In systems such as Radar, GPR, satellite communication systems, SIW transitions are reported to integrate components like power dividers [42], [48], antenna [53], and filter [60].

Rectangular waveguides being bulky still find usage in various high frequency microwave and millimetre-wave applications, due to its lower loss and power handling capabilities. However, for a complete system a transition between SIW and rectangular waveguide is necessary. Due to the cross-sectional width and dielectric differences between both the guides, there is an impedance mismatch between them which lead to loss. Therefore, proper transitions which match the impedance between both the waveguides have been designed. The first

## LITERATURE REVIEW

---

transition between waveguide to SIW is reported in 2003, which demonstrates that the energy is transferred through an input-coupling aperture made on the bottom conductor layer of the PCB [43]. The Ka-Band transition presents a 15dB return loss bandwidth of 8%. In [44], the transition is initiated from a radial probe extended from the SIW, which is inserted in a height-tapered waveguide. Though it exhibits a higher bandwidth of 33.03%, the insertion loss is poor. Longitudinal slots are also used to couple energy from SIW to the waveguide. When the substrate with a longitudinal slot etched on the broad wall of the SIW is surface mounted to the standard flange of the waveguide, it acts as the window to transfer energy [45], however, the design suffers from narrow bandwidth of 800MHz. In order to increase the bandwidth upto 1.72 GHz, two longitudinal slots of different lengths can be simultaneously resonated at close frequencies [46]. The longer slot is resonating at the lower frequencies, whereas the shorter slot is excited at the upper edge of the frequency band. A multiple substrate layered V-Band transition is documented in [47], where the signal propagates from the bottom SIW substrate to the second substrate level through a longitudinal slot. The second substrate acts as a short vertical waveguide section. The signal now couples from the second substrate to the third substrate through another longitudinal slot. The upper layer of the topmost substrate behaves as an aperture coupled patch antenna, which transfers the signal into the waveguide. The structure gives an effective 10 dB bandwidth of 35%. Transverse slot is also used in SIW transitions to develop a power divider, where an extra substrate layer is sandwiched in between the etched transverse slot SIW and rectangular waveguide [48]. The middle substrate has only one copper layer facing the rectangular waveguide, which acts as the radiating microstrip patch. The power divider could present a narrow bandwidth of 5.6% only. However, both [47],[48] are bulky. An 8 GHz broadband SIW transition is developed by realising an antipodal quasi-Yagi Antenna probe on the same SIW substrate, and then inserted vertically into the waveguide at the centre

## LITERATURE REVIEW

---

[49]. In [50], along with two stepped ridges in the waveguide flange, an additional arrangement of etched coupling aperture on the broad wall of the SIW is made to obtain a 7.05 GHz broadband response in Ka-Band. An improved, compact and broadband transition technique had been proposed in [51], where the aperture is designed to create three coupled resonators. In another new type of back-to-back W-Band transition, the SIW is tapered to increase its width and then extended as a wave-impedance transformer into a smooth height tapered waveguide [52]. The measured bandwidth is 26%. Instead of tapering the height of the waveguide, height-stepped waveguides are also incorporated [53] in the design of transitions. The structure can be further extended along with an arrangement of either a single-step widening transformer [54] or normal inserted substrate taper [55] for better performance. Recently, antipodal finline tapers are reported in the construction of SIW to waveguide transition [56].

SIW proves to be a technology that bridges the gap between waveguides and microstrip lines by having better loss characteristics [41]. However, it occupies a larger area than microstrip [42]. Though both SIW and microstrip are planar, they exhibit different dominant modes and characteristic impedance. An SIW to microstrip transition overcomes these difficulties over the operating bandwidth. The basic transition from microstrip to SIW is proposed in [57]. In order to interface signals between the technologies, a tapered microstrip line connects the 50 microstrip line to the planar SIW. The entire design is realised on the same substrate. As the signals in both the cases propagate in the same direction and the electric fields are of similar orientation, the taper is able to transform the quasi-TEM mode of the microstrip line to the dominant  $TE_{10}$  mode of an SIW. Since there is a mismatch between the width of the 50 microstrip line and the SIW width, the taper length has to be taken into consideration for matching the impedance between them. The analytical equations to design the mentioned

## LITERATURE REVIEW

---

transition in [57] are elaborated in [58]. To derive the equations the transition is divided into two parts: the tapered microstrip line and the step between the SIW and 50 microstrip line. The step is further analysed by considering the SIW to be a dielectric filled rectangular waveguide having a height equal to the substrate and by modelling the microstrip to an equivalent TEM waveguide. The return loss of the tapered transition is improved by placing an extra pair of metallic via at the tapered line and SIW junction [59]. In another transition, a pair of quarter-wavelength short circuited slots and grounded coplanar waveguide impedance transformer is connected between the microstrip line and the SIW on the same substrate [60]. As the dominant  $TE_{10}$  mode enters the transition structure from the SIW, the stronger electric fields at the centre enters the GCPW, and the rest gets eliminated by the slots. After the parallel plate modes generated in the GCPW are suppressed by the via-holes on the GCPW planes, the fields are launched in the microstrip line. The measured transition resulted in a 50% bandwidth at V-band. Transition between microstrip and SIW is achieved over a broadband with lower loss in multilayered substrate environment, as well. The structure is using tapered and multi-sectional ridged SIW and tapered microstrip line for the required transition [61].

In applications like GPR, radar where low frequency RF signal is fed to any SIW component through coaxial lines, transformation of TEM waves from the coaxial line to the  $TE_{10}$  mode in the lower impedance SIW is necessary. Direct transitions from coaxial line to SIW were reported in [62]-[66]. The designs proposed in [62]-[65] make use of a short-circuited back wall, placed at a quarter wavelength distance from the inner conductor of the coaxial connector. In [62], three different transition techniques are investigated. The primary design has a coaxial Line appended onto the top plane of the SIW such that the inner conductor is inserted into the substrate and shorted onto the ground plane. However, due to mismatch of

## LITERATURE REVIEW

---

impedance the bandwidth got restricted to 1.1%. To lower the impedance of the coaxial line to that of the SIW, instead of inserting the inner conductor till the ground plane, a step or taper is installed at the end of the inner conductor midway in the dielectric. The structures present a bandwidth of 14.7% and 13.2 % bandwidth, respectively. A further modification of [62] is suggested through simulation, where an inductive septum is formed after the signal is launched in the SIW [63] and a ring is cut around the contact between the inner conductor and the top conductor of the SIW [64]. In [65], a triangular slot around the inner conductor is used to improve the bandwidth to 30%. Coaxial Line to SIW transitions without the use of any short-circuited back wall have also been reported [66]. Such structures have a ring etched at a certain radius from the inner conductor of the coaxial line. The SMA connector pin is soldered between the top and bottom conductor through a via at the centre of the patch. Since no short-circuited back wall is used, both the transitions are wide band. The same concept is applied to transitions between Coaxial lines to ESIW guides [67].

Literature reveals transitions from SIW to CPW as well. In [68], by widening the gap between the parallel lines of the grounded coplanar waveguides (GCPW) to form a stub and further bending it by  $90^\circ$  to form a slot into the SIW, a transition between GCPW and SIW is designed [68]. The stubs are used for impedance matching and the slot radiates into the substrate to excite the SIW. However, it radiates outside the structure as well. A metallic post can initiate the coupling between GCPW and SIW as well [69]. To avoid parallel plate modes, rows of metallic-via on each side of GCPW are used. To nullify the parasitic effect of an open GCPW, an open circuited-stub is inserted between the coupling post and the open GCPW. 70% bandwidth is achieved in a three layer transition design that uses an elevated CPW [70].



## LITERATURE REVIEW

---

Stepped resonator is applied along with the  $90^\circ$  bent in [71] to design transitions. This type of transition makes integration of active and passive components simple and inexpensive.

Transitions between SIW and other transmission lines such as waveguide, microstrip, coaxial line, CPW for various microwave and millimetre-wave applications are reviewed through standard literature. An overview of the designs and performances are listed in this paper. SIW has been presented as an emerging technology to integrate various transmission lines on a single substrate and thus facilitate advancements in SIC approach. The future scope includes the development of transitions between other substrate integrated circuits (SICs) and to modify the existing bulky transitions with compact, low cost designs at different bandwidths.

### 2.3 Review on various SIW power dividers and couplers

In a microwave and millimeter wave system, the power divider plays a very important role as a passive component. The recent challenge in the communication industry is that the electromagnetic spectrum is becoming more crowded with wireless signals. The future generation of wireless communication systems along with other industrial electronic applications would demand critical spectral channelization of coexisting bandwidths, which might be already in use for other applications. Researchers are also getting ready to introduce multiple-input multiple-output (MIMO) techniques in the above mentioned systems and applications. It is hence evident that to support these techniques, power dividers with more than two ways of division i.e. multiway power dividers/combiners are immensely required. Several multiway power dividers are reported in both planar and non-planar forms of transmission media, such as waveguide [72], coaxial waveguide [73], stripline [74], microstrip [75].

## LITERATURE REVIEW

---

However, the upcoming systems and technologies including MIMO involve a large number of hardwares and hence the components should be compact, low loss, economical which can be easily integrated. SIW, thus, acts as a very important transmission line to design components, including multiway power dividers, which would meet the needs of the emerging industry trends and hence SIC systems.

The first SIW power dividers were developed in 2003 [76]. They were the standard T-junction and straight Y-junction waveguide power dividers but developed on a PCB for Ka band operations. At the T-junction, a metallic via is drilled to act as an inductive post, similar to the septum in a waveguide, to achieve better input return loss. The diameter of the post along with its placement, determined the level and the peak frequency of return loss at the input port. In order to widen the bandwidth, multiple posts were suggested [77], which can easily be implemented in SIW. The entire X-band has a return loss better than 15 dB with a power division of around 3.4 dB with hardly any variation in the magnitude and phase between both the outputs. The same work was further extended to achieve arbitrary power division as well [78]. The paper showcases power dividers with division ratios of 1:4 and 1:8 at 6 GHz. The bandwidths measured are 53% and 63.3%, respectively. In the Y-junction SIW power divider [76], the guide was bifurcated into two channels of equal width, with a coupling region in between the two discontinuities. The dominant mode  $TE_{10}$  from the input port enters the coupling region to form a higher order  $TE_{20}$  mode, which gets divided between the output channels to form  $TE_{10}$  modes. The output channels are separated by a series of metallic vias. To avoid reflections and other higher order modes, the coupling length should be properly optimized.

## LITERATURE REVIEW

---

A very well established power divider in waveguides is the Riblet coupler and recently, its SIW counterpart was also reported in [79], where the return losses are over 11dB, insertion losses are  $4.5 \pm 0.5$  dB and isolation over 15dB throughout a bandwidth of 36% in Ku-band. As  $TE_{10}$  mode is excited from the input or from the three outputs if used as a combiner, the longitudinal axis symmetry of the structure makes it useful to further re-excite  $TE_{30}$  mode in the coupling area. The divider is tapered in the coupling region in order to widen the bandwidth.

Whenever there is a requirement of high power level along with higher degrees of isolation between the output ports, Wilkinson power divider is preferred, but they are practically not implemented in waveguide. However, with the SIW technology, Wilkinson power dividers can be developed. A standard Wilkinson power divider includes quarter wavelength transformers in its two arms, which individually has an impedance of  $\sqrt{2}$  times the input characteristic impedance ( $Z_0$ ). In [80], the quarter wavelength transformers are realised in HMSIW. In the gap between the HMSIW branches, a surface mount component (SMC) isolation resistor is placed. The measured fabricated power divider operates in the X-band with a 71% 10dB isolation bandwidth. In order to achieve a broadband response along with size reduction, polyline unit cells can be etched on the surface [81]. This power divider reported a measured 10 dB isolation bandwidth of 91.7% and 15 dB bandwidth of 43.4%. There is also a size reduction of 40% when compared with similar performances in various SIW power dividers. Ring shaped Wilkinson power dividers were also suggested in both SIW and HMSIW [82]. In order to maintain the quarter wavelength shift, the output ports are arranged in a  $60^\circ$  rotation configuration. A slot is realised in the main circular section in order to place the SMC isolation resistor. The HMSIW equivalent can also be implemented with multiple parallel resistors (for

## LITERATURE REVIEW

---

better isolation) or avoid resistors and instead replace them with the equivalent resistance of resonant slots to simplify the circuit and reduce the size. All the four power dividers, when fabricated, presented a bandwidth of more than 23% at X-band and less than 0.3 dB loss.

Gysel power dividers which are usually constructed in microstrip have better power handling capability than Wilkinson power dividers. These power dividers when designed in waveguides results in a complex and a bulky construction [83] but, SIW proves to be a better alternative [84], [85]. In the SIW design [84], apart from the input port, there are two distributing (output) ports and two isolated ports which are terminated by isolation resistors. The same structure can be built in multilayered SIW PCBs, by stacking them vertically. Folded SIW structures have also been used in the design, so that a difference in electrical length of  $\lambda g/4$  and  $\lambda g/2$  remain between the distributing ports and isolation ports, and that between the distributing ports, respectively. Within a frequency range of 17-19 GHz, a return loss, insertion loss and isolation loss of 12.5, 5.25, 20 dB is found in the fabricated planar structure and those for the non planar structure are 10, 8, 10 dB. Gysel power dividers can also be achieved with the help of HMSIW [85].

It is thus apparent from the literature that SIW is beneficial in designing power dividers which are usually realized in non-planar transmission lines. It is also used in developing power dividers which are otherwise not possible to design in rectangular waveguides, like Wilkinson and Gysel power dividers. As discussed that multifunctional components are the recent and upcoming requirements of the industry, power dividers with filtering characteristics are in great demand, and, SIW triangular cavities [86] and circular cavities [87] are used to design dual band filtering power dividers (FPD) as well. The triangular cavity FPD results in divided power

## LITERATURE REVIEW

---

passbands at 5.5 and 8.3 GHz. The circular cavity FPD results in divided powers a single passband at 5.61 GHz with 7.8% 3-dB bandwidth.

With the advancement of research in the development of power dividers and couplers in SIW, multiway division or coupling has also been explored, a very important application in MIMO systems. Initially, multiway power dividers were formed by combining various configurations of basic power dividers. Such topologies are often called corporate feeders. Similarly, either by using a single configuration or multiple configurations of well established two way power dividers, SIW multiway power dividers were designed. The most common SIW multiway power dividers were constructed out of T-junction and Y-junction power dividers. The first developed SIW multiway power divider was reported in 2005 [88], where seven T-junction and eight Y-junction power dividers were arranged and combined together using fourteen bends to develop a sixteen-way SIW power divider in X-band. As the input  $TE_{10}$  mode is initiated, it gets divided in the first T-junction. These divided powers get further divided in the subsequent T-junctions. The bends help these divided powers to move into another divider as their input. At the last step, these signals are finally divided by the Y-junctions to achieve a 16-way division. The power divider has a 15dB return loss bandwidth of 1.75 GHz with an insertion loss of  $14.5\text{dB} \pm 0.5\text{dB}$ . This approach was further carried out to develop various types of multiway power dividers [89]-[94]. [89]consists of T-junctions, Y-junctions and smooth bends at X-band. The power divider is fed by a GCPW transition instead of usual microstrip. In [90]-[93], the same arrangement were utilized with only T-junction power dividers to attain  $2^N$  ways of power division. By adjusting the power division ratios in the elementary T-junctions at each step, difference of power in the final output ports can be achieved to build unequal power dividers [90]. The configuration has been further extended in

## LITERATURE REVIEW

---

planar ridge waveguides known as Ridge SIWs [91] which upon fabrication presented a bandwidth of 55% and an insertion loss less than  $-9.7 \pm 0.3\text{dB}$  for eight ways of division. In [95], a single T-junction SIW power divider is used to design a four-way power divider. In addition to the two way power divider, it utilizes a slot based multi-layered transition between SIW and microstrip to carry out the further division. The power initially enters the T-junction through a microstrip line. The divided power from the T-junction is further captured on two microstrip lines. Each of these microstrip lines are further branched out into two more lines, with an isolation resistor in between, to provide a X band four way power divider having good amplitude and phase balance, 1.75 GHz return loss (12 dB) bandwidth which has an isolation of more than 12 dB. Similar structure was reported in [96],[97] as well. [97] suggests the usage of an extra isolation resistor in the centre of the short-circuited slotline, which would provide an isolation of more than 17 dB over 1.6 GHz of bandwidth in the X-band. The topologies mentioned above require basic two way power dividers to be combined in such a topology that  $2^N$  ways of power division are achieved. However, with such a topology, odd number of divisions is not possible. To facilitate odd ways of division, [98] suggested a technique where in the first step, the input power is divided into two ways using a Y-junction power divider. As discussed, Y-junctions [88] include a step junction just after the input channel that bifurcates into two output channels. These divided powers further enter into another step junction or the coupling area, which trifurcates into three output channels to divide the power in three ways. The fabricated divider resulted in a bandwidth of almost 10 GHz bandwidth in the E-band. However, there is a shift of  $7^\circ$  in the phase, which might have resulted due to additional bends in the circuit required for measurements. The authors have analyzed the superposition of the sinusoidal functions generated from the Y-junction and hence proposed the technique to design power dividers with any even or odd ways of division. For example, to achieve four ways of

## LITERATURE REVIEW

---

division, these three way divided powers should further broaden into another step junction and finally quadfurcated into four output channels.

SIWs are known to exhibit three types of loss [99], [100]. The presence of metallic via holes in the circuit contributes to conductor losses and the presence of dielectric, in the PCB, contributes to dielectric loss. The gaps between the metallic via holes too can lead to radiation losses. Since, the dielectric results in the major loss in SIW systems, hence larger the area more will be the overall loss. With the above mentioned topologies, it was found that even though several ways of equal and unequal power division with good isolation characteristics were possible, the overall footprint of the circuitry increases which not only might result in the increase of overall loss but are not compact. The power dividers investigated in this section are, however, built of separate topologies where they do not cascade any basic two-way power dividers, instead the input power is directly divided into multiple ways after it propagates through a coupling area.

In order to reduce dielectric losses and circuit footprints, simple designs of multi way power dividers, without using multiple T- or Y-junction two way power dividers, were proposed in [101]- [104]. Equal power division with uniform phase division at each output was observed in [104], where the structure was a modified T-junction. An extra arm was added to the structure, at the junction of the regular T-junction output ports, opposite to the input port. The central via placed at the junction of the output ports was highly responsible in controlling the reflection characteristics and hence adjusted the magnitude and the phase of the divided power. It measured an insertion loss of 4.77 dB, 17.5% bandwidth for a return loss better than 18.5 dB at X-band. Similar structure was demonstrated in HMSIW as well, which helped in the

## LITERATURE REVIEW

---

further reduction of the size [101]. Primarily, all the three branches of the basic T-junction were developed in HMSIW, where an input vertical branch was connected to a horizontal branch having both the outputs. To avoid unwanted energy coupling, due to the direct connection between the half-open dielectric walls of both the vertical and horizontal HMSIW branch, an air gap was etched out on the top metal layer of the PCB along with a row of metallic via. This structure was further modified in two ways to present two types of four way power dividers. In one of the structures, the horizontal branch was connected to three parallel and equispaced vertical branches. One of the ends of the horizontal branch was ended by a  $90^\circ$  bend and made parallel to the vertical branches. All the vertical branches and the bend acted as the four outputs. The return loss was better than 14.5 dB over 3GHz in the Ku-band with a loss of  $1.1 \pm 0.3$  dB. In the second structure, two vertical branches were appended to the horizontal branch, and both the ends had a  $90^\circ$  bend. The input branch was however in SIW, which connected to the horizontal branch directly to the wall in which the via holes were drilled. The SIW branch was the input. In all the above structures, it was the air gap which played a role in the equal division of the power. This power divider achieved a bandwidth of 2 GHz, with  $0.6 \pm 0.5$  dB loss and a return loss better than 12.5 dB. Just like T-junctions, Y-junction power dividers were also redesigned to develop multi way power dividers as shown in [102]. In these dividers, multilayered SIW and HMSIW concepts were used. Two identical PCBs were sandwiched back to back, such that both the guides had a common metal layer. Each PCB had an SIW channel which finally bifurcated into two HMSIW output channels. The output channels had a common via wall at the centre. The power entered the circuit from the top PCB, with the help of a tapered microstrip to SIW transition. This input power is first divided vertically between the two SIW layers and from each of the SIW layers it is further laterally coupled to the HMSIW output channels, to achieve four way power division. This out of phase



## LITERATURE REVIEW

---

divider was fabricated and measured to operate in X-band between 7.63 GHz to 11.12 GHz, where the insertion losses were within  $7 \pm 0.5$  dB and the return loss was better than 10 dB. However, the isolation was poor. In order to improve the isolation, the authors suggested the use of isolation resistors between the two HMSIW channels in each layer. Unlike the previous design, the output HMSIW channels did not have a common via wall boundary, instead they were in continuity with the SIW via-walls, and the open ended via walls were towards the centre with an air gap between the channels in the metal (not in the common metal layer). Isolation resistors were placed between the magnetic walls of the HMSIW output channels. Usually in a Y-junction, the output branches have one of its sidewall as common, but the common wall can also be separated with a certain angle between the output embranchments and this can be realized in SIW and HMSIW as well. In [103] this concept of 90° Y-junction was used to design a four way power divider, by combining two adjacent Y-junctions. The input branch was designed in SIW, and the output branches were in HMSIW. A 15 dB bandwidth was observed in almost the entire X-band, but the amplitudes of output ports were not equivalent.

Several multilayered structures also facilitate multiple ways of power division. The X-band out-of-phase power divider in [105], utilized a two layer SIW, with the input in one layer and four outputs in the other. The power from the input was coupled to the output SIW through a coupling slot, etched at the common metal layer. The power divider however presented a lot of loss. The power divider presented in [106] was a structure with two PCBs, SIW and microstrip, sandwiched together and having a common middle metal/ground layer. It consisted of an SIW which was short circuited at one end. Four rectangular slots were etched on the middle metal/ground layer, such that one-fourth of the input power from the SIW PCB was

## LITERATURE REVIEW

---

coupled to the microstrip PCB. This divided power was available at the output through four microstrip lines on the topmost PCB. The short wall was placed at the quarter-guided wavelength of the SIW. The slots width, length and the position were chosen carefully to avoid higher order modes and poor coupling. The measured results showed narrowband characteristics of 250 MHz bandwidth with more than 15 dB return loss and less than 1.5 dB of insertion loss. Similar divider was reported in [107] as well where it operated in the W-band. To avoid possible overlapping of the reflection generated by each of the slots, their positions were optimised such that all the four slots are not placed and aligned near to only one side wall, and instead alternatively placed. It had a narrowband performance but with high insertion loss. Filtering anti-phase power dividers like [108] were also explored in Ka-band. The input power, after getting filtered, is coupled to the above  $TE_{20}$  mode SIW through a longitudinal slot (longitudinal to the  $TE_{20}$  mode SIW). The  $TE_{20}$  mode SIW had two output branches on its two sides and hence the filtering anti-phase four way power division response was obtained.

In a system it might so happen that its constituent components are built on various transmission lines. These transmission lines might not be restricted to only planar forms, but non-planar structures, such as waveguides, might be a part as well. We are already aware that out of all available SICs, SIW is the most developed technology and it supports transition between various planar and non planar structures, but with the requirement of miniaturization in the current and upcoming manufacturing scenario, a component should be multifunctional. SIW is favourable as a guide which carries out both the functions of transitioning and power dividing. Four multilayered SIWs stacked on top of each other were tapered and inserted into the reduced height waveguide (transition) in [109]. Since the SIW was a reduced height dielectric waveguide of reduced width, in order to match the impedance between the SIW and

## LITERATURE REVIEW

---

the reduced height waveguide, the waveguide taper and the SIW taper was realized. As the power transits from the waveguide to the SIW, it gets divided in just one step, as compared to series or tree structures. In [110], instead of substrate taper, substrate wedges are realized in between the width tapered SIW and height tapered waveguide. Both the structures operated in Ka-band and had a broad bandwidth, but the losses were more.

A Ka-band six-way power divider is presented in [111], where the structure involves a single mode SIW input channel opening up to a coupling area in order to generate multiple modes. At the other end of the multimode SIW, six single mode SIW channels are connected. The divider is excited with  $TE_{10}$  mode which finally generates  $TE_{m0}$  modes (odd modes) in the multimode SIW. Just before the output channels, six-fold multiple imaging of the E-field is achieved, which the six channels captures individually and hence present  $TE_{10}$  divided power at the output. It achieves a 15 dB return loss bandwidth of 2GHz, however losses are more. Using this technique N-way power division can be carried out and the length of the multimode SIW can be determined accordingly.

A ten-way SIW power divider is investigated using shape optimization technology to reconstruct the diffraction field at Ka-band [112]. Good power splitting, amplitude and phase balance are achieved in simulation. It is expected that such a work would provide a new idea to the design of the millimeter wave device such as the application to filtering-power divider based on hybrid SIW-spoof surface plasma filter.

The Riblet coupler is originally a four port device, when designed in waveguides, but when realized in SIW to design a two way power divider, it is modified to a five port device

## LITERATURE REVIEW

---

[79] with an extra isolation port. In order to split powers in three ways, the five port device is further upgraded to a six port device, by adding an extra output channel to the already existing two output channels [113]- [117]. The  $TE_{10}$  mode which enters into the divider input, is allowed to generate  $TE_{30}$  mode in the coupling region, and the interaction between coupling section and the output arms are so designed that it gets divided into them equally as  $TE_{10}$  modes. The first reported six port three way power divider was proposed in 2013, as an X-band device with 10% bandwidth [113]. Resonating cavities were introduced through inductive irises in each arm to increase the bandwidth. In order to provide better isolation between adjacent channels, unsymmetrical apertures were used in the lateral port arms. The insertion loss was better than 1.6 dB whereas the isolation and the return loss was below 19 dB. Six port three way dividers were further presented as a more compact option in [115] at X-band itself. It achieved 12 % bandwidth, with less than 1 dB variation in the insertion loss and the reflection was better than 15 dB. The isolation was, however, not reported. Another alternative to a compact structure is suggested in [117], where the lateral arms were realised in HMSIW, such that the via walls of the SIW and the HMSIWs were common. It was an unequal power divider which operates in the X-band as a  $90^\circ$  phase shifter. The structure also included a longitudinal slot at the centre of the structure, in the coupling region. After passing through the SIW line, as the input power reached the slot, it was divided into two. These divided powers were again individually halved at each of the SIW and HMSIW output junctions, such that the HMSIW junctions receive -6 dB and the central SIW output arm received two in-phase -6 dB powers, which added up to -3 dB. The fractional bandwidth was 23.5 %. The basic structure of a Riblet Coupler is basically two guides appended together with a common narrow wall, but the common wall has a short slot or a gap in between which forms the coupling region. Similarly in the above mentioned dividers, there were three SIW/HMSIW guides, with a gap in their

## LITERATURE REVIEW

---

common walls. But, it is also possible to design three way (both equal and unequal) power dividers using multi-apertures in the common walls [114], [116]. The equal division coupler is a uniform structure, which is symmetrical in its axial direction, and the two coupling windows are of the same length, while the unequal division one was designed with an asymmetrical structure, in which the two coupling windows were of different lengths. Both the dividers operated from 12.5 to 16.5 GHz with a measured isolation was more than 18 dB.

In most of the SIW power dividers studied above, the input or the output of the SIW can't be measured directly using a coaxial SMA connector. A tapered transition between SIW input/output channels and microstrip is first designed and the SMA connector is soldered to the  $50\Omega$  microstrip line. This results in additional loss and a certain increase in the circuit footprint due to the taper. In the paper [118], a method is suggested in order to avoid the microstrip taper transition in the input, a stepped coaxial line transformer is directly connected to feed the SIW power divider, at the centre. This transformer connects with an axially symmetric dual disk probe, in order to achieve a broader impedance matching between the coaxial line and the SIW. From the dual disk probes, four rectangular SIW channels branch out in a radial fashion, to divide the power equally in four ways. The output is however, measured through the SMA soldered at the tapered transition. A prototype is fabricated to work in C-band and is measured to obtain a bandwidth of 4.4 GHz, covering almost the entire C-band. The return loss of the divider is below 10 dB throughout the bandwidth. This technique is further carried out to design a C-band six way out-of-phase power divider [119]. By placing three alternate output channels on the top plane and the rest three on the bottom, the polarity of their potential changes and hence  $180^\circ$  phase shift is achieved. The results are broadband with 3 GHz of bandwidth. Further reduction of size and complexity can be achieved by getting rid of the

## LITERATURE REVIEW

---

dependency on microstrip and its transition, at the outputs as well [120]. Here, instead of guides, four SIW rectangular cavities, with tapered openings to the central coaxial feed, are connected. All the four output probes and the input probes are current probes and don't include the coaxial transformer, instead SMA connectors are directly appended. Such power dividers can be developed using  $100\Omega$  impedance transition between the SIW and the coaxial lines, instead of regular  $50\Omega$  impedance transition [121]. Similar four way power divider is built on ESIW platform [122], as well. The tapered openings act as inductive posts, which helps in the reduction of transmission loss and reflections. Within a band of 5.15 to 5.85 GHz, the return loss is less than 10 dB and the insertion losses are less than 1 dB. These power dividers are very much useful in feeding antenna arrays for mobile satellite TV receptions, high performance, cost effective applications in 5G communications, and smart surface systems.

Cavities designed in SIW can be used in the design of direct coaxial fed SIW power dividers [123], which sometimes provide the power division with additional filtering characteristics as well [124], [125]. It is known how the quarter mode of an SIW, QMSIW, is obtained from a rectangular SIW cavity. When a QMSIW is bisected diagonally, the structure is known as 1/8th mode SIW, which looks like an isosceles triangle. If it is further bisected diagonally, 1/16th mode SIW is formed and when the 1/16th mode SIW is bisected, it is known as 1/32th mode SIW. This 1/32th mode SIW if placed radially across the central coaxial feed, multiway power dividers can be built [123]. The feeding for the output is a  $50\Omega$  microstrip line connected to the perpendicular edge of the wedged-shape 1/32th mode SIW with an offset from the short wall. Four way and eight way power dividers were fabricated. While the 10 dB bandwidth for the four way power divider was 39.3%, that of the eight way power divider was 13%. The size was very compact with  $0.49\lambda_g^2$  area. The isolation of the four way divider was

## LITERATURE REVIEW

---

more than 13.5 dB and that of the eight way divider was 19 dB across their respective bandwidths. Similarly, in [124] a four way power divider was realized in the  $1/8$ th mode of a circular SIW cavity. The design was a multilayered structure, in which one substrate acted as a regular SIW cavity. Power was fed into the cavity using a coaxial feed. In the second substrate, four  $1/8$ th mode of circular cavities were aligned radially. The output power was measured using SMA connectors appended to microstrip lines. Circular perforations of various radius across different layers of the PCB was made to solder the inner conductor pin of the input SMA connector, and power was coupled from one substrate to the other. Filtering characteristics were observed in the circuit, and it acted as a narrow S-band divider with isolations more than 15 dB. In [125], a square patch was fed with a coaxial probe at the centre, resulting in  $TE_{20}$  mode only. The patch was further loaded with a square SIW cavity resonator to widen the bandwidth, which depended on the interaction between the  $TE_{110}$  mode of the resonator and  $TE_{20}$  mode of the patch. Four open ended coupling lines were connected to each  $50\Omega$  microstrip output feed lines and four isolation resistors were loaded between each output port linked by the transmission line stubs. The fractional bandwidth of the S-band FPD was 21.3% which had a return loss less than 10 dB, but insertion loss less than 2 dB. Another technique to reduce the size in designing four way SIW power dividers was proposed in [126], by incorporating complementary split ring resonators (CSRR) in HMSIW. The structure includes two HMSIW with a loaded CSRR connected at their magnetic wall and at the centre, the input power is fed using a coaxial line. The power then divides into the two HMSIW sections. These divided powers in the HMSIW sections are again divided by placing two microstrip lines at both the ends of each section, and hence four way power division is attained. A narrow bandwidth of 3.2% in the C-band was observed with return loss less than 15 dB, insertion loss within 1.1 dB and isolation better than 12 dB. The size came to be around  $0.079\lambda_g^2$ .

## LITERATURE REVIEW

---

With the development of feeding power directly to waveguides or SIW, via coaxial lines and the radial alignment of cavities around the central feed to design power dividers, a new topology for multiway power divider was presented in the literatures [127]-[135], where instead of using segmented cavities, an entire circular SIW cavity is used. The input power is fed at the centre of the cavity via a coaxial line and the output probes are placed radially around the cavity as peripheral probes. The peripheral probes are also fed by coaxial lines. Such power dividers are known as radial power dividers. In [127], a four way radial power divider was presented in Ku band. The SIW radial cavity was synthesized on a planar substrate by drilling arrays of a metallic via holes to form a circumferential wall. These metallic vias act as an electrical wall and suppress the parallel-plate leaky modes. Four identical peripheral current probes were placed radially, on the opposite side of the substrate. Since the peripheral current probes were symmetrical with the centre probe, the power divider structure can be viewed to be radially divided into four sectors and each sector forms a branch of the power divider. Each sectoral waveguide consisted of an input and an output with a short at the back and the sectors were separated by magnetic side walls. In order to achieve proper power division, the impedance of the current probe is to be matched with a current probe in a sectoral waveguide with magnetic side walls and a short at the back. Based on these assumptions, the existing technique of conventional radial cavity was analysed and other multiway SIW radial cavity power dividers were designed. At 12.3 GHz, the measured minimum insertion loss was approximately 0.6 dB and return loss was better than 30 dB. The measured 15 dB return loss bandwidth was around 600 MHz. Another prototype for four-way SIW radial power divider/combiner operating at Ka band was fabricated and measured [128]. Experiments on the back-to-back design showed a minimum insertion loss of 1.5 dB at 31.1 GHz which



## LITERATURE REVIEW

---

corresponded to 84% power-combining efficiency. The measured 10-dB return loss bandwidth was 2.2 GHz. Similar approach is extended to the design of eight way radial SIW power dividers. The power divider in [129] was developed in C-band using simple electromagnetic modelling. This narrow band power divider provided an advantage of low insertion loss. The broadband power dividers are however not so good with their isolation. In 2020, [136] presented a microstrip structure which acted as the isolation network for the broadband power divider. This overall structure was multilayered, with an extra layer having the microstrip isolation network, which was a star network with lines from the centre to each output port. Usually a signal from the output port will pass the SIW cavity, the microstrip circuit and finally arrive at other output ports, due to poor isolation. But, since there were two path signals having  $180^\circ$  phase difference between them, they were cancelled out and good isolation performance was observed. There were eight resistors in the isolation circuit and they balanced the output ports and played an isolation role. The 15 dB bandwidth was 25% with more than 16 dB of isolation. Differential radial power dividers in SIW for both four ways and eight ways of division were also reported [130],[132]. In both the structures this is obtained by not placing every consecutive peripheral probe on the same metal plane. Such arrangements provide  $180^\circ$  out of phase, without any dependency on the frequency, and hence change the electric field polarity for every consecutive probe which results in power division with a differential operation. The four way divider presented a 350 MHz of bandwidth with losses less than 1 dB and excellent amplitude and phase balance [130]. Additional pairs of radial slots were etched out around each peripheral probe in order to improve the out-of-band rejection level [132]. Since, the currents of higher order modes are not along the radial direction, they will be cut off by these radial slots. This will result in the suppression of the higher order modes and extension of the upper stopband bandwidth. The radial slots were parallel to the current direction of the

## LITERATURE REVIEW

---

dominant mode and hence would not change the performance of the divider. To achieve broadband input impedance matching, multiple-via probes were used in the central patch of the input probe. More than 84% of bandwidth was achieved. There might be issues for realizing these power dividers at higher frequencies because as the overall size decreases and the number of ways of division increases, appending coaxial SMA connectors to the feed becomes difficult or impossible. However, with multilayered structure it becomes possible. The authors of [133] hence suggested a technique and used it to design a prototype for a seven way SIW radial power divider in K band. The SIW PCB was sandwiched between two microstrip PCB layers. The input power was fed to the microstrip layer, at one side of the structure and not to the centre. It was the microstrip line, which carried it to the centre. At the centre, this power was captured through a patch and with the via and the normal current probe (in the SIW metal layer), it was transmitted to the SIW cavity for power division. Similarly, the output powers were captured by coaxial feeds away from the ports. -10 dB reflection bandwidth of 45% was observed in the K-band at 20 GHz. The power dividers being low profile, simple and having high power-combining efficiency finds usage in sub 6-GHz 5G base stations and satellite communication applications such as multiplexers, power amplifiers, antenna arrays [134], switches [131].

### References:

- [1] J. Hirokawa and M. Ando, "Single-Layer Feed Waveguide Consisting of Posts for Plane TEM Wave Excitation in Parallel Plates," *IEEE Trans. Ant. Propag.*, vol.46, no.5, pp.625-630, May 1998.
- [2] H. Uchimura, T. Takenoshita, M. Fujii, "Development of a Laminated Waveguide," *IEEE Trans. Microw. Theory Tech.*, vol. 46, no. 12, pp.2438-2443, Dec. 1998
- [3] J. Hirokawa and M. Ando, "Efficiency of 76 GHz Post-Wall Waveguide-Fed Parallel Plate Slot Arrays," in *Proc. 29<sup>th</sup> Eur. Microw. Conf. (EuMC)*, Munich, pp. 271-274, Oct. 1999.

## LITERATURE REVIEW

---

- [4] K. Wu, D. Deslandes, and Y. Cassivi, "The Substrate Integrated Circuits—A New Concept for High-Frequency Electronics and Optoelectronics," *Telecommun. Modern Satellite, Cable, Broadcast. Service*, vol. 1, pp. P-III–P-X, Oct. 2003.
- [5] A. Zeid and H. Baudrand, "Electromagnetic Scattering by Metallic Holes and its Applications in Microwave Circuit Design," *IEEE Trans. Microw. Theory Tech.*, vol. 50, no. 4, pp. 1198–1206, Apr. 2002.
- [6] A. Suntives and R. Abhari, "Characterizations of Interconnects Formed in Electromagnetic Bandgap Substrates," in *Proc. 9th IEEE Workshop Signal Propagation Interconnects (SPI)*, Garmisch-Partenkirchen, Germany, May 10–13, 2005, pp. 75–78, 2005.
- [7] A. Suntives and R. Abhari, "Design and Characterization of the EBG Waveguide-Based Interconnects," *IEEE Trans. Adv. Packag.*, vol. 30, no. 2, pp. 163–170, May 2007.
- [8] D. Deslandes and K. Wu, "Design Considerations and Performance Analysis of Substrate Integrated Waveguide Components," in *Eur. Microw. Conf.*, pp. 881–884, Sep. 2002.
- [9] Y. Cassivi, L. Perregriani, K. Wu, and G. Conciauro, "Low-Cost and High-Q Millimeter-Wave Resonator Using Substrate Integrated Waveguide Technique," in *Proc. 32nd Eur. Microwave Conf.*, vol. 2, Milan, Italy, Sep. 23–27, 2002, pp. 737–740, 2002.
- [10] D. Deslandes and K. Wu, "Single-Substrate Integration Technique of Planar Circuits and Waveguide Filters," *IEEE Trans. Microw. Theory Tech.*, vol. 51, no. 2, pp. 593–596, Apr. 2003.
- [11] Y. Cassivi, L. Perregriani, P. Arcioni, M. Bressan, K. Wu, and G. Conciauro, "Dispersion Characteristics of Substrate Integrated Rectangular Waveguide," *IEEE Microw. Wireless Compon. Lett.*, vol. 12, no. 9, pp. 333–335, Sep. 2002.
- [12] F. Xu, Y. Zhang, W. Hong, K. Wu, and T.J. Cui, "Finite-Difference Frequency-Domain Algorithm for Modeling Guided-Wave Properties of Substrate Integrated Waveguide," *IEEE Trans. Microw. Theory Tech.*, vol. 51, no. 11, pp. 2221–2227, Nov. 2003.
- [13] L. Yan, W. Hong, K. Wu, and T.J. Cui, "Investigations on the Propagation Characteristics of the Substrate Integrated Waveguide Based on the Method of Lines," *Proc. Inst. Elect. Eng.—Microw. Ant. Propag.*, vol. 152, pp. 35–42, Feb. 2005.
- [14] D. Deslandes and K. Wu, "Accurate Modelling, Wave Mechanisms, and Design Considerations of a Substrate Integrated Waveguide," *IEEE Trans. Microw. Theory Tech.*, vol. 54, no. 6, pp. 2516–2526, June 2006.
- [15] F. Xu and K. Wu, "Guided-Wave and Leakage Characteristics of Substrate Integrated Waveguide," *IEEE Trans. Microw. Theory Techn.*, vol. 53, no. 1, pp. 66–73, Jan. 2005.
- [16] M. Bozzi, L. Perregriani, and K. Wu, "Modeling of Radiation, Conductor, and Dielectric Losses in SIW Components by the BI-RME Method," in *Proc. 3<sup>rd</sup> Eur. Microw. Int. Circuits Conf.*, Netherlands, pp. 230–233, Oct. 2008.
- [17] A.A. Khan, M. K. Mandal, S. Sanyal, "Unloaded Quality Factor of a Substrate Integrated Waveguide Resonator and its Variation with the Substrate Parameters," in *Proc. Int. Conf. Microw. Photo. Dhanbad*, pp. 1–4, Dec. 2013.

## LITERATURE REVIEW

---

- [18] W. Che, K. Deng and Y. L. Chow, "Equivalence between Waveguides with Side Walls of Cylinders (SIRW) and of Regular Solid Sheets," *Asia Pacific Microwave Conference APMC 2005*, Dec. 2005.
- [19] W. Che, K. Deng, D. Wang, and Y. L. Chow, "Analytical Equivalence between Substrate-Integrated Waveguide and Rectangular Waveguide," *IET Microwaves, Antennas and Propag.*, vol. 2, no. 1, pp. 35–41, 2008.
- [20] F. Shigeki, "Waveguide Line (in Japanese)," *Japan Patent 06-053 711*, Feb. 25, 1994.
- [21] R.Q. Li, X.H. Tang and F. Xiao, "Substrate Integrated Waveguide Dual-Mode Filter Using Slot Lines Perturbation," *Electron. Lett.*, vol. 46, no. 12, pp. 845-846, June 2010.
- [22] J. X. Chen, W. Hong, Z. C. Hao, H. Li, and K. Wu, "Development of a Low Cost Microwave Mixer Using a Broad-Band Substrate Integrated Waveguide (SIW) Coupler," *IEEE Microw. Wireless Compon. Lett.*, vol. 16, no. 2, pp. 84–86, Feb. 2006.
- [23] Y. Cassivi and K. Wu, "Low Cost Microwave Oscillator Using Substrate Integrated Waveguide Cavity," *IEEE Microw. Wireless Compon. Lett.*, vol. 13, no. 2, pp. 48–50, Feb. 2003.
- [24] M. Abdolhamidi and M. Shahabadi, "X-band Substrate Integrated Waveguide Amplifier," *IEEE Microw. Wireless Compon. Lett.*, vol. 18, no. 12, pp. 815–817, Dec. 2008.
- [25] Y. Li, W. Hong, G. Hua, J. X. Chen, K. Wu and T. J. Cui, "Simulation and Experiment on SIW Slot Array Antennas," *IEEE Microw. Wireless Compon. Lett.*, vol. 14, no. 9, pp. 446–448, Sep. 2004.
- [26] A. J. M. Ros, J.L. G. Tornero, and G. Goussetis, "Multifunctional Angular Bandpass Filter SIW Leaky-Wave Antenna," *IEEE Ant. Wave Propag. Lett.*, vol. 16, pp. 936-939, Oct. 2016.
- [27] W. D'Orazio and K. Wu, "Substrate-Integrated-Waveguide Circulators Suitable for Millimeter-Wave Integration," *IEEE Trans. Microw. Theory Tech.*, vol. 54, no. 10, pp. 3675–3680, Oct. 2006.
- [28] M. Bozzi, A. Georgiadis, and K. Wu, "Review of Substrate-Integrated Waveguide Circuits and Antennas," *IET Microw. Antennas Propag.*, vol. 5, no. 8, pp. 909–920, June 2011.
- [29] M. Bozzi, L. Perregrini, K. Wu and P. Arcioni, "Current and Future Research Trends in Substrate Integrated Waveguide Technology," *Radio Engineering*, vol. 18, no. 2, pp. 201–209, Jun. 2009.
- [30] W. Hong, B.Liu,Y.Q.Wang,Y.Q.Wang, Q. H. Lai andK.Wu,"Half Mode Substrate Integrated Waveguide: A New Guided Wave Structure for Microwave and Millimeter Wave Application," in *Proc. Joint 31st Int. Conf. Infr. Millim. Waves 14th Int. Conf. Terahertz Electron.*, Shanghai, China, Sep. 18–22, 2006
- [31] Y. J. Cheng, W. Hong, and K. Wu, "Half Mode Substrate Integrated Waveguide (HMSIW) Directional Filter," *IEEE Microw. Wireless Compon. Lett.*, vol. 17, no. 7, pp. 504–506, Jul. 2007.
- [32] Z. Zhang, N. Yang, and K. Wu, "5-GHz Bandpass Filter Demonstration Using Quarter-Mode Substrate Integrated Waveguide Cavity for Wireless Systems," in *Proc. IEEE Radio Wirel. Symp.*, pp. 95–98, Jan. 2009.
- [33] C. Jin, R. Li, A. Alphones, and X. Bao, "Quarter-Mode Substrate Integrated Waveguide and its Application to Antennas Design," *IEEE Trans. Antennas Propag.*, vol. 61, no. 6, pp. 2921–2928, Jun. 2013.

## LITERATURE REVIEW

---

- [34] N. Grigoropoulos, B. Sanz-Izquierdo and P. R. Young, "Substrate Integrated Folded Waveguides (SIFW) and Filters," *IEEE Microw. Wireless Compon. Lett.*, vol. 15, no. 12, pp. 829–831, Dec. 2005.
- [35] C. Zhao, C. Fumeaux and C. –C. Lim, "Folded Substrate-Integrated Waveguide Band-Pass Filters," *IEEE Microw. Wireless Compon. Lett.*, vol. 27, no. 1, pp. 22–24, Jan. 2017.
- [36] A. Belenguer, H. Esteban, and V. E. Boria, "Novel Empty Substrate Integrated Waveguide for High-Performance Microwave Integrated Circuits," *IEEE Trans. Microw. Theory Techn.*, vol. 62, no. 4, pp. 832–839, Apr. 2014.
- [37] F. Parment, A. Ghiotto, T.P. Vuong, J.M. Duchamp, and K. Wu, "Air-Filled Substrate Integrated Waveguide for Low-Loss and High Power-Handling Millimeter-Wave Substrate Integrated Circuits," *IEEE Trans. Microw. Theory Tech.*, vol.63, no.4, pp.1228-1238, Apr.2015.
- [38] G. H. Zhai, W. Hong, K. Wu *et al.*, "Folded Half Mode Substrate Integrated Waveguide 3-dB Coupler," *IEEE Microw. Wireless Compon. Lett.*, vol. 18, no. 8, pp. 512–514, Aug. 2008.
- [39] K. Wu, D. Deslandes, and Y. Cassivi, "The Substrate Integrated Circuits—A New Concept for High-Frequency Electronics and Optoelectronics," *6th International Conference on Telecommunications in Modern Satellite, Cable and Broadcasting Service, 2003. TELSIKS 2003., Nis, Yugoslavia*, pp. P-III–P-X, 2003.
- [40] Y. Ding and K. Wu, "Coaxial End-Launch and Microstrip to Partial H-Plane Waveguide Transitions," *IEEE Trans. Microw. Theory Tech.*, vol. 63, no. 10, pp. 3103–3108, Oct. 2015.
- [41] F. Xu and K. Wu, "Guided-wave and Leakage Characteristics of Substrate Integrated Waveguide," *IEEE Trans. Microw. Theory Tech.*, vol. 53, no. 1, pp. 66–73, Jan. 2005.
- [42] A. A Khan and M. K. Mandal, "Miniaturized Substrate Integrated Waveguide (SIW) Power Dividers," *IEEE Microw. Wireless Compon. Lett.*, vol. 26, no. 11, pp. 888–132, Nov. 2016.
- [43] Y. Huang and K. L. Wu, "A Broadband LTCC Integrated Transition of Laminated Waveguide to AirFilled Waveguide for Millimeter Wave Applications," *IEEE Trans. Microw. Theory Tech.*, vol. 51, no. 5, pp. 1613–1617, May 2003.
- [44] L. Xia, R. Xu, B. Yan, J. Li, Y. Guo, and J. Wang, "Broadband Transition between Air-Filled Waveguide and Substrate Integrated Waveguide," *Electron. Lett.*, vol. 42, no. 24, pp. 1403–1405, Nov. 2006.
- [45] L. Li, X. P. Chen, R. Khazaka, and K. Wu, "A Transition from Substrate Integrated Waveguide (SIW) to Rectangular Waveguide," *Proc. Asia Pacific Microw. Conf.*, pp. 2605–2608, 2009.
- [46] R. Gogowski, J. F. Zürcher, C. Peixeiro and J. R. Mosig, "Broadband Ka-Band Rectangular Waveguide to Substrate Integrated Waveguide Transition," *Electron. Lett.*, vol. 49, no. 9, Apr. 2013.
- [47] April 2013, pp. 602-604. 9. Y. Li and K. M. Luk, "A Broadband V-Band Rectangular Waveguide to Substrate Integrated Waveguide Transition," *IEEE Microw. Wireless Compon. Lett.*, vol. 24, no. 9, pp. 590-592, Sept. 2014.

## LITERATURE REVIEW

---

- [48] C. Li, D. Wu and K. Seo, "Rectangle Waveguide to Substrate Integrated Waveguide Transition and Power Divider," *Microwave and Optical Technology Letters*, vol. 52, no. 2, pp. 375-378, Feb. 2010.
- [49] H. Jin, W. Chen and G. Wen, "Broadband Transition between Waveguide and Substrate Integrated Waveguide based on Quasi-Yagi Antenna," *Electron. Lett.*, vol. 48, no. 7, pp. 355-356, Mar. 2012.
- [50] W. Dou and T. Li, "Broadband Right-Angle Transition from Substrate-Integrated Waveguide to Rectangular Waveguide," *Electron. Lett.*, vol. 50, no. 19, pp. 1355-1356, Sept. 2014.
- [51] X. Huang and K. L. Wu, "A Ka-Band Broadband Integrated Transition of Air-Filled Waveguide to Laminated Waveguide," *IEEE Microw. Wireless Compon. Lett.*, vol. 22, no. 20, pp. 515-517, Oct. 2012.
- [52] D. Dousset, K. Wu and S. Claude, "Millimetre-Wave Broadband Transition of Substrate-Integrated Waveguide to Rectangular Waveguide," *Electron. Lett.*, vol. 46, no. 24, pp. 1610-1611, Nov. 2010.
- [53] Z. Li, X. P. Chen and K. Wu, "A Surface Mountable Pyramidal Horn Antenna and Transition to Substrate Integrated Waveguide," *International Symposium on Signals, Systems and Electronics*, pp. 607-610, 2007.
- [54] J. L. Cano, A. Mediavilla and A. R. Perez, "Full-Band Air-Filled Waveguide-to-Substrate Integrated Waveguide (SIW) Direct Transition," *IEEE Microw. Wireless Compon. Lett.*, vol. 25, no. 2, pp. 79-81, Feb. 2015.
- [55] H. Lee, S. Yun, M. Uhm and I. Yom, "Full-Band Transition from Substrate Integrated Waveguide to Rectangular Waveguide," *Electron. Lett.*, vol. 51, no. 14, pp. 1089-1090, July 2015.
- [56] C. Rave and A. F. Jacob, "A Design Approach for Tapered Waveguide to Substrate-Integrated Waveguide Transitions," *IEEE Trans. Microw. Theory Tech.*, vol. 64, no. 8, pp. 2502-2510, Aug. 2003.
- [57] D. Deslandes and K. Wu, "Integrated Microstrip and Rectangular Waveguide in Planar Form," *IEEE Microw. Wireless Compon. Lett.*, vol. 11, no. 2, pp. 68-70, Feb. 2001.
- [58] D. Deslandes, "Design Equations for tapered microstrip-to-Substrate Integrated Waveguide Transitions," in *IEEE MTT-S Int. Microwave Symp. Dig.*, pp. 704-707, 2010.
- [59] Z. Kordiboroujeni and J. Bornemann, "New Wideband Transition from Microstrip Line to Substrate Integrated Waveguide," *IEEE Trans. Microw. Theory Tech.*, vol. 62, no. 12, pp. 2983-2989, Dec. 2014.
- [60] S. T. Choi, K. S. Yang, K. Tokuda and Y. H. Kim, "A V-band Planar Narrow Bandpass Filter Using a New Type Integrated Waveguide Transition," *IEEE Microw. Wireless Compon. Lett.*, vol. 14, no. 12, pp. 545-547, Dec. 2004.
- [61] Y. Ding and K. Wu, "Substrate Integrated Waveguide-to-Microstrip Transition in Multilayer Substrate," *IEEE Trans. Microw. Theory Tech.*, vol. 55, no. 12, pp. 2839-2844, Dec. 2007.
- [62] T. Kai, Y. Katou, J. Hirokawa, M. Ando, H. Nakano and Y. Hirachi, "A coaxial line to post-wall waveguide transition for a cost-effective transformer between a RF device and a planer slot array in 60 GHz band," *IEICE Trans. Commun.*, vol. E89-B, no. 5, pp. 1646-1653, May 2006.

## LITERATURE REVIEW

---

- [63] A. Morini, M. Farina, C. Cellini, T. Rozzi, G. Venanzoni, "Design of low-cost non-radiative SMA-SIW launchers," in *Proc. 36th Eur. Microw. Conf. (EuMC)*, Manchester, UK, pp. 526-529, Sept. 2006.
- [64] E. Arnieri, G. Amendola, L. Boccia and G. D. Massa, "Coaxially fed substrate integrated radiating waveguides," in *Proc. Int. Symp. Ant. Propag.*, pp. 2718- 2721, June 2007.
- [65] S. Mukherjee, P. Chongder, K. V. Srivastava, A. Biswas, "Design of a broadband coaxial to substrate integrated waveguide (SIW) transition," in *Proc. Asia-Pacific. Microwave Conference*, pp. 896-898, Nov. 2013.
- [66] A.A. Khan and M. K. Mandal, "A compact broadband direct coaxial line to SIW transition," *IEEE Microw. Wireless Compon. Lett.*, vol. 26, no. 11, pp. 894- 896, Nov. 2016.
- [67] A.A. Khan, M.K. Mandal, and R. Shaw, "A compact and wideband SMA connector to empty substrate integrated waveguide (ESIW) transition," in *IEEE MTT-S Int. Microwave RF Conf.*, 2015, pp. 246–248, 2015.
- [68] D. Deslandes and K. Wu, "Integrated Transition of Coplanar to Rectangular Waveguides," in *IEEE MTT Symp. Dig.*, 2, Phoenix, AZ, 2001, pp. 619–622, 2001.
- [69] D. Deslandes and K. Wu, "Analysis and design of current probe transition from grounded coplanar to substrate integrated rectangular waveguides," *IEEE Trans. Microw. Theory Tech.*, vol. 53, no. 8, pp. 2487-2494, Aug. 2005.
- [70] S. H. Lee, S. W. Jung, and H. -Y. Lee, "Ultra-Wideband CPW-to-substrate integrated waveguide transition using an elevated-CPW section," *IEEE Microw. Wireless Compon. Lett.*, vol. 18, no. 11, pp. 746– 748, Nov. 2008.
- [71] R.Y. Fang, C.F. Liu and C.L. Wang, "Compact and Broadband CB-CPW-to-SIW Transition Using Stepped Impedance Resonator With 90°-Bent Slot," *IEEE Trans. Comp. Pack. Manufac. Tech.*, vol. 3, no. 2, pp. 247-252, Feb. 2013.
- [72] J. Zhou, K. A. Morris and M. J. Lancaster, "General Design of Multiway Multisection Power Dividers by Interconnecting Two-Way Dividers," *IEEE Trans. Microw. Theory Techn.*, vol. 55, no. 10, pp. 2208-2215, Oct. 2007.
- [73] K. Song and Q. Xue, "Planar Probe Coaxial-Waveguide Power Combiner/Divider," *IEEE Trans. Microw. Theory Techn.*, vol. 57, no. 11, pp. 2761-2767, Nov. 2009.
- [74] C. Sun and J. Li, "Design of planar multi-way differential power division network using double-sided parallel stripline," *Electron. Lett.*, vol. 53, no. 20, pp. 1364-1366, 2017.
- [75] T. Yu and J. Tsai, "Design of multiway power dividers including all connecting lines," *IET Microwaves, Antennas & Propagation*, vol. 12, no. 8, pp. 1367-1374, July 2018.
- [76] S. Germain, D. Deslandes and K. Wu, "Development of substrate integrated waveguide power dividers", in *Proc. IEEE Canadian Conf. Electrical Computer Engineering (CCECE'03)*, vol. 3, pp. 1921-1924, May 2003.
- [77] A. Akbarzadeh and Z. Shen, "Waveguide power dividers using multiple posts," *Microw. Opt. Technol. Lett.*, vol. 50, no. 4, pp. 981-984, Apr. 2008.

## LITERATURE REVIEW

---

- [78] T. Li and W. Dou, "Broadband substrate-integrated waveguide T-junction with arbitrary power-dividing ratio," *Electron. Lett.*, vol. 51, no. 3, pp. 259-260, Feb. 2015.
- [79] Y. M. Huang et al., "Substrate-Integrated Waveguide Power Combiner/Divider Incorporating Absorbing Material," *IEEE Microw. Wireless Compon. Lett.*, vol. 27, no. 10, pp. 885-887, Oct. 2017.
- [80] A. Suntives, N. Smith and R. Abhari, "Analytical design of a half-mode substrate integrated waveguide Wilkinson power divider," *Microw. Opt. Technol. Lett.*, vol. 52, no. 5, pp. 1066-1069, May 2010.
- [81] Y. Zhou et al., "Slow-Wave Half-Mode Substrate Integrated Waveguide 3-dB Wilkinson Power Divider/Combiner Incorporating Nonperiodic Patterning," *IEEE Microw. Wireless Compon. Lett.*, vol. 28, no. 9, pp. 765-767, Sept. 2018.
- [82] T. Djerafi, D. Hammou, K. Wu and S. O. Tatu, "Ring-Shaped Substrate Integrated Waveguide Wilkinson Power Dividers/Combiners," *IEEE Trans. Compon. Packag. Manuf. Technol.*, vol. 4, no. 9, pp. 1461-1469, Sept. 2014.
- [83] K. Song et al., "Ka-Band Rectangular-Waveguide Gysel Power Divider with Low Insertion Loss and High Output Isolation," *Journal of Infrared, Millimeter, and Terahertz Waves*, vol. 39, pp. 996-1004, July 2018.
- [84] H. Chen, W. Che, X. Wang and W. Feng, "Size-Reduced Planar and Nonplanar SIW Gysel Power Divider Based on Low Temperature Co-fired Ceramic Technology," *IEEE Microw. Wireless Compon. Lett.*, vol. 27, no. 12, pp. 1065-1067, Dec. 2017.
- [85] H. Chen, X. Wang, W. Che, Y. Zhou and Q. Xue, "Development of Compact HMSIW Gysel Power Dividers With Microstrip Isolation Networks," *IEEE Access*, vol. 6, pp. 60429-60437, Oct. 2018.
- [86] Y. Wang, C. Zhou, K. Zhou and W. Wu, "Compact dual-band filtering power divider based on SIW triangular cavities," *Electron. Lett.*, vol. 54, no. 18, pp. 1072-1074, Aug. 2018.
- [87] A. R. Moznebi et al., "Compact filtering power divider based on corrugated third-mode circular SIW cavities," *Microw. Opt. Technol. Lett.*, vol. 62, no. 5, pp. 1900-1905, Jan. 2020.
- [88] Z. C. Hao, W. Hong and K. Wu, "Multiway broadband substrate integrated waveguide (SIW) power divider," in *Proc. IEEE Int. Symp. Antennas Propagation*, pp. 639-642, July 2005.
- [89] R. Kazemi, R. Sadeghzadeh and A. E Fathy, "Design of a wide band eight-way compact SIW power combiner fed by a low loss GCPWTO-SIW transition," *Progress In Electromagnetics Research C*, vol. 26, pp. 97-110, 2012.
- [90] S. Contreras & A. Peden, "Graphical design method for unequal power dividers based on phase-balanced SIW tee-junctions," *International Journal of Microwave and Wireless Technologies*, vol. 5, no. 5, pp. 603-610, Oct. 2013.
- [91] R. Kazemi and A. E. Fathy, "Design of a wideband eight-way single ridge substrate integrated waveguide power divider," *IET Microw. Antennas Propag.*, vol. 9, no. 7, pp. 648-656, Jul. 2015.



## LITERATURE REVIEW

---

- [92] Z. Hao, M. He, K. Fan and G. Luo, "A Planar Broadband Antenna for the E-Band Gigabyte Wireless Communication," *IEEE Trans. Antennas Propag.*, vol. 65, no. 3, pp. 1369-1373, Mar. 2017.
- [93] W. Mazhar, D. Klymyshyn, A. Qureshi, "Design and analysis of wideband eight-way SIW power splitter for mm-wave applications," *International Journal of RF and Microwave Computer-Aided Engineering*, vol. 28, no. 2, Feb. 2018.
- [94] Y. Wu, Z. Hao and Z. Miao, "A Planar W-Band Large-Scale High-Gain Substrate-Integrated Waveguide Slot Array," *IEEE Trans. Antennas Propag.*, vol. 68, no. 8, Aug. 2020.
- [95] G. Li, K. Song, F. Zhang and Y. Zhu, "Novel Four-Way Multilayer SIW Power Divider With Slot Coupling Structure," *IEEE Microw. Wireless Compon. Lett.*, vol. 25, no. 12, pp. 799-801, Dec. 2015.
- [96] K. Song, W. Lu, S. Guo and Y. Fan, "Four-way hybrid SIW/microstrip-line power divider with improved output isolation," *Electron. Lett.*, vol. 55, no. 1, pp. 36-38, 10 01 2019.
- [97] K. Song, F. Xia, Y. Zhou, S. Guo and Y. Fan, "Microstrip/Slotline-Coupling Substrate Integrated Waveguide Power Divider With High Output Isolation," *IEEE Microw. Wireless Compon. Lett.*, vol. 29, no. 2, pp. 95-97, Feb. 2019.
- [98] T. Djerafi, A. Patrovsky, K. Wu and S. O. Tatu, "Recombinant Waveguide Power Divider," *IEEE Trans. Microw. Theory Techn.*, vol. 61, no. 11, pp. 3884-3891, Nov. 2013.
- [99] D. Deslandes and K. Wu, "Design considerations and performance analysis of substrate integrated waveguide components," in *Proc. Eur. Microw. Conf.*, pp. 881-884, Sep. 2002.
- [100] M. Bozzi, M. Pasian, L. Perregini, & K. Wu, "On the losses in substrate-integrated waveguides and cavities," *International Journal of Microwave and Wireless Technologies*, vol. 1, no. 5, pp. 395-401, Oct. 2009.
- [101] B. Liu, W. Hong, L. Tian, H.-B. Zhu, W. Jiang and K. Wu, "Half mode substrate integrated waveguide (HMSIW) multi-way power divider", in *Proc. Asia-Pacific Microw. Conf.*, pp. 917-920, Dec. 2006.
- [102] D. Eom, J. Byun and H. Lee, "Multilayer Substrate Integrated Waveguide Four-Way Out-of-Phase Power Divider," *IEEE Trans. Microw. Theory Techn.*, vol. 57, no. 12, pp. 3469-3476, Dec. 2009.
- [103] X. Zou, C. -M. Tong and D. -W. Yu, "Y-junction power divider based on substrate integrated waveguide," *Electron. Lett.*, vol. 47, no. 25, pp. 1375-1376, Dec. 2011.
- [104] O. Kiris, V. Akan, M. Gokten and L. Kuzu, "Implementation of three-way power divider based on substrate integrated waveguide", *USNC-URSI Radio Science Meeting (Joint with AP-S Symposium) 2017*, pp. 111-112, 2017.
- [105] Q. Chen and J. Xu, "Out-of-phase power divider based on two-layer SIW," *Electron. Lett.*, vol. 50, no. 14, pp. 1005-1007, July 2014.
- [106] K. Song, L. Xue, G. Li, M. Fan & Y. Fan, "Novel Four-Way Slotted-Substrate Integrated Waveguide Power Divider Using Identical Coupling Circuits," *Electromagnetics*, vol.37, no. 4, 233-239, May 2017.

## LITERATURE REVIEW

---

- [107] Z. Li, J. Li, Y. Huang, and G. Wen, "W-Band SIW Power Combiner/Divider Based on the Antipodal Fin-Line SIW-RW Transition and Longitudinal-Slot Coupling Techniques," *Progress In Electromagnetics Research C*, Vol. 72, 43-54, 2017.
- [108] H. Jin, G. Q. Luo, W. Wang, W. Che and K. Chin, "Integration Design of Millimeter-Wave Filtering Patch Antenna Array With SIW Four-Way Anti-Phase Filtering Power Divider," *IEEE Access*, vol. 7, pp. 49804-49812, 2019.
- [109] K. Song, F. Zhang, F. Chen & Y. Fan, "Wideband millimetrewave four-way spatial power combiner based on multilayer SIW," *Journal of Electromagnetic Waves and Applications*, vol. 27, no. 13, pp. 1715-1719, Aug. 2013.
- [110] K. Song, F. Chen, F. Zhang & Y. Fan, "Ka-Band Four-Way Power Combiner Based on Multi-layer Substrate Integrated Waveguide," *Wireless Personal Communications*, vol. 79, pp. 1703-1711, Oct. 2014.
- [111] Ning Yang, C. Caloz and Ke Wu, "Substrate integrated waveguide power divider based on multimode interference imaging," *2008 IEEE MTT-S International Microwave Symposium Digest, Atlanta, GA, USA, 2008*, pp. 883-886, Sept. 2008.
- [112] F. Zhang, K. Song and Y. Fan, "Diffraction Field Reconstruction in Millimeter-Wave SIW Ten-Way Power Divider by Shape Optimization Technology," *IEEE Plasma Sci.*, vol. 45, no. 12, pp. 3177-3181, Dec. 2017.
- [113] M. Salehi, J. Bornemann and E. Mehrshahi, "Wideband Substrate-Integrated Waveguide Six-Port Power Divider/Combiner," *Microw. Opt. Technol. Lett.*, vol. 55, no. 12, pp. 2984-2986, Dec. 2013.
- [114] Z. Liu and G. Xiao, "New multi-way SIW power dividers with high isolation," in *Proceedings of Asia-Pacific Microwave Conference*, pp. 702-704, 2014.
- [115] G. Venanzoni et al., "Compact substrate integrated waveguide six-port directional coupler for X-band applications," *Microw. Opt. Technol. Lett.*, vol. 57, no. 11, pp. 2589-2592, Nov. 2015.
- [116] Z. Liu and G. Xiao, "Design of SIW-Based Multi-Aperture Couplers Using Ray Tracing Method," *IEEE Trans. Compon. Packag. Manuf. Technol.*, vol. 7, no. 1, pp. 106-113, Jan. 2017.
- [117] S. Karamzadeh, V. Rafei, and H. Saygin, "A New Multi-Functional Half Mode Substrate Integrated Waveguide Six-Port Microwave Component," *Progress In Electromagnetics Research Letters*, Vol. 69, 71-78, 2017.
- [118] K. Song and Y. Fan, "Broadband travelling-wave power divider based on substrate integrated rectangular waveguide," *Electron. Lett.*, vol. 45, no. 12, pp. 631-632, June 2009.
- [119] K. Song et al., "Broadband six-way out-of-phase SIW power divider," *International Journal of Microwave and Wireless Technologies*, vol. 8, no. 2, pp. 165-170, Mar. 2016.
- [120] J. Huang et al., "A New Compact and High Gain Circularly-Polarized Slot Antenna Array for Ku-Band Mobile Satellite TV Reception," *IEEE Access*, vol. 5, pp. 6707-6714, 2017.
- [121] B. Feng, J. Lai, K. L. Chung, T. Chen, Y. Liu and C. Sim, "Communication A Compact Wideband Circularly Polarized Magneto-Electric Dipole Antenna Array for 5G Millimeter-Wave Applications," *IEEE Trans. Antennas Propag.*, vol. 68, no. 9, Sept. 2020.

## LITERATURE REVIEW

---

- [122] K. Y. Kapusuz, S. Lemey and H. Rogier, "Substrate-Independent Microwave Components in Substrate Integrated Waveguide Technology for High-Performance Smart Surfaces," *IEEE Trans. Microw. Theory Techn.*, vol. 66, no. 6, pp. 3036-3047, June 2018.
- [123] A. A. Khan and M. K. Mandal, "Miniaturized Substrate Integrated Waveguide (SIW) Power Dividers," *IEEE Microw. Wireless Compon. Lett.*, vol. 26, no. 11, pp. 888-890, Nov. 2016.
- [124] A. Moznebi, K. Afrooz, M. Danaeian and P. Mousavi, "Four-Way Filtering Power Divider Using SIW and Eighth-Mode SIW Cavities With Ultrawide Out-of-Band Rejection," *IEEE Microw. Wireless Compon. Lett.*, vol. 29, no. 9, pp. 586-588, Sept. 2019.
- [125] M. Yang, J. Wang, X. Wang and W. Wu, "Design of wideband four-way filtering power divider based on SIW loaded square patch resonator," *Electron. Lett.*, vol. 55, no. 7, pp. 389-391, Apr. 2019.
- [126] A. Moznebi, M. Danaeian, E. Zarezadeh and K. Afrooz, "Ultracompact two-way and four-way SIW/HMSIW power dividers loaded by complementary split-ring resonators," *International Journal of RF and Microwave Computer-Aided Engineering*, vol. 29, no. 10, 2019.
- [127] K. Song, Y. Fan and Y. Zhang, "Radial cavity power divider based on substrate integrated waveguide technology," *Electron. Lett.*, vol. 42, no. 19, pp. 1100-1101, Sept. 2006.
- [128] K. Song, Y. Fan and Y. Zhang, "Design of Low-Profile Millimeter-Wave Substrate Integrated Waveguide Power Divider/Combiner," *International Journal of Infrared and Millimeter Waves*, vol. 28, pp. 473-478, 2007.
- [129] K. Song, Y. Fan and Y. Zhang, "Eight-Way Substrate Integrated Waveguide Power Divider with Low Insertion Loss," *IEEE Trans. Microw. Theory Techn.*, vol. 56, no. 6, pp. 1473-1477, June 2008.
- [130] Y. -p. Hong, Y. -j. An and J. -g. Yook, "Differential radial power combiner using substrate integrated waveguide," *Electron. Lett.*, vol. 46, no. 24, pp. 1607-1608, Nov. 2010.
- [131] D. -. Lee, Y. -. An and J. -. Yook, "An Eight-Way Radial Switch Based on SIW Power Divider," *Journal of Electromagnetic Engineering And Science*, vol. 12, no. 3, pp. 216-222, Sep. 2012.
- [132] K. Song et al., "Broadband Eight-Way Differential SIW Power Divider with Bandpass-Filtering Response Using Novel Hybrid Multiple-via Probe and Multiple Radial Slots," *Wireless Personal Communications*, vol. 78, pp- 1103-1114, 2014.
- [133] C. Rave and A. F. Jacob, "A wideband radial substrate integrated power divider at K-band," in *Proc. German Microw. Conf.*, pp. 84-87, Mar. 2015.
- [134] A. P. Saghati, A. Pourghorban Saghati and K. Entesari, "A SIW Uniform Circular Antenna Array for 5G Applications Fed by a Radially-symmetric Eight-way SIW Power Divider," *Proc. IEEE International Symposium on Antennas and Propagation and USNC-URSI Radio Science Meeting*, pp. 1343-1344, 2019.
- [135] K. Song, Y. Chen, T. Kong and Y. Fan, "Broadband Eight-Way Substrate Integrated Waveguide Radial Power Divider/Combiner With High-Isolation," *IEEE Access*, vol. 8, pp. 69268-69272, 2020.

# CHAPTER 3

## ***SIW THEORETICAL CONCEPTS AND TRANSITIONS***

---

### **3.1 Objective**

To understand the basic SIW theory and analyze the design of a Substrate Integrated Waveguide (SIW) for proper operation in circuits. Various transitions between SIW and other technologies are also studied. Simulation based investigations are carried out to design compact transitions between a SIW and microstrip, waveguide and an empty substrate integrated waveguide (ESIW), respectively, to efficiently transfer power from one transmission line to the other through proper matching of impedances and fields between the two lines. These approaches may be useful in the substrate integrated circuit (SIC) technology.

### **3.2 Introduction to SIW**

In the past few decades, a rapid progress in the microwave and millimeter wave components at higher frequency range having desired performances is reported. The increased research interest is mainly due to the availability of high frequency simulation softwares (with advantages of faster iterations of accurate design models), precision fabrication techniques and advancements in planar structures. The wireless and communication systems having microwave and millimeter wave components, like power

## SIW THEORETICAL CONCEPTS AND TRANSITIONS

---

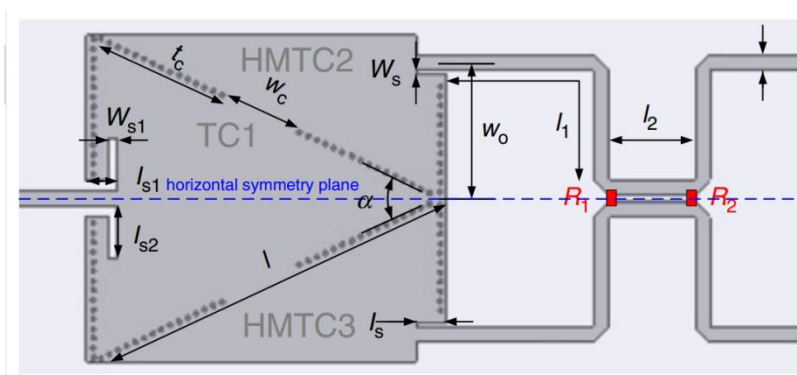
dividers, couplers, filters, antennas etc, thus find its usage in various industrial, scientific and medical applications.

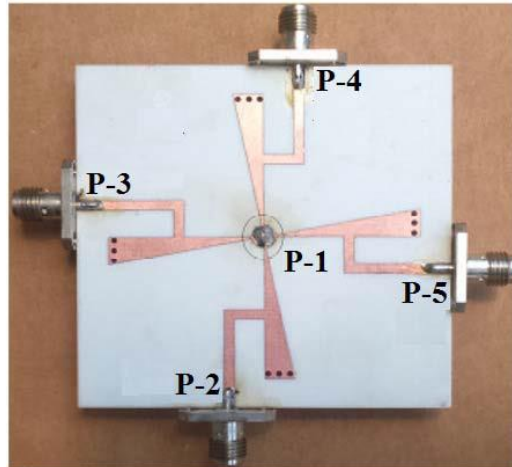
Till now, high performance microwave and millimeter wave components in various technologies are developed. The earliest transmission line technology to design such components is waveguide. Waveguide is known to present lower losses. It can handle high power and has a higher quality factor. But, the technology is however bulky, complex, expensive and face difficulty in the integration with other non-planar structures. To overcome the problems faced by waveguides, planar circuit technology is developed in the later stage. Some of the common planar structures include microstrip, coplanar waveguide and stripline. But, they are lossy and have lower Q- Factor.

In the last ten years, a lot of research is carried out in developing transmission line technologies which could fill in the technology gap. One such emerging technology is the Substrate Integrated Waveguide (SIW), which is first introduced in 1998 [1],[2]. SIW is a substrate based transmission line, which has metallic via holes drilled in a standard printed circuit board (PCB), which connects the top and bottom conductors [3]. The via-holes are arranged in an array on both the sides and act as the side wall of the waveguide in the substrate itself. The SIW combine the advantages of both waveguide and planar circuits [4].

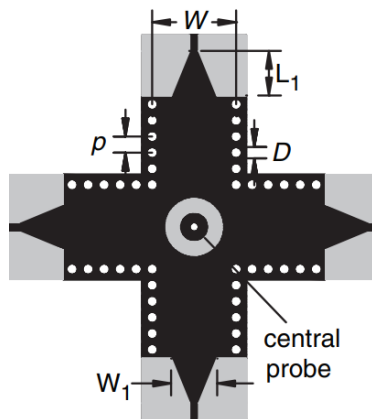
The SIW inherits a lot of properties from the waveguide due to the construction of the sidewalls and thus, it can handle power at higher frequencies [5],[6]. It presents lower loss and also has a higher quality factor [7]. Planar SIW is light weight, simple and

## SIW THEORETICAL CONCEPTS AND TRANSITIONS





(b)



(c)

Fig. 3.1. SIW power dividers: (a) 2-way dual band [20], (b) 4-way [21], (c) 4-way broadband [22]

### 3.3. Construction of an SIW

#### 3.3.1. Basic Geometry of an SIW

The basic geometry of a substrate integrated waveguide is similar to a rectangular waveguide which is filled with a dielectric [23]. Unlike waveguides, SIW is constructed using the standard PCB fabrication process, used for microstrip and this reduces the

## SIW THEORETICAL CONCEPTS AND TRANSITIONS

height of an SIW drastically to that of the substrate thickness. The two metallic broad walls of the rectangular waveguide are substituted with deposition of copper sheets on each side of the substrate. The narrow walls of the waveguide are replaced by an array of periodically placed metallic vias which are drilled through the substrate. Alternatively, the sidewalls can be realized using techniques of sputtering copper on laser cut troughs in the substrate, as well. Fig. 3.2 shows the basic structure of a substrate integrated waveguide (SIW) along with the geometric parameters for via diameter, via spacing, SIW's physical width, substrate height as:  $d$ ,  $s$ ,  $w$  and  $h$ , respectively.

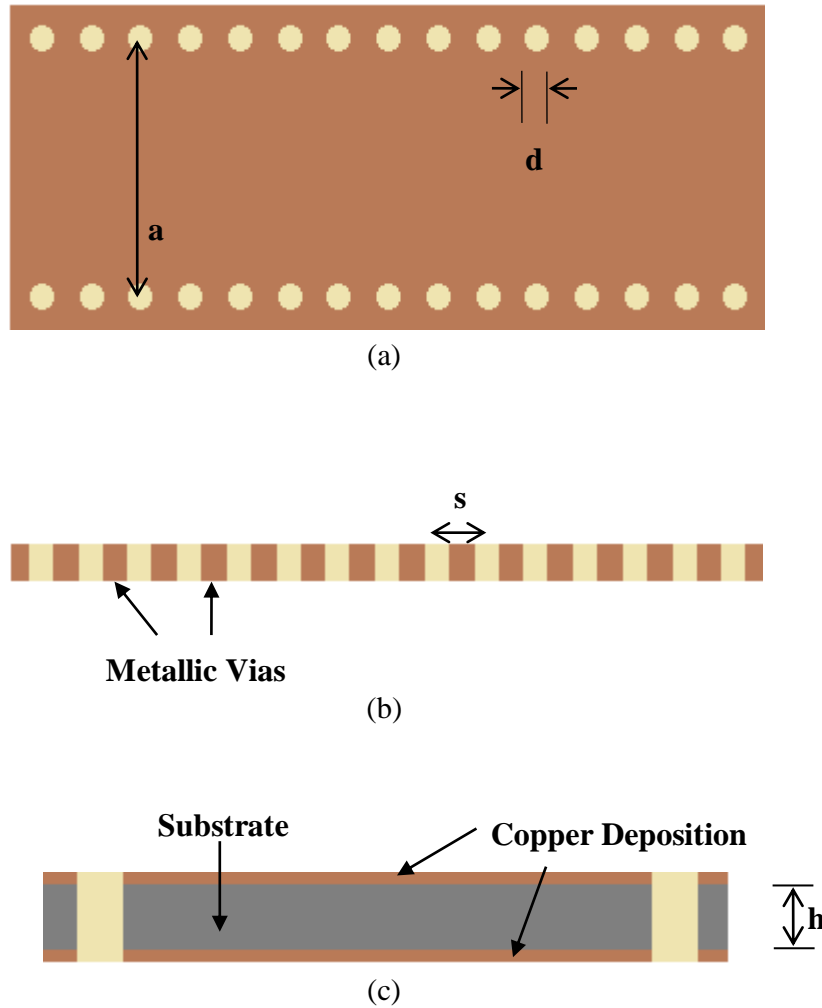


Fig. 3.2. (a) Top View of an SIW, (b) Side View of an SIW, (c) Front View of an SIW



### 3.3.2. Construction Parameters of an SIW

Since, substrate integrated waveguides are the planar realization of a dielectric filled metallic rectangular waveguides, it has an inherit cut-off frequency. Any signal having a frequency below this cut-off frequency will not propagate through the SIW. The width of the SIW determines the cut-off frequency of the dominant mode. Just like a waveguide, the width of an SIW is the distance between the two metallic via rows, measured from the center of the metallic via in each row.

The other important construction parameter of an SIW is its metallic via sidewall. During the design of an SIW, the metallic vias are placed appropriately, all with the same diameter, in order to support guide wave propagation with minimized radiation loss. It is the spacing between the vias that limits the amount of leakage of field outside the waveguide. Placing the vias too far apart from each other leads to compromised isolation. If the spacing between the vias are close enough, the two arrays becomes equivalent to electric walls for the electromagnetic waves propagating in the SIW.

$$a_{eqv} = a - 1.08 \cdot \frac{d^2}{s} + 0.1 \cdot \frac{d^2}{a} \quad (3.1)$$

The equivalent width of an SIW  $a_{eqv}$  is the width of a dielectric field waveguide having the same dominant mode cut-off frequency as the substrate integrated waveguide having width  $a$ . The width of an SIW and a dielectric filled rectangular waveguide is nearly identical if the correction factor is taken into account. This correction factor [24] is reflected in equation (3.1) and thus presents a relation between the equivalent width of an

SIW  $a_{eqv}$  and the other design parameters of an SIW, like  $d$ ,  $p$  and  $a$ , where  $d$  is the diameter of the metallic via and  $p$  is the space between the vias. The cut-off frequency  $f_c$  of a dielectric filled rectangular SIW having width  $a_{eqv}$  and height  $h$ , can be calculated from equation (3.2).

$$f_c = \frac{c}{2\pi\sqrt{\epsilon_r}} \sqrt{\left(\frac{m\pi}{w_{eqv}}\right)^2 + \left(\frac{n\pi}{h}\right)^2} \quad (3.2)$$

### 3.3.3. Design Procedures of an SIW

It can be viewed from equation (3.1), that by proper adjustment of the periodicity of the metallic via arrays, the diameter of the metallic via and the width of the SIW, we can reduce the leakage losses for the operating frequency and bandwidth.

When the diameter of the metallic via  $d$  is increased, the space between the vias  $p$  should be decreased in order to reduce the leakage loss. However, when the value of  $d/a$  is more, larger  $d$  and smaller  $p$  will cause the dispersion characteristics of an SIW to degrade. Thus, from equation (3.1), it is understood that the ratios  $p/d$  and  $d/a$  should be as small as possible. It is suggested to follow a design rule where  $p/d$  is less than 2.0 and  $d/a$  is less than 1.5 for better dispersion characteristics and lower leakage loss.

The design procedure is as follows [24]:

- Step 1) Select  $p/d$  less than 2.0.
- Step 2) Select  $d/a$  less than 1.5.
- Step 3) Calculate  $a_{eqv}$  based on the cut-off frequency defined in equation (3.2).
- Step 4) Calculate  $a$  from equation (3.1).
- Step 5) Calculate  $d$  and  $p$  from  $p/d$  and  $d/a$ .

### 3.4. Field configuration of an SIW

Conventional rectangular waveguides support both transverse electric ( $TE$ ) modes and transverse magnetic ( $TM$ ) modes. The transverse electric ( $TE$ ) modes have no electric field components in the direction of propagation, while the transverse magnetic ( $TM$ ) mode is mode of propagation when there is no longitudinal component of the electric field and have no magnetic field in the direction of propagation. Hence, the magnetic fields are transverse to the direction of propagation in  $TM$  mode. Similarly, for transverse electric modes, there is no longitudinal component of the magnetic field and have no electric field in the direction of propagation. The electric fields are thus transverse to the direction of propagation in  $TE$  mode. The transverse electric and transverse magnetic fields in a waveguide are denoted by  $TE_{mn}$  and  $TM_{mn}$ , respectively, where  $m$  and  $n$  are the mode numbers. Mode number  $m$  represent the sinusoidal half-wave variation in the  $x$ -direction and the mode number  $n$  represents the sinusoidal half-wave variation in the  $y$ -direction. By calculating the half sinusoidal variations of the fields and considering the cross-section of the waveguide, the field distribution patterns are identified. The propagation of the modes are independent without any coupling between them, which means they are orthogonal to each other. The boundary conditions, width and the height of the uniform waveguide structure, defines the number of half modes, independent of the operating frequency of the waveguide.

One of the major difference between an SIW and a rectangular waveguide lies in the surface current. In the case of transverse magnetic mode propagation, longitudinal surface currents propagate along the narrow walls. Similarly, for  $TE_{mn}$  transverse electric mode

## SIW THEORETICAL CONCEPTS AND TRANSITIONS

propagation, where  $n \neq 0$ , longitudinal narrow wall surface currents propagate for efficient propagation. Now, if the standard waveguide is modified to a structure having vertical slits on its narrow walls, then it will become a waveguide with discontinuous side walls. In case of  $TM$  and  $TE_{mn}$ , where  $n \neq 0$ , mode of propagation, the vertical slits will cut through the longitudinal surface currents along the side walls. This will produce a large amount of radiation through the narrow wall. Similarly, for an SIW, which has discontinuous narrow walls realized by the row of metallic vias, there will be a considerable amount of radiation through the spacing between the vias, when it will be trying to propagate  $TM$  and  $TE_{mn}$  modes, where  $n \neq Z$ . It is essential to establish a conducting connection between the metalized vias to preserve the longitudinal currents along it for the propagation of  $TM$  and  $TE_{mn}$ , where  $n \neq 0$ , modes. Substrate integrated waveguides, thus, support only transverse electric modes with no sinusoidal half-wave variation in the  $y$ -direction, i.e.,  $TE_{m0}$  modes and as a result, the first mode called dominant mode is the  $TE_{10}$  mode. Fig. 3.3 shows the surface currents for the dominant  $TE_{10}$  mode for an SIW which has its metalized via side walls replaced by solid conducting walls with vertical slits.

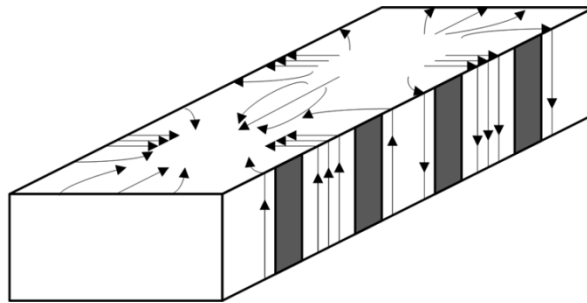


Fig. 3.3.  $TE_{10}$  mode surface current distribution on an SIW. The metalized via holes are replaced with narrow slot openings on the side wall [24].

It can be thus observed that in waveguides, the surface currents circulate freely in any direction along the sidewall. But, in the case of an SIW, the current flow is limited to vertical direction along the sidewall. Due to the periodically spacing of the via holes, the narrow wall longitudinal current component cannot circulate alongside the SIW across each regular interval for  $TM$  and  $TE_{mn}$  modes, where  $n \neq 0$ . SIW allows propagation of vertical and longitudinal surface currents along the side walls.

### 3.5. Losses in an SIW

Just like, substrate integrated waveguide preserves the well known advantages of both rectangular waveguides and planar structure, it also suffers from losses. In an SIW, there are three major loss mechanisms [25]. First, the ohmic losses, which it inherits from the standard metallic waveguide. The second loss is the dielectric loss, though this is avoided in air filled metallic waveguides but, it is present in any substrate based planar circuits. Last but not the least is the radiation losses, which are very much prevalent in planar circuits due to lack of shielding. The major issue in the application of SIWs to the design of microwave and millimeter-wave components is related to these losses.

Both, SIW and standard waveguides being similar metallic structures, they exhibit ohmic losses due to the presence of the conductor in the metal broad and narrow walls. Ohmic losses depends on the height of the structure and the conductivity of the metal. The conductor losses are lower if the SIW is of a more thickness. This is because, with height the power handling capability of the SIW increases. Since, SIW is a planar structure and is based on PCB substrates, it suffers from dielectric losses due to the loss tangent of the

## SIW THEORETICAL CONCEPTS AND TRANSITIONS

---

dielectric material present in the chosen PCB board. Dielectric losses are disadvantageous to not only planar structures but, to non planar dielectric filled waveguides as well. It is dependent on the substrate thickness and width. In an SIW structure, the dielectric is confined between the top and bottom copper sheets and the two arrays of metallic vias. If the area of the dielectric increases, it will be storing more energy and this energy will be transformed into heat, thus producing loss. Radiation loss can occur when the conditions on the diameter and the spacing between two vias are not fulfilled. Since, other planar structures are not shielded, they present more radiation losses, but in comparison to waveguides, due to the presence of discontinuity in the narrow walls of an SIW, the shielding is lower and thus produces radiation losses. These are the primary losses that SIW suffers from and during the design of any SIW component they are taken into consideration.

In [26], the three main loss mechanisms are separately investigated. It states that the power  $P(z)$  flowing through a section  $z$  can be denoted by the following equation.

$$P(z) = P(0)e^{-2\alpha z} \quad (3.3)$$

where,  $\alpha$  denotes the overall attenuation constant. Now, if the losses are reasonably small, the overall attenuation constant would be a sum of all the other losses as shown in equation (3.4), as the evaluation of losses is based on the determination of the attenuation constant.

$$\alpha = \alpha_c + \alpha_d + \alpha_r \quad (3.4)$$

where, the attenuation constant due to ohmic loss is denoted by  $\alpha_c$ , the attenuation constant due to dielectric loss is denoted by  $\alpha_d$ , and  $\alpha_r$  is the attenuation constant due to radiation losses. The attenuation constant can be derived from the S-parameters as follows

$$\alpha = -\frac{1}{d} 10 \log_{10} \left( \frac{|S_{21}|^2}{1 - |S_{11}|^2} \right) \quad dB \quad (3.5)$$

In equation (3.5),  $d$  is used to denote the length of the SIW structure and it is chosen in such a manner that the insertion loss is close to unity.

In order to determine the three attenuation constants, three separate analysis is followed in the sequence as follows:

Step 1) Firstly, we consider a perfect conductor ( $\sigma=\infty$ ) and ideal dielectric ( $\tan \delta=0$ ). Hence, the only source of loss is the radiation loss. Thus,  $\alpha_r$  can be calculated from (3.5) and (3.4). As, all the attenuation constants are zero,  $\alpha = \alpha_r$ .

Step 2) We now consider a finite conductivity for the conductor but, the dielectric is still considered to be ideal. In this case, the losses are due to the conductor and the radiation. Thus,  $\alpha_d = 0$  and  $\alpha_r$  is known from the previous step. The overall attenuation constant is calculated from equation (3.5), and  $\alpha_c = \alpha - \alpha_r$ .

Step 3) In the third analysis, we again consider the SIW to have a perfect conductor, but with a lossy dielectric. Here, the losses are contributed by

## SIW THEORETICAL CONCEPTS AND TRANSITIONS

---

the dielectric and the radiation. Thus,  $\alpha_c = 0$  and  $\alpha_r$  is known from the

Step 1. The overall attenuation constant is calculated from equation (3.5),

and  $\alpha_d = \alpha - \alpha_r$ .

From, the analysis of the attenuation constants mentioned above, it can be concluded that the radiation losses are large when the metallic vias have a small diameter and are placed far apart from each other. The radiation losses are negligible when the vias are large and gaps between them are lower. In this case, SIW tends to be completely shielded like rectangular waveguides. If the vias are large and closely spaced, the conducting losses are also less. This happen because, when the vertical electric currents on the metal vias flows on a wider surface, the current density decreases and hence the power dissipated is more, leading to lower loss. But, it is limited. However, if the via diameter is too large, the modulation in the width of the waveguide hampers the propagation characteristic. In an SIW, the dielectric losses are the major source of loss and is significantly more than the ohmic and radiation losses. It affects mainly the region where the amplitude of the electric field is more, and hence at the middle of the SIW. Since, the field pattern is slightly affected by the via size and spacing, there is a small variation in the dielectric loss. The ohmic losses and the dielectric losses are slightly higher in an SIW than a rectangular waveguide. Table 3.1, shows the comparison of various losses in different planar transmission lines- microstrip, stripline and SIW. The losses in microstrip are primarily from the dielectric material and the the radiations arising out of the fringing fields. In stripline, the radiation losses are much lower due to the confinement of the fields between the ground planes. However, the dielectric losses remain. Compared to SIW and stripline, ohmic losses are comparatively more in microstrip, as the current gets concentrated in the edges. Since, the SIW is a confined structure like a waveguide, hence



## SIW THEORETICAL CONCEPTS AND TRANSITIONS

there is minimal radiation loss. The ohmic loss is also less due to the discrete arrangement of the vias unlike the continuous conducting structures like microstrip, stripline or even waveguide. The dielectric loss in SIW is also the least due to the enclosed dielectric in the structure.

TABLE 3.1  
Comparison of Losses in Planar Transmission Lines

Transmission line	Dielectric losses	Ohmic losses	Radiation losses
Microstrip line	Higher	Moderate	Moderate
Strip line	Moderate	Lower	Lower
SIW	Lower	Lower	Lower

### 3.6. Miniaturization of SIW

#### 3.6.1. Basic Requirement of Miniaturization

Substrate integrated waveguide proves to be a popular technology in high integration, dense packaging applications like space exploration communication systems and satellites. This is due to the reduction in the weight payload of the SIW components that would be incorporated into a space craft or other dense packaging systems. However, miniaturization of existing technologies still plays an attractive research area. It requires microwave engineers to design components and systems with further decreased footprint and weight. Recently, researchers have proposed several structures which are modification to the standard SIW, but with a reduced overall dimension. Some of the popular structures like, Half-mode substrate integrated waveguide [27],[28], Quarter-

Mode substrate integrated waveguide [29],[30], Substrate integrated folded waveguide [31]-[33] and Empty substrate integrated waveguide [34],[35] are mentioned below.

### 3.6.2. *Half-Mode Substrate Integrated Waveguide*

Half-mode substrate integrated waveguide (HMSIW), as the name suggests, is just the half of a conventional substrate integrated waveguide. It is constructed if the SIW is cut into half longitudinally from the center [27],[28]. HMSIW can retain the field properties and cut-off characteristics of an SIW. The symmetric plane along the direction of propagation is equivalent to a magnetic wall, where there is no current available. Hence, by bisecting the SIW into half from the magnetic wall, the structure retains the half field distribution unchanged. HMSIW can have a nearby perfect magnetic wall by having a high ratio between its width and height. The dominant mode of an HMSIW is thus  $TE_{10}$ . HMSIW is capable of achieving 50% reduction of size without any multilayer or additional dielectric requirements. Due to the minimization of the overall conductor and dielectric layers, it produces much lower ohmic and dielectric losses, and with a higher ratio between the width and height, it can also present lower radiation loss than the conventional SIW. Fig. 3.4 shows the top view of the HMSIW structure.

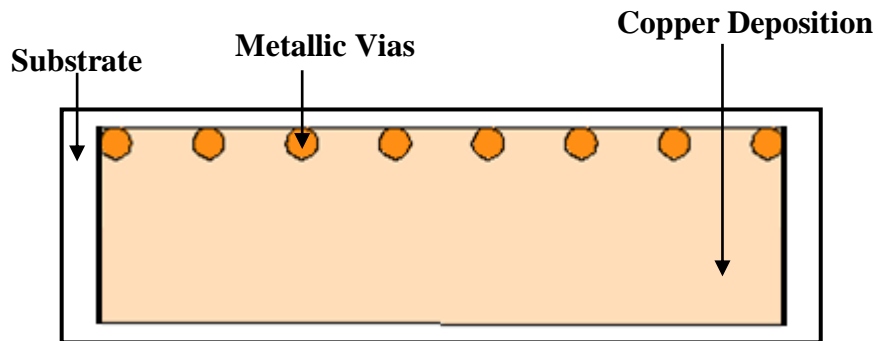


Fig. 3.4. Top view of HMSIW.

### 3.6.3. *Quarter-Mode Substrate Integrated Waveguide*

Previously, we have discussed that by bisecting a standard SIW longitudinally into two halves, we obtain two HMSIW. Similarly, if we further bisect the HMSIW cavity into two sections equally from the plane of symmetry, the structure that we get is a Quarter-mode substrate integrated waveguide (QMSIW) [29],[30]. To realize a cavity in an SIW, we place the equally spaced metallic vias in all the four boundaries and thus create an electrical wall. If we cut this SIW cavity along its two magnetic walls, we achieve four sections of QMSIW cavity. The structure can retain a quarter of the field distribution of an SIW. QMSIW has a further reduced size than HMSIW and is only a quarter of the SIW cavity. QMSIW is a very promising technology in designing antennas, especially circularly polarized antennas and filters. The top view of a quarter-mode substrate integrated waveguide is presented in Fig. 3.5. Since, it has an area almost a quarter of an SIW, the ohmic and dielectric losses are much lower.

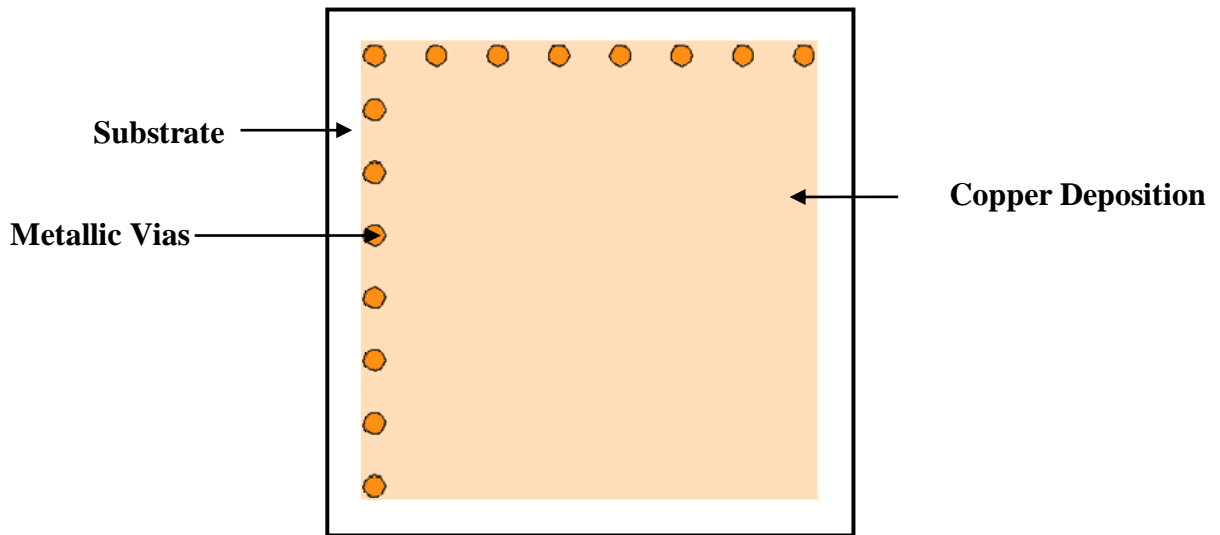


Fig. 3.5. Top view of QMSIW.

### 3.6.4. *Folded Substrate Integrated Waveguide*

Folded substrate integrated waveguides (FSIW) are based upon the concept of folded rectangular waveguides [31],[32]. FSIW inherits the same propagation and cutoff characteristics as the conventional SIW. Though, there is a reduction of almost half in the area but, at the cost of introducing additional dielectric layer. FSIW are constructed in PCBs using double-layer substrates. It can be realized by the folding of the SIW along certain longitudinal axes and the plane of symmetry appears between the two dielectric layers. FSIWs with size reduction of more than 50% can be obtained through various folding configurations, but they require additional substrate layers. Due, to the folding, the electromagnetic field in the FSIW, undergo an appropriate folding. Hence, the mode is similar to the conventional  $TE_{10}$  but folded round under itself. The maximum field is present at the edge of the guide between the side wall and the center of the structure. The cross-sectional view of the folded substrate integrated waveguide propagating the dominant  $TE_{10}$  mode is shown in Fig. 3.6. The compactness can be further improved by the folded structure of the existing HMSIW designs and they are known as folded half-mode substrate integrated waveguides (FHMSIW) [33].

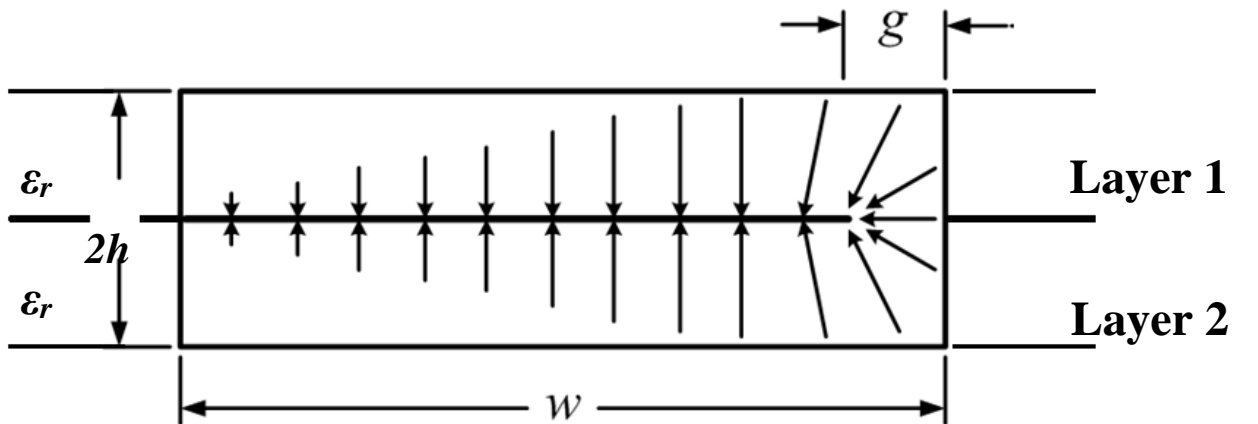


Fig. 3.6. Cross-sectional view of FSIW showing dominant  $TE_{10}$  type mode [31].

### 3.6.5. *Empty Substrate Integrated Waveguide*

Substrate integrated waveguides, as studied so far reported better quality factor and lower losses than other planar structures. But, these characteristics are worse than rectangular air filled waveguides, and this is because the presence of dielectric in the SIWs. In order to improve the quality factor and the losses, mainly the dielectric losses, SIWs can be replaced with a new technology which is known as an empty substrate integrated waveguide (ESIW) [34],[35]. It can be also regarded as hollow substrate integrated waveguide. The ESIW is nothing but the same conventional SIW, but without the substrate in it. It instead has air or vacuum as the dielectric. The structure can be manufactured using the standard PCBs by emptying a rectangular hole in the planar substrate and then metalizing the side walls by electroplating procedure. The top and the bottom conductor are formed by soldering two thin copper sheets to the substrate. The electromagnetic fields in an ESIW propagate through the air or vacuum confined within the four metallic walls. The layout of an empty substrate integrated waveguide is presented in Fig. 3.7. ESIW presents a higher quality factor and lower loss than the standard SIWs.

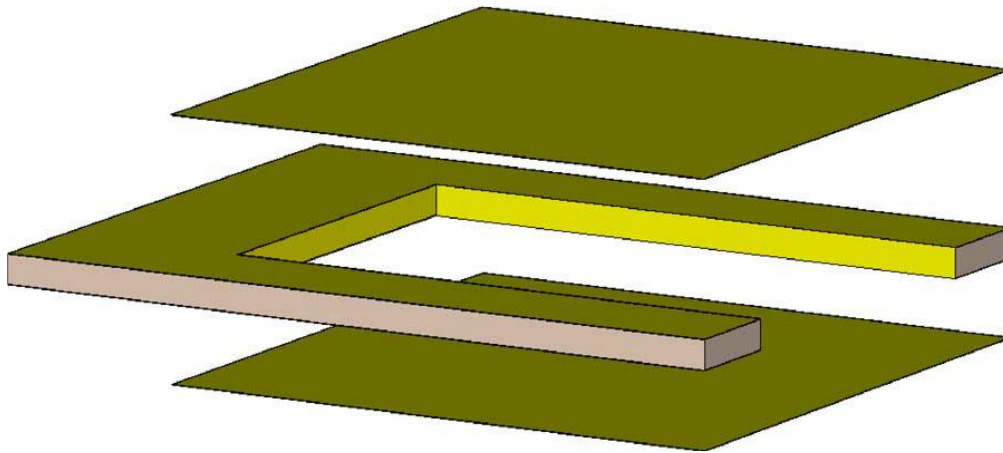


Fig. 3.7. Layout of ESIW [34].

### 3.7. Simulation Study of Basic SIW

In order to understand the functionality of a substrate integrated waveguide, a study based on simulations have been presented on both SIW and ESIW. The aim behind the parametric analysis is to showcase how the important parameters of an SIW design vary and hence it is helpful for designers to achieve an optimum result.

#### 3.7.1. Simulated Parametric Analysis of SIW

In the parametric analysis of an SIW, we first start with the initial calculations using the formula presented in (3.1) and the design steps mentioned in section 3.3.3. We choose to design the structure in a RT Duroid 5880 substrate which has a dielectric constant ( $\epsilon_r$ ) of 2.2. The height of the substrate has been fixed to 20 mil or 0.5 mm.

- a. We initially select  $p = 1.5$  mm and  $d = 1$  mm.  $p/d$  is  $1.5 < 2.0$ .
- b. We calculate  $a_{eqv} = 12.64$  mm by considering the cut-off frequency to be 8 GHz for X-band and the equation defined in (3.2).
- c. Now, we calculate  $a$  from equation (3.1), which comes to be around 13.35 mm.
- d. We find that  $d/a$  is much less than 1.5, and hence we may proceed with our initial simulations.

The simulation of the structure has been carried out using Ansys HFSS. The reflection loss S11 and the insertion loss S21 as per the initial calculated dimensions are shown in

## SIW THEORETICAL CONCEPTS AND TRANSITIONS

Fig. 3.8. The initial simulation doesn't result in a wideband response across the entire X-Band. The return loss is better than 15 dB at around 9.9 GHz across 0.2 GHz bandwidth.

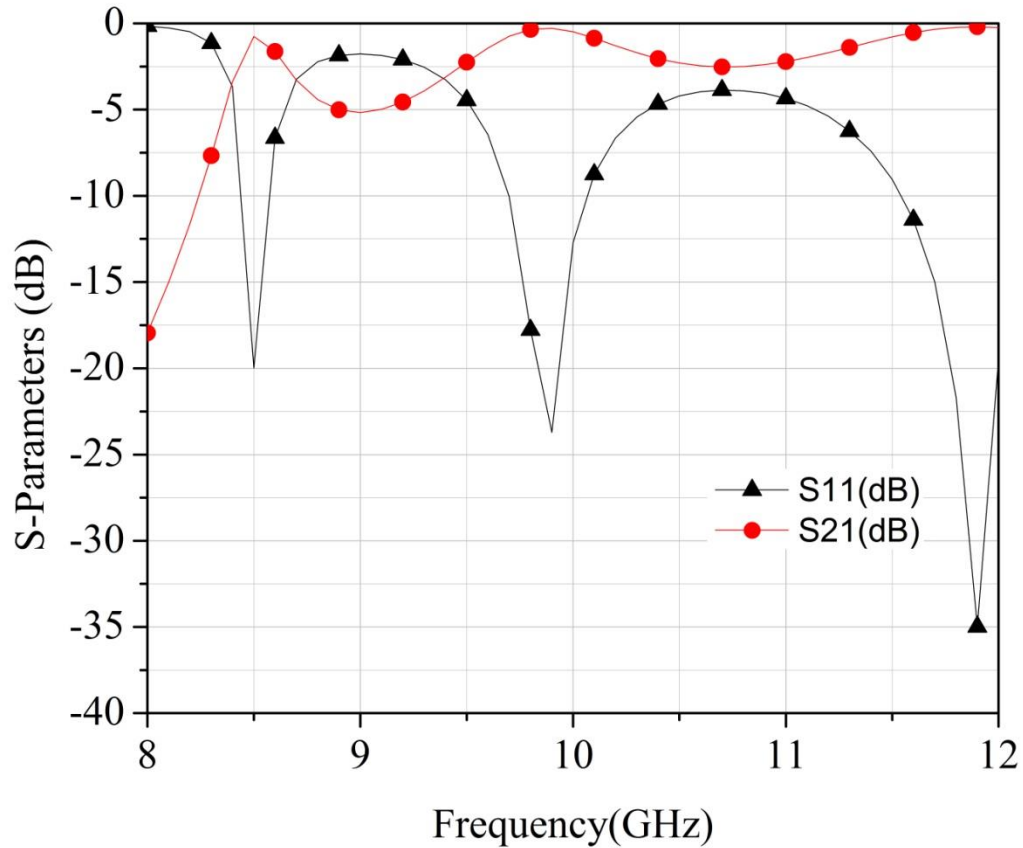


Fig. 3.8. Simulated S11 and S21 for SIW having  $a = 13.35$  mm,  $p = 1.5$  mm and  $d = 1$  mm.

In order to achieve an optimum result and simultaneously study the response of the structure on the  $a$  dimension, or the width of the SIW, we run a parametric simulation over the same structure with all the other dimensions fixed to their initial values. Fig. 3.9 shows the simulated return loss S11 response and Fig. 3.10 shows the simulated insertion loss S21 for the  $a$  dimensions : 13mm, 13.5mm, 15mm, 17mm, 17.5mm and 18 mm.

## SIW THEORETICAL CONCEPTS AND TRANSITIONS

From the plots, we find that 17.5 mm results in an optimum result covering the entire X-band with a return loss better than 15 dB and an insertion loss better than 0.2 dB.

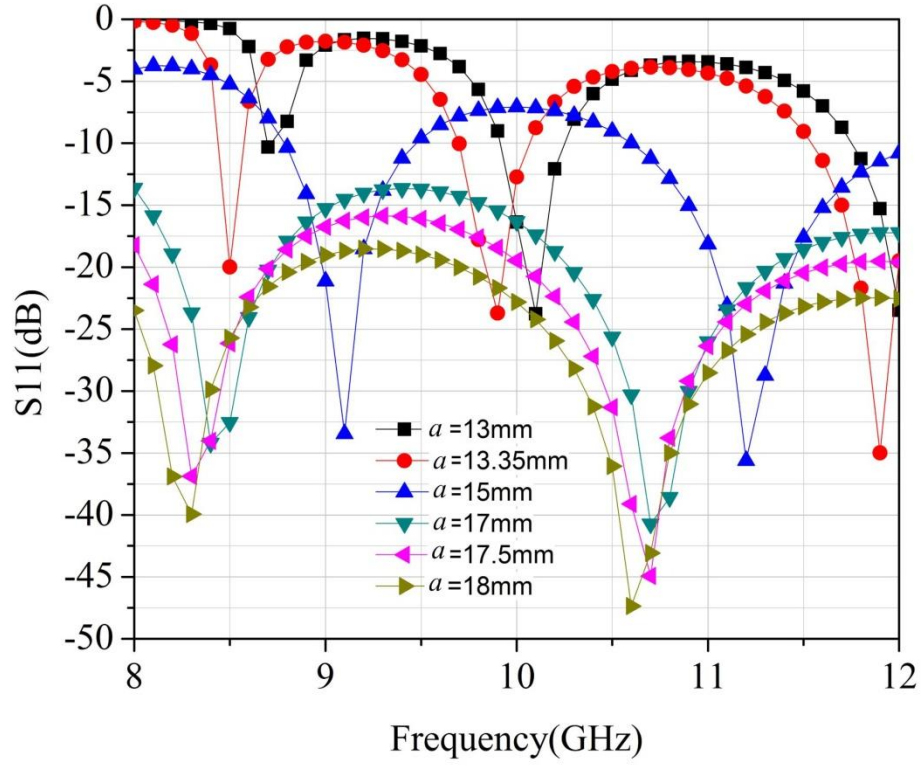


Fig. 3.9. Simulated S11 for SIW having  $a$  (in mm) = 13, 13.35, 15, 17, 17.5, 18,  $p = 1.5$  mm and  $d = 1$  mm.



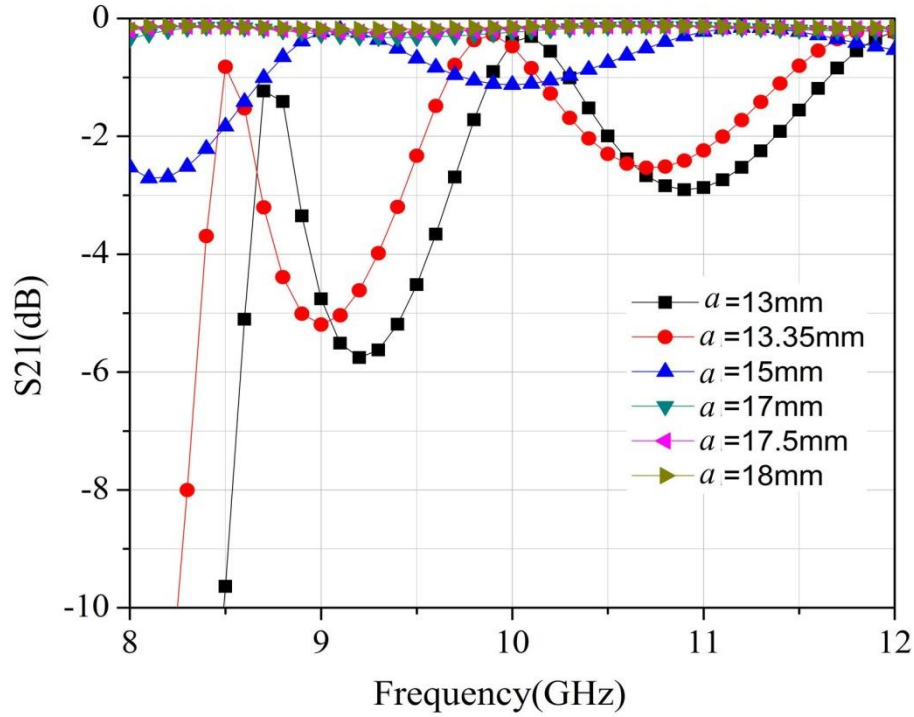


Fig. 3.10. Simulated  $S_{21}$  for SIW having  $a$  (in mm) = 13, 13.35, 15, 17, 17.5, 18,  $p = 1.5$  mm and  $d = 1$  mm.

We infer from the results that as the width of the SIW is increased, the cut off frequency is shifted to the lower frequency side and hence we get a stable frequency response. But we cannot keep increasing the width indefinitely as spurious higher order modes will be excited and power will get distributed among them.

To further study the effects of the via dimension  $d$  and its periodicity  $p$  on the response, parametric simulations are done on the same Ansys HFSS design but with the optimum  $a$  dimension value 17.5 mm. Fig. 3.11 shows the simulated return loss  $S_{11}$  response for the periodicity  $p$  having dimensions: 1mm, 1.2mm, 1.4mm, and 1.5 mm.

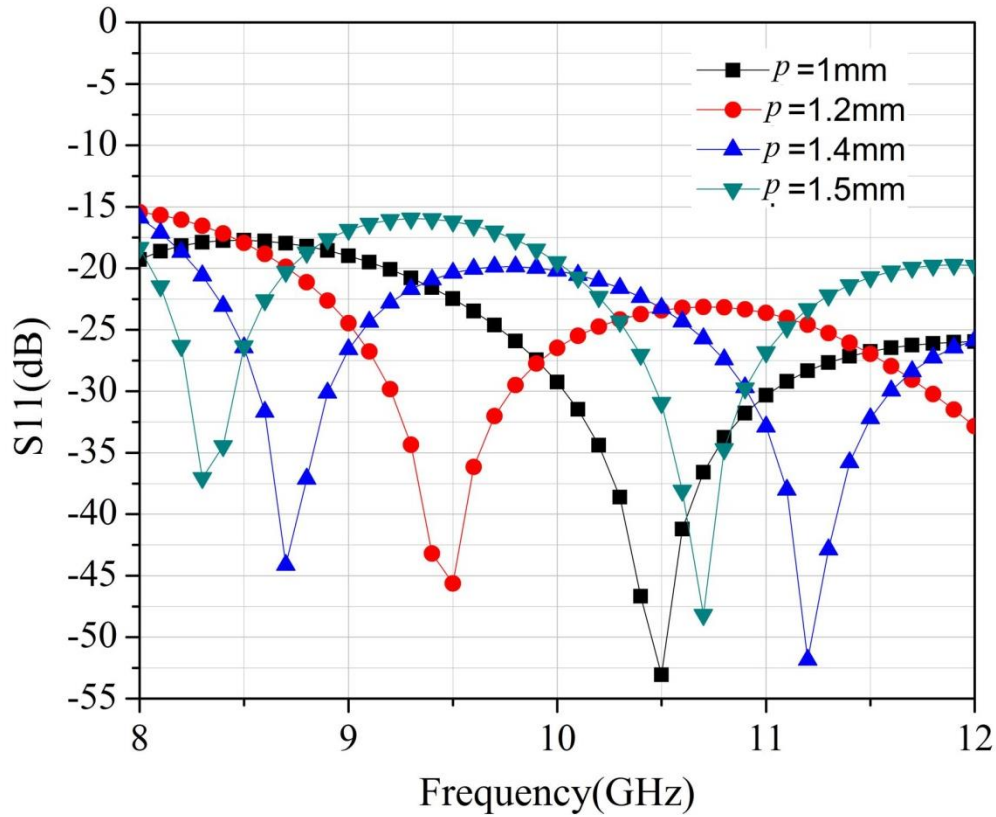


Fig. 3.11. Simulated S11 for SIW having  $p$  (in mm) = 1, 1.2, 1.4, 1.5,  $a = 17.5$  mm and  $d = 1$  mm.

From the Fig. 3.11 we choose optimum pitch  $p$  to be of 1mm because a larger value of pitch will result in more leakage radiation. At this value the return loss is better than 20 dB in the entire X- band. Using these optimum values of  $a$  and  $p$ , further parametric analysis is carried out on the via diameter  $d$ . Fig. 3.12 presents the simulated return loss S11 response for the via diameter  $d$  having dimensions: 0.8 mm, 0.9 mm, 1mm 1.1mm, and 1.2 mm.

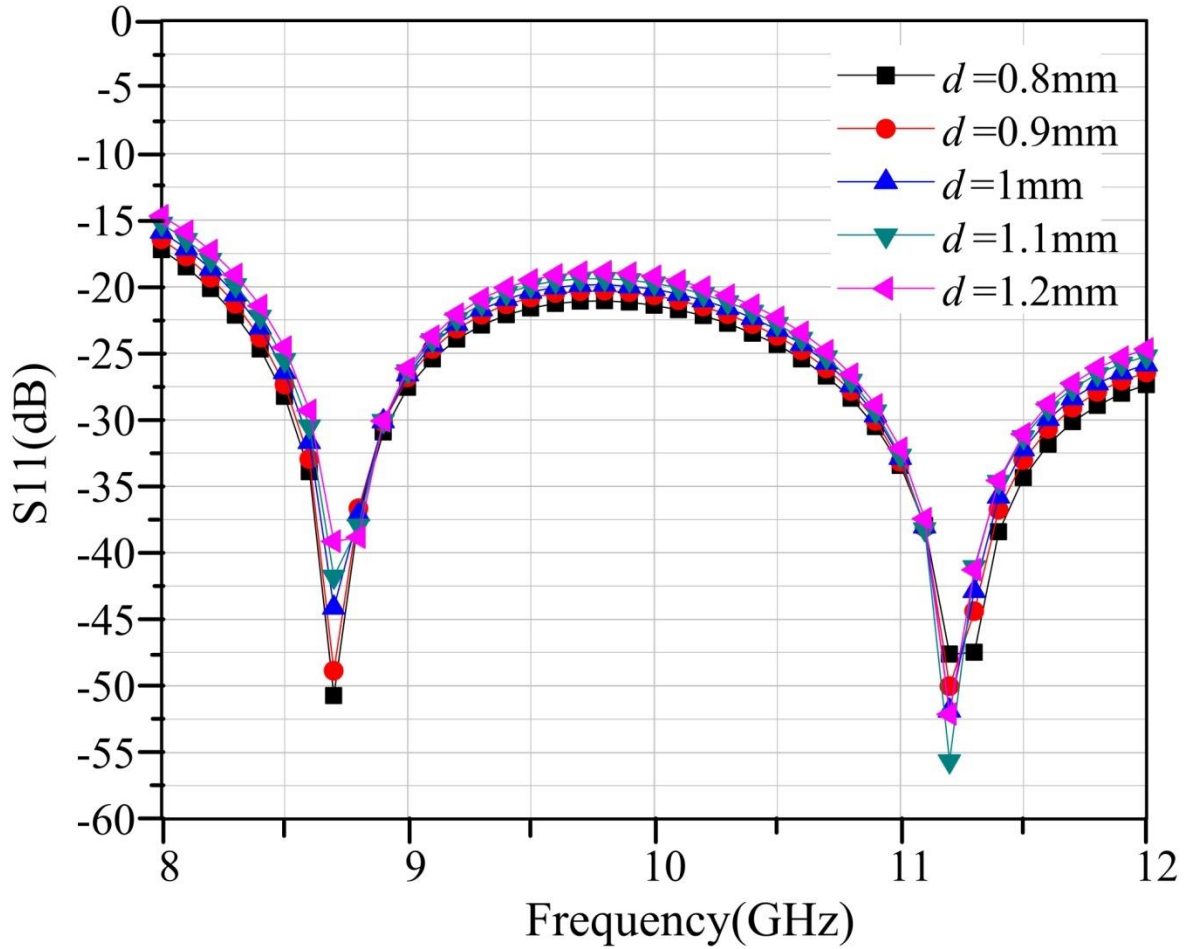


Fig. 3.12. Simulated S11 for SIW having  $d$  (in mm) = 0.8, 0.9, 1, 1.1, 1.2,  $a = 17.5$  mm and  $p = 1$  mm.

As seen from the plots in Fig. 3.12, there is very little variations in the return loss results. However, for a value of 0.8 mm of the via diameter  $d$ , the response is slightly better, but there might be fabrication difficulty at the lower values. Hence optimum value of  $d$  is selected to be of 1mm as fabrication is feasible and realizable.

Using these optimum values of the width of the SIW  $a = 17.5$  mm, via diameter  $d = 1$  mm and the periodicity  $p = 1$  mm, we have run a final simulation to obtain the plots for the

## SIW THEORETICAL CONCEPTS AND TRANSITIONS

reflection loss S11 and the insertion loss S21. Hence, the optimum results are in Fig. 3.13. Almost the entire X-band has a return loss better than 20 dB and the insertion loss is better than 0.15 dB.

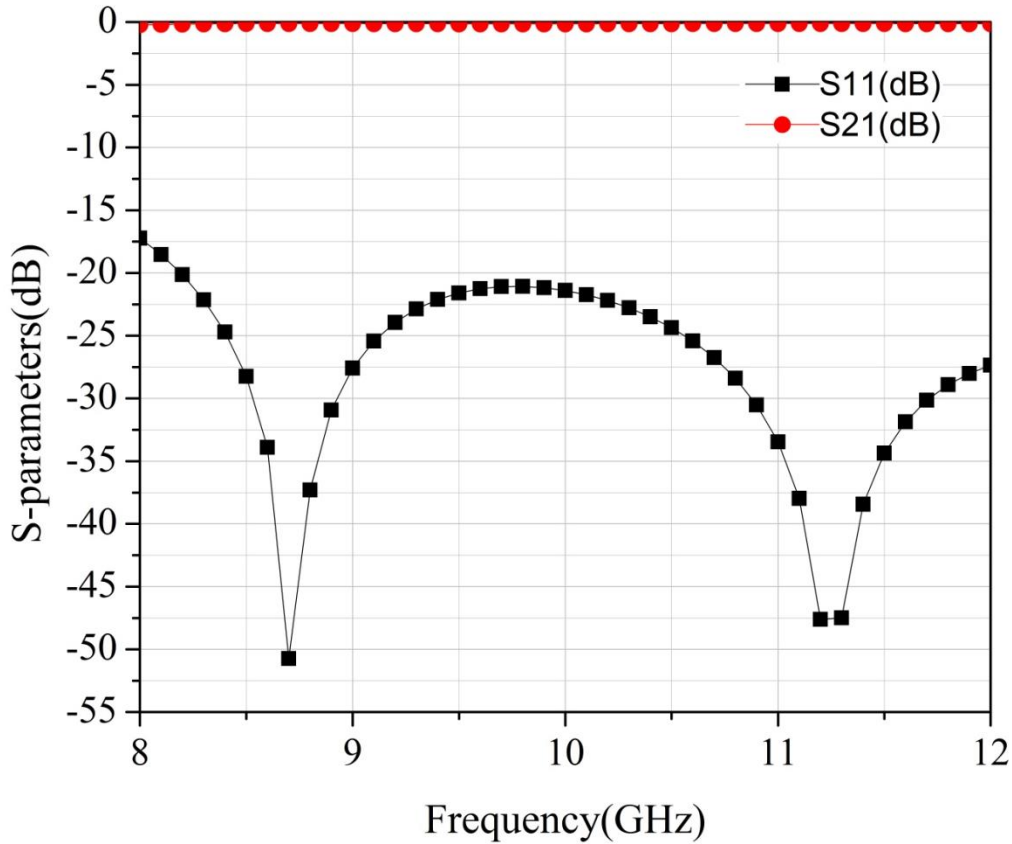


Fig. 3.13. Simulated S11 and S21 for SIW having  $a = 17.5$  mm,  $d = 1$  mm and  $p = 1$  mm.

Parametric analysis on SIW in HFSS was carried out for different values of width  $a$ , pitch  $p$  and diameter  $d$  of vias and optimum values were selected from the results obtained. It was observed that these optimum values are  $a=17.5$ mm,  $p=1$ mm and  $d=1$ mm where almost in the entire X-band return loss better than 20 dB and the insertion loss is better than 0.15 dB.

### 3.7.2. Simulated Parametric Analysis of ESIW

An ESIW, unlike an SIW does not have much parameter to be dependent on when it comes to its response. Since, ESIW does not have any dielectric and instead of via walls it has continuous wall. Hence, for an ESIW the width matters the most, to achieve an optimum result. In the parametric analysis of the ESIW, we first start with the initial calculations using the formula presented in (3.2) where the  $a$  dimensions come to 18.75 mm. The height of the substrate has been fixed to 20 mil or 0.5 mm. Fig. 3.14 represents the initial results with the reflection loss S11 and insertion loss S21 plots. Entire X-band has a reflection loss better than 40 dB.

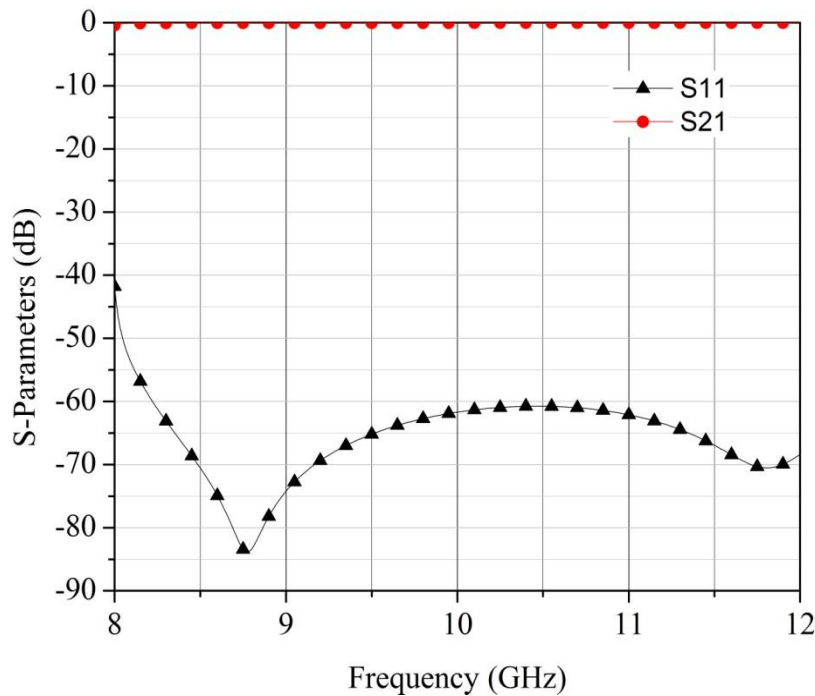


Fig. 3.14. Simulated S11 and S21 for ESIW having  $a = 18.75$  mm.

## SIW THEORETICAL CONCEPTS AND TRANSITIONS

In order to study the effects of variations in the width of the ESIW, further parametric simulation has been carried on for values of 18 mm, 20 mm, 22.86 mm, 24 mm. The simulation results are presented in Fig. 3.15. The optimum results are obtained at  $a = 20$  mm. Optimum value of 20mm is selected as with higher values than that may lead to excitation of higher and spurious modes thus taking away power from the dominant mode. In Fig. 3.16, the optimum reflection loss S11 and the optimum insertion loss S21, together are presented.

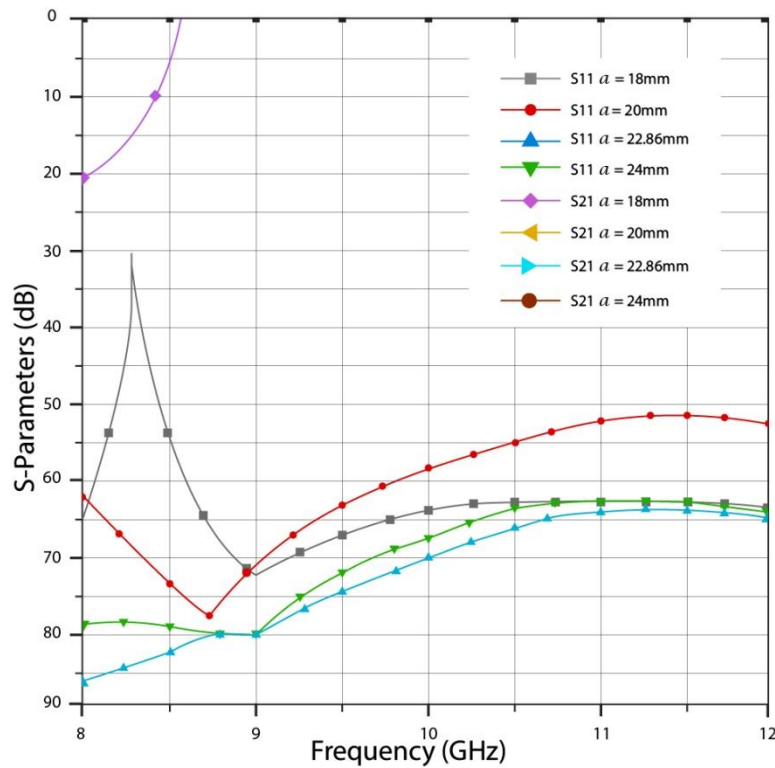


Fig. 3.15. Simulated S11 and S21 for ESIW having  $a$  (mm) = 18, 20, 22.86, 24.

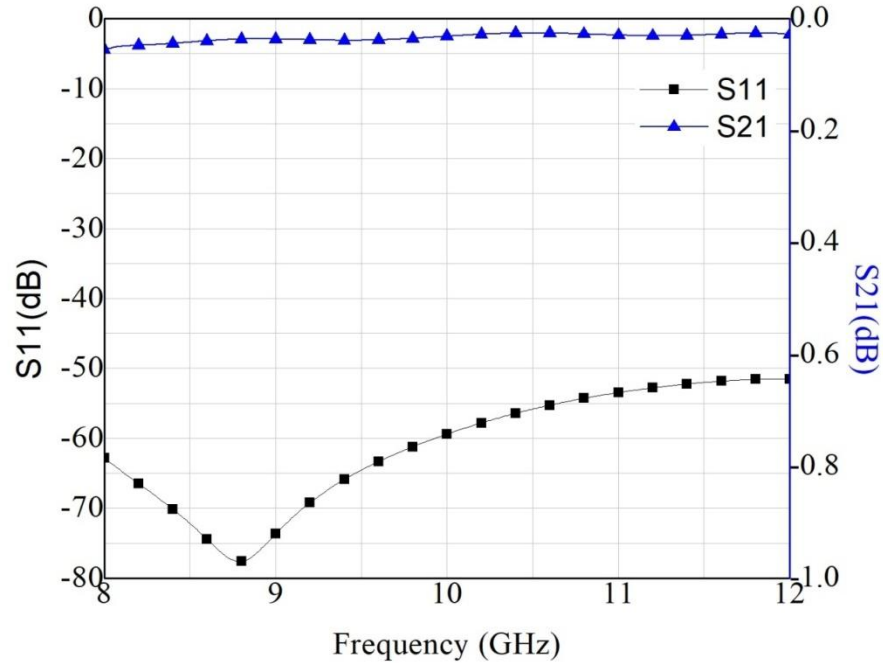


Fig. 3.16. Simulated S11 and S21 for ESIW having  $a = 20$  mm.

Parametric analysis of ESIW was carried out in HFSS by varying the width  $a$  of ESIW (as this is the only parameter that can be varied) and the optimum dimension of  $a$  is selected at 20mm where the in almost the entire X-band, the return loss is better than 50 dB and the insertion loss is better than 0.03 dB.

### 3.8. Transition

Substrate integrated circuit (SIC), as discussed, emerged as a solution to address the limitations of both non-planar and planar configurations [4]. In the context of SIC, an integrated system is developed within a single substrate. This is achieved by transforming non-planar circuitry into a planar format and then seamlessly integrating it with the pre-existing planar circuitry on the same substrate. Given the capability of SIC technology to

establish connections among diverse transmission lines, it becomes imperative to establish smooth transitions between SIW and other technologies. Beyond antennas, wireless systems encompass an array of microwave and millimeter wave components, which are not necessarily constructed using a uniform technology. As a result, achieving optimal impedance and mode matching between the transition's ports and the associated technologies is of paramount importance. Traditionally, transitions connecting various planar and non-planar structures like waveguides, coaxial cables, and microstrips have been cumbersome and intricate due to their bulky nature and the intricate mechanical processes required for their fabrication. In contrast, the planar nature and adaptable characteristics of SIC technology facilitate straightforward interconnection of diverse transmission lines through uncomplicated transitions. By leveraging the compactness and cost-effectiveness of SIWs, the integration process between SIW and alternative structures becomes more streamlined. Furthermore, the flexibility of SIC technology enables its seamless integration with both planar and non-planar structures, thus enabling higher degrees of integration and denser packaging within complex systems. Simulation based design of various transitions between SIW and other technologies like waveguide, microstrip and ESIW is presented.

### ***3.8.1 SIW to Microstrip***

The first ever SIW transition that was realized was the tapered microstrip design [36], which remains the most commonly employed method of transitioning from a microstrip line to a SIW in single-layered circuits. This transition design utilizes a microstrip line with a linear taper, effectively transforming the quasi-TEM mode present in the 50Ω



## SIW THEORETICAL CONCEPTS AND TRANSITIONS

microstrip line into the  $TE_{10}$  mode within the same dielectric medium as the SIW. The simple and straightforward design enables the efficient excitation of the SIW, as the electric fields of the both the lines align in a similar direction and share a common profile. Experimental measurements of the fabricated back-to-back arrangement yields a bandwidth exceeding 12%, ensuring a 20 dB return loss within the frequency range of 26.65 to 30.20 GHz.

In this section of the chapter, a broadband microstrip-to-SIW transition is studied and designed. It features the same design with the tapering microstrip as in [36], however, this structure has a stepped linear microstrip taper instead of one. This transition results in a return loss better than 15 dB over the entire X band and thus showcases an improvement over [36]. The layout of back-to-back transition structure is shown in Fig. 3.17.

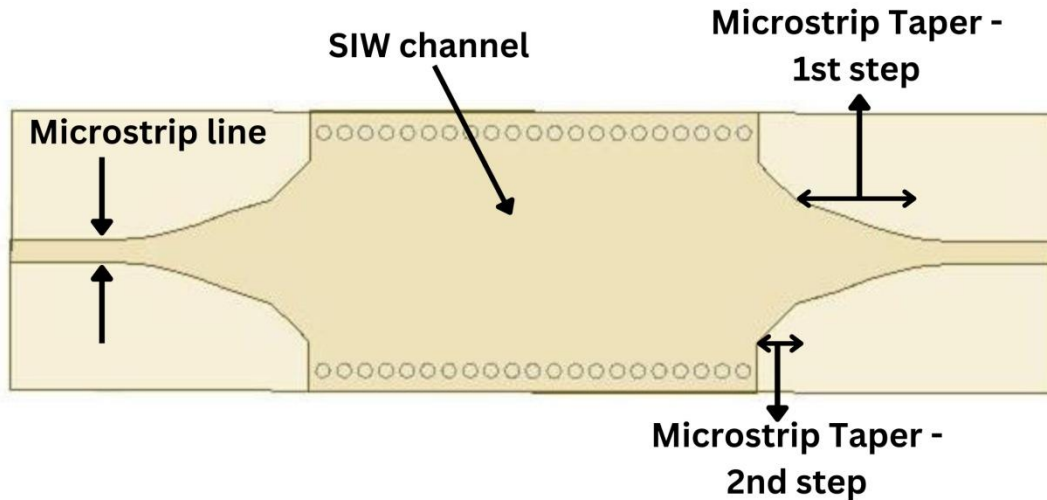


Fig. 3.17. Basic layout of the proposed microstrip-SIW transition.

The dimensions and optimized values of the coupler's structure are shown in Fig. 3.18 and Table 3.2, respectively.

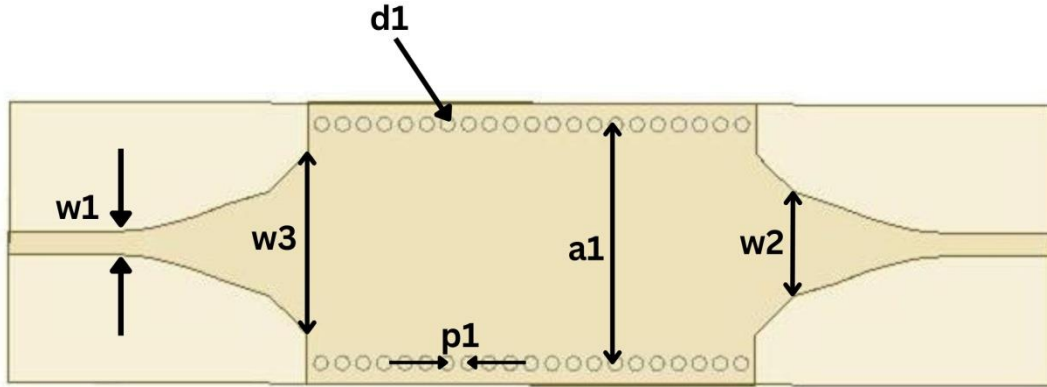


Fig. 3.18. Design parameters of the proposed microstrip-SIW transition.

TABLE 3.2

Dimensions of the Proposed Microstrip to SIW Transition

Dimensions	a1	p1	d1	w1	w2	w3
Optimized Values (in mm)	17	1.5	1	1.6	7.4	13

The entire configuration is designed using a 0.5mm thick Rogers RT/Duroid substrate which features a dielectric constant of 2.2 and a loss tangent of 0.0009. Ansys HFSS is used to carry out the simulation study. Fig. 3.19 shows that the structure has a return loss better than 15 dB in the entire X-band with a bandwidth of 40% and the return loss is better than 20 dB for a bandwidth of 14.78%. The proposed transition is compared with [36] in Table 3.3. It is evident from the comparison that the proposed stepped linear microstrip taper transition to SIW is resulting in a broader band than [36].

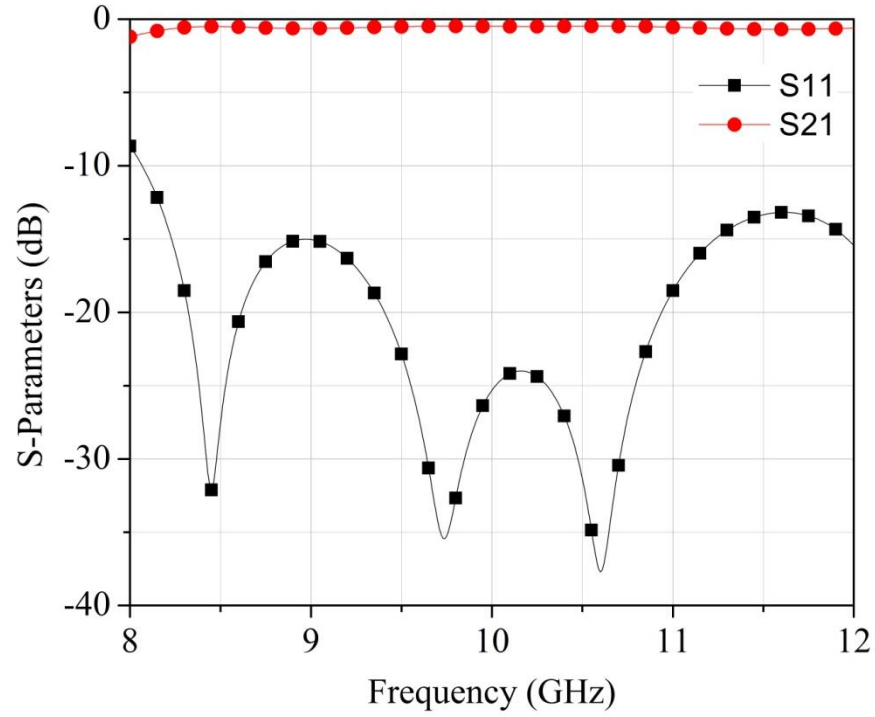


Fig. 3.19. HFSS simulation result of the proposed microstrip-SIW transition.

TABLE 3.3

Comparison of Microstrip Taper Transitions in *Ref* [36] and This Work for Return Loss more than 20dB and Return Loss more than 15 dB

Reported papers	<i>Ref</i> [36]	<i>Ref</i> [36]	This work	<i>Ref</i> [36]	<i>Ref</i> [36]	This work
Taper technology	Single taper	Single taper	Stepped taper	Single taper	Single taper	Stepped taper
Simulation/Measured	Simulation	Measured	Simulation	Simulation	Measured	Simulation
Return Loss (dB)	>20	>20	>20	>15	>15	>15
Frequency (GHz)	27.4-31	26.65-30.2	9.4-10.9	25-31.75	26.4-30.5	8-12
Fractional Bandwidth (%)	12.33	12.49	14.78	23.79	14.41	40

### 3.8.2 *SIW to Waveguide*

Despite the bulky nature of a rectangular waveguide, it continues to find applications in various high-frequency microwave and millimeter-wave contexts, primarily due to its favorable attributes of lower loss and higher power handling capacities. However, within substrate integrated circuit (SIC) based systems, achieving a comprehensive system on a single substrate isn't always feasible. As a result, a transition between the most widely adopted and effective non-planar guide and the most efficient SIC planar guide becomes imperative. This specific section of the chapter delves into the intricacies of transitioning the common  $TE_{10}$  field between a substrate integrated waveguide (SIW) and a traditional waveguide. Given the disparities in cross-sectional width and dielectric characteristics of these guides, an impedance mismatch surfaces, leading to signal losses. Hence, meticulous designs for transitions that harmonize the impedance between both the waveguide is necessary. The transition in [37] has a right-angled based configuration where the axes of both the guides are perpendicular. The approach involves integrating a waveguide flange onto the broad wall of the SIW, with coupling achieved through a single slot. This method presents a straightforward mechanical arrangement with no additional bulky arrangements. However, the application of this transition is inherently limited to narrowband systems and components, due to the resonant behavior of the coupling slot. The example showcased demonstrates a fractional bandwidth of merely 2.3% (with a 15 dB return loss) within the Ka-band.

## SIW THEORETICAL CONCEPTS AND TRANSITIONS

A modification of the structure proposed in [37] is designed and simulated to provide a broader bandwidth. The technique is to use a pair of slots, instead of one as in [37] to couple both the guides [38]. The layout of the transition is shown in Fig. 3.20.

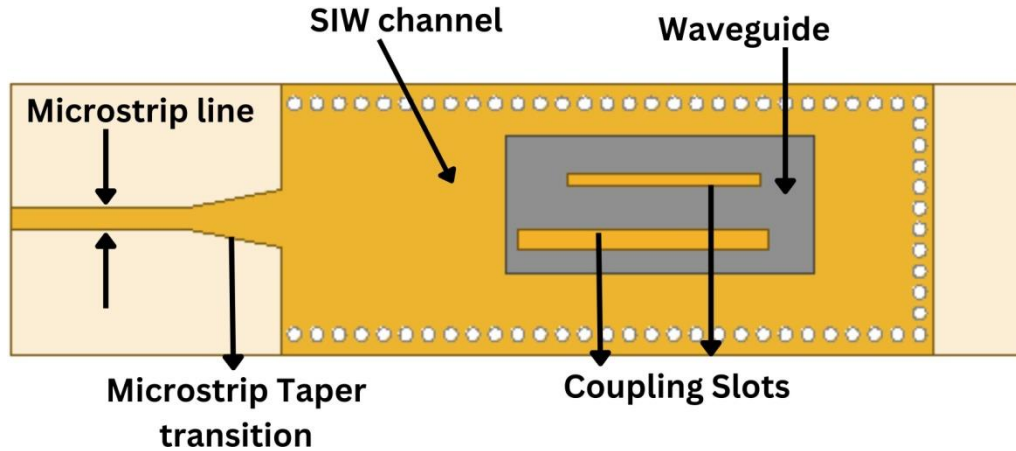


Fig. 3.20. Basic layout of the proposed transition between SIW and waveguide with dual slot configuration.

Similar to [37], the SIW substrate is directly appended to the waveguide flange. Energy transfer is enabled through the utilization of two slots that are etched into the top broadwall of the SIW. To operate over a broader range of frequencies, the slots are deliberately given distinct lengths, resulting in the creation of two resonances at two close frequencies. To obtain the broader bandwidth, the SIW is terminated with a short placed at a distance approximately equivalent to three quarter-wavelengths from the central point of the slots. This strategic placement transforms the impedance of the short so that it effectively behaves like an open when considered at the plane of the slots. A similar effect could be achieved by incorporating a short at any odd multiple of the quarter-wavelength distance. However, adopting a quarter-wavelength distance for this purpose is unfeasible as it would limit the slot lengths, which is undesirable. At the lower frequency band, the

## SIW THEORETICAL CONCEPTS AND TRANSITIONS

longer slot becomes active and resonates, while at higher frequencies, the shorter slot resonates. The design parameters are presented in Fig. 3.21 and the dimensions are mentioned in Table 3.4.

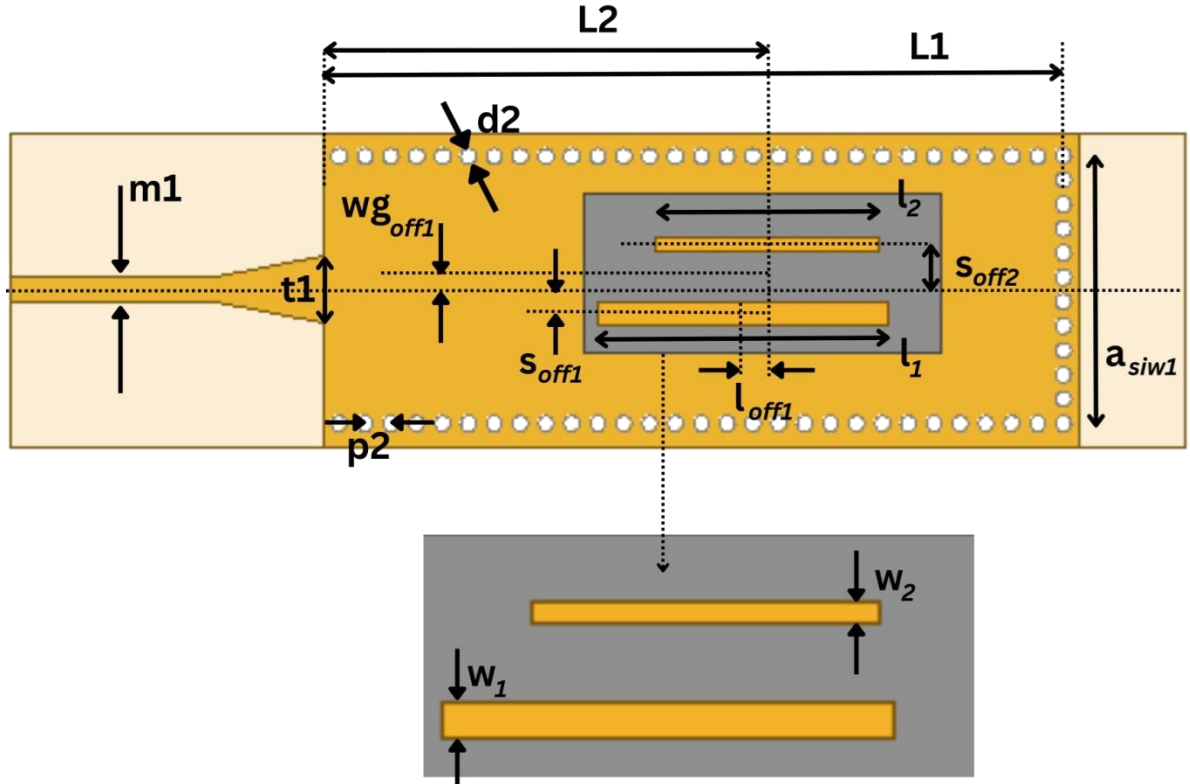


Fig. 3.21. Design parameters of the proposed single band transition between SIW and waveguide.

TABLE 3.4

Dimensions of the proposed single band SIW to waveguide transition

Dimensions	$a_{siw1}$	$m_1$	$t_1$	$w_{g_{off1}}$	$p_2$	$d_2$	$L_2$	$L_1$
Optimized Values (in mm)	17	1.6	4.8	1	1.55	1	27.44	48.36
Dimensions	$w_1$	$w_2$	$l_1$	$l_2$	$s_{off1}$	$s_{off2}$	$l_{off1}$	$l_{off2}$
Optimized Values (in mm)	1.5	0.9	18.5	14.25	1.56	3	1.31	0

The single band transition is designed using a 0.5 mm thick Rogers RT/Duroid substrate which features a dielectric constant of 2.2 and a loss tangent of 0.0009 and simulated using Ansys HFSS. Fig. 3.22 shows that the structure has a return loss better

than 10 dB for a bandwidth of 1.43 GHz and a bandwidth of 1 GHz having return loss better than 15 dB. The insertion loss is better than 0.92 dB in the entire pass band.

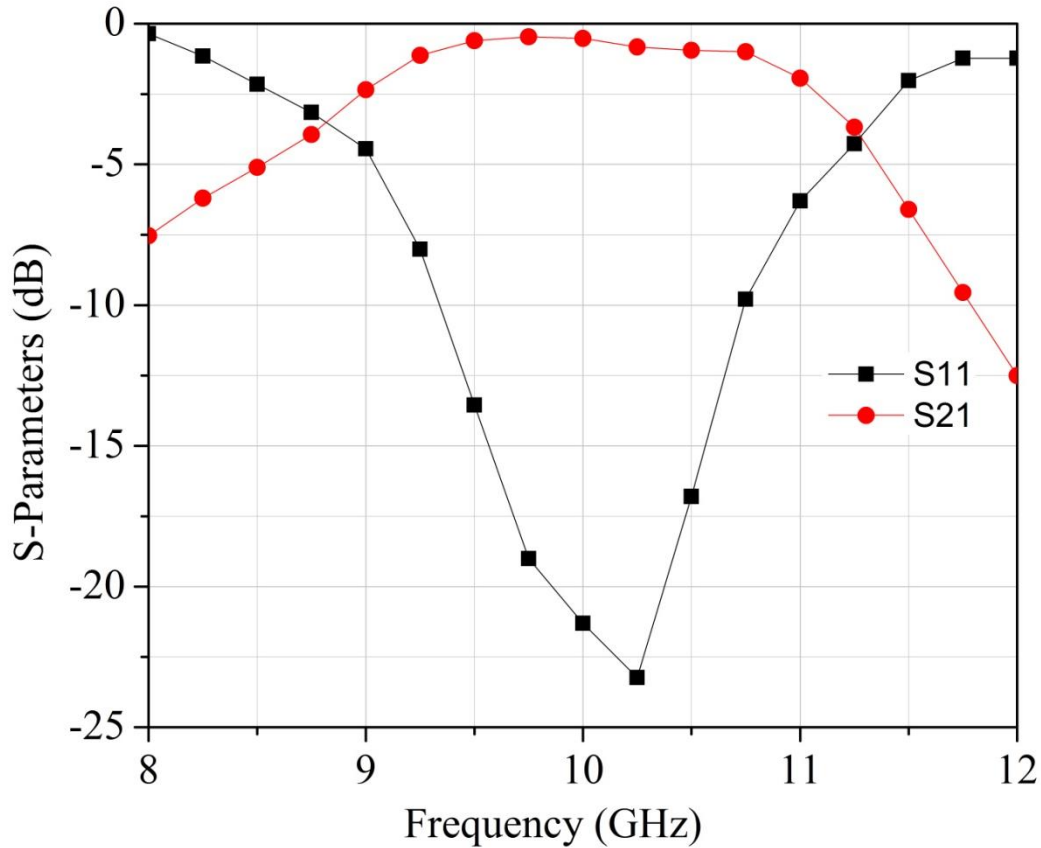


Fig. 3.22. HFSS Simulation of the proposed single band transition between SIW and waveguide.

The same structure can be further tuned and optimized to develop a dual band transition for multiband applications. The layout and the configuration of the transition remain same as shown in Fig. 3.19. The only difference lies in the technique to resonate the two slots at two different frequencies which are not close to each other, unlike the broadband design. The dual band design parameters are presented in Fig. 3.23 and the dimensions are mentioned in Table 3.5.

## SIW THEORETICAL CONCEPTS AND TRANSITIONS

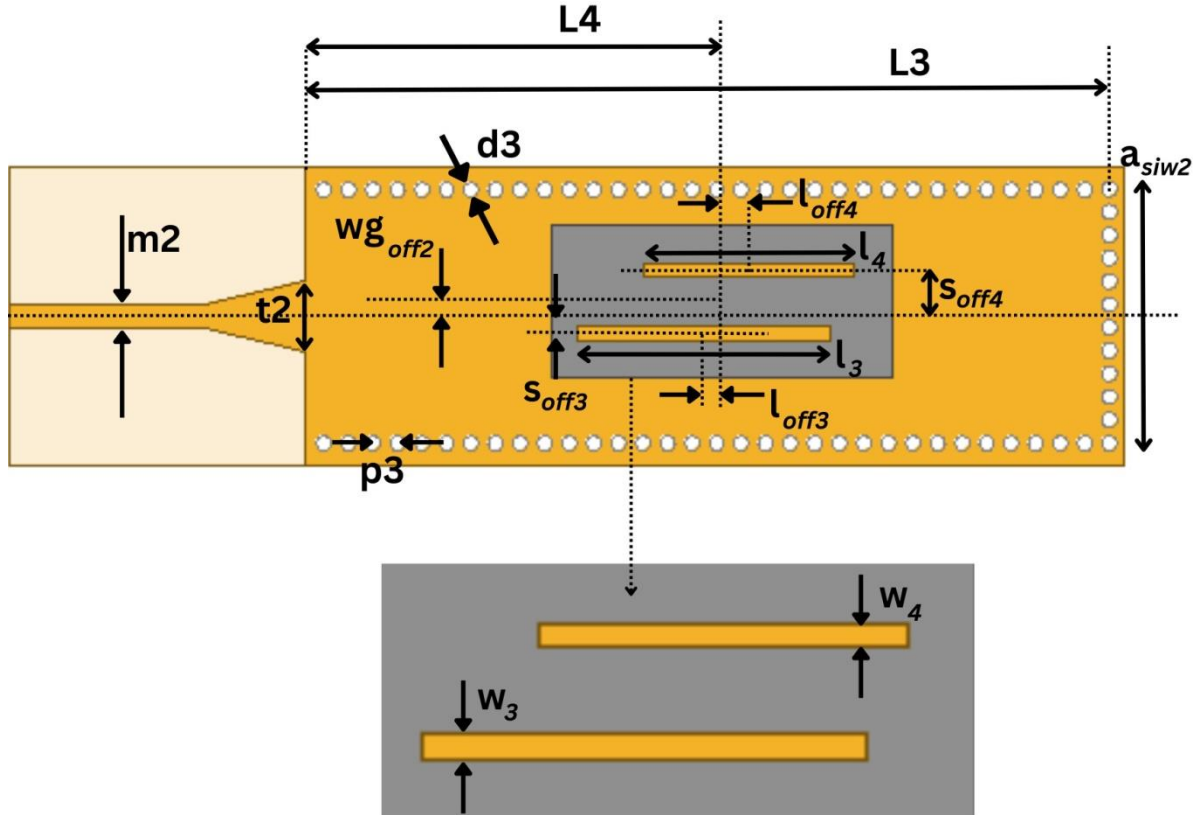


Fig. 3.23. Design parameters of the proposed dual band transition between SIW and waveguide.

TABLE 3.5

Dimensions of the proposed dual band SIW to waveguide transition

Dimensions	$a_{siw2}$	$m2$	$t2$	$wg_{off2}$	$p3$	$d3$	$L3$	$L4$
Optimized Values (in mm)	17	1.6	4.8	1	1.55	1	55	27.26
Dimensions	$w3$	$w4$	$l3$	$l4$	$s_{off3}$	$s_{off4}$	$l_{off3}$	$l_{off4}$
Optimized Values (in mm)	1	1	17	14.2	1.43	2.3	0.89	4.25

The dual band transition is designed using a 0.5 mm thick Rogers RT/Duroid substrate which features a dielectric constant of 2.2 and a loss tangent of 0.0009. The structure is simulated using Ansys HFSS. Fig. 3.24 shows that the structure has a return



## SIW THEORETICAL CONCEPTS AND TRANSITIONS

loss better than 10 dB in the X-band at two pass bands. The centres frequencies of the two passbands are at 8.97 GHz and 11.26 GHz and the 10 dB bandwidth of the passbands are 300 MHz and 255 MHz.

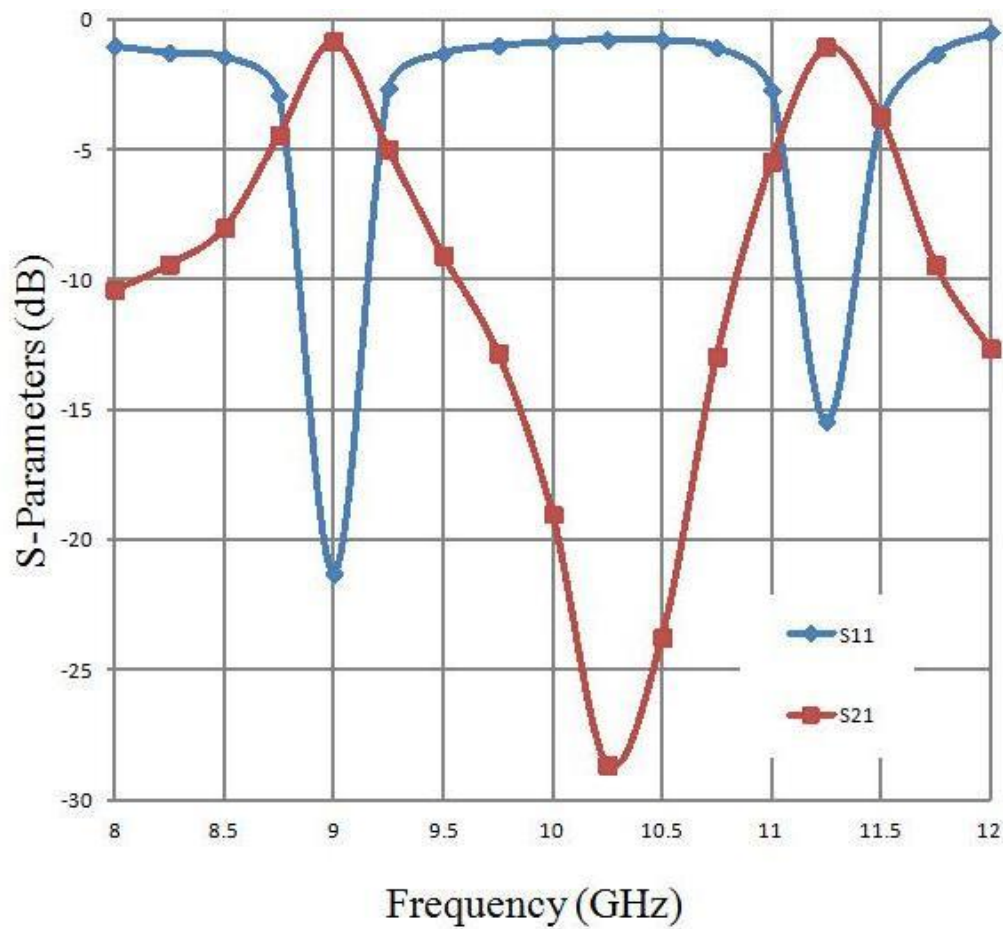


Fig. 3.24. HFSS Simulation of the proposed dual band transition between SIW and waveguide.

### 3.8.3 SIW to ESIW

A design for a multilevel transition is formulated to facilitate power transfer from one SIW to another ESIW positioned on distinct levels. Our proposal involves an investigation into an efficient and compact multilayered transition design connecting SIW and ESIW. This design is accomplished through the integration of a complimentary split ring resonator (CSRR), strategically positioned within the shared broadwall of both the SIW and ESIW. The transition exhibits a desirable return loss of less than 10 dB, sustained over a frequency bandwidth spanning 300 MHz. This multilayered arrangement holds potential for applications in establishing coupling structures within SIC, allowing for enhanced connectivity and functionality.

The basic structure of the proposed transition between an SIW and the ESIW is shown in Fig. 3.25. As shown in the figure, the ESIW sits right on top of the SIW, such that the top broadwall of the SIW and bottom broadwall of the ESIW are common. In order to initiate a multi-layered transition between the SIW layer and the ESIW layer, a single ring complementary split ring resonator (CSRR) is etched out at the common broadwall of the two guides. The developed CSRR is placed at a half-wavelength distance from the input port of the SIW and at another half-wavelength distance from the CSRR, along the SIW guide, a short wall is realized. The SRR used in the structure helps in feeding the incident power from the SIW into the ESIW cavity. The ESIW guide is of quarter-wavelength distance and the SRR is placed at the centre. The other end of the ESIW line is short-circuited. The short-circuit and the side walls in the ESIW can be achieved through gold-plating.

## SIW THEORETICAL CONCEPTS AND TRANSITIONS

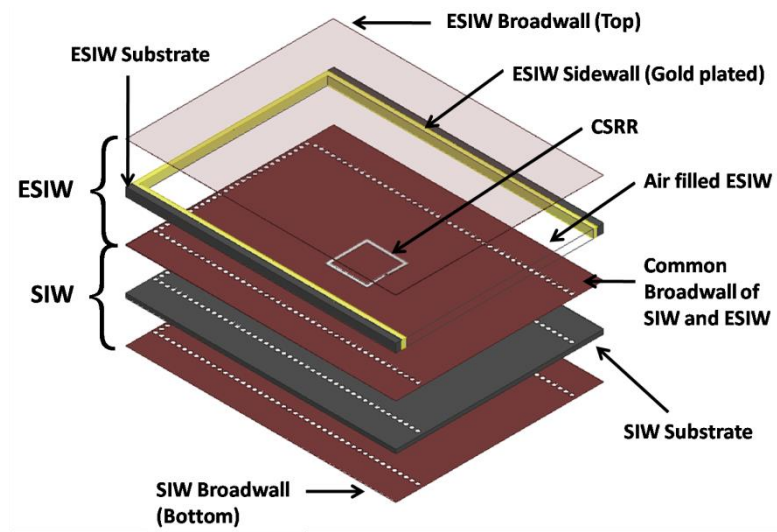


Fig. 3.25. Basic structure of the proposed transition between SIW and ESIW.

The top-view illustration of the structure along with the dimension parameters is presented in Fig. 3.26, and the values for the parameters are shown in Table 3.6.

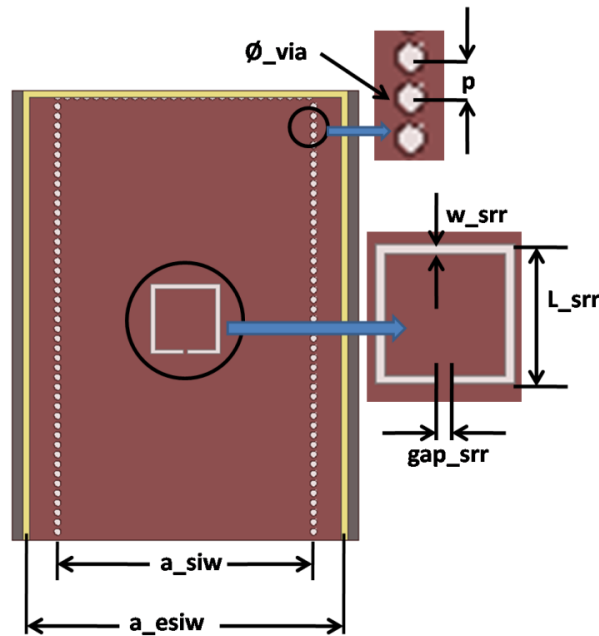


Fig. 3.26. Design parameters of the proposed multilayered SIW-ESIW transition in top view.

## SIW THEORETICAL CONCEPTS AND TRANSITIONS

TABLE 3.6  
Dimensions of proposed transition (Unit: millimeters)

Dimensions	a <sub>siw</sub>	a <sub>esiw</sub>	Ø <sub>via</sub>	p
Optimized Values	18.5	22.5	0.5	0.7
Dimensions	L <sub>srr</sub>	w <sub>srr</sub>	gap <sub>srr</sub>	
Optimized Values	5	0.3	0.3	

The structure is entirely designed using a Rogers RT/Duroid substrate with a dielectric constant of 2.2 and loss tangent of 0.0009. The thickness of the substrate is 0.5 mm for the SIW and 1mm for the ESIW. The simulation of the structure is carried out using Ansys HFSS. The results are displayed in Fig. 3.27, where, the simulated transmission loss and return loss of the complete transition structure is displayed. It also includes the results which take into the effect of  $\pm 20$  micron tolerances. The minimum return loss obtained is 30.42 dB at 7.1 GHz. The structure has a bandwidth of 300 MHz for 10 dB return loss. The E-field plot, in Fig. 3.28, shows the transition of  $TE_{10}$  mode from SIW to the ESIW through the CSRR, etched out in the common broadwall of the SIW and the ESIW transmission lines.

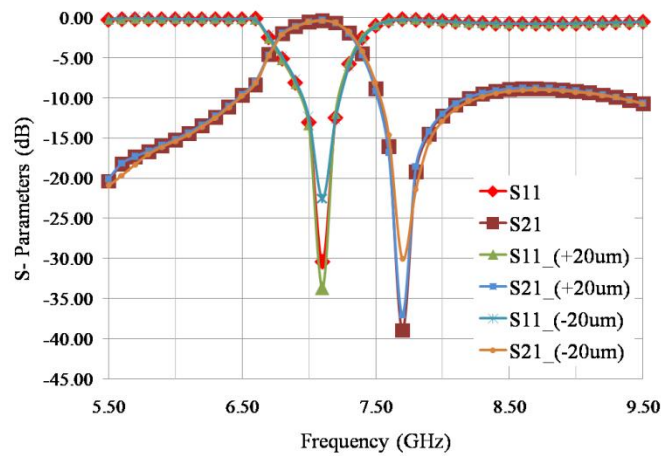


Fig. 3.27. HFSS simulation result of the proposed multilayered SIW-ESIW transition.

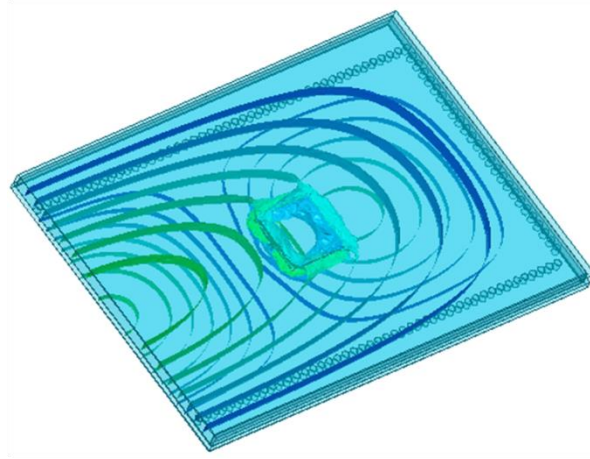


Fig. 3.28. HFSS E-Field plot of the proposed multilayered SIW-ESIW transition.

The PCB fabrication facilities which are nowadays commercially available can develop the circuit with dimensional deviations within  $15\text{ }\mu\text{m}$  and since the results considering the  $\pm 20\text{ }\mu\text{m}$  tolerances, in Fig. 3.27, are within acceptable limits, this structure is easily realizable and it may closely match with the measured results.

### 3.9. Conclusion

The basic theory of a SIW is studied along with its working principle. It is a planar analogue of the standard rectangular waveguide. It can be manufactured using the standard PCB fabrication process and drilling array of metalized holes on both the sides. SIWs are light, low cost and planar unlike waveguides. They have a high quality factor and lower losses than other planar structures. They can also be integrated to other planar and non planar structures. It can propagate in  $TE_{m0}$  mode only. The losses in an SIW are composed of losses from the conductor, dielectric and radiation, which can be minimized by selecting proper large vias and placing them closely. It finds application in various

## SIW THEORETICAL CONCEPTS AND TRANSITIONS

---

high intensity, dense packaging systems like space explorations and ISM devices. Miniaturization of SIW is also been achieved with structures like FSIW, HMSIW, QMSIW and ESIW.

A parametric study of SIW in HFSS was performed for various values of width  $a$ , pitch  $p$ , and diameter  $d$ , and the optimum values were chosen based on the results. It was discovered that the optimum values are  $a = 17.5\text{mm}$ ,  $p = 1\text{mm}$ , and  $d = 1\text{mm}$ , where the return loss is less than 20 dB and the insertion loss is less than 0.15 dB across the whole X-band. The optimum values were chosen based on trade off between stability of plots within X band and higher and spurious order modes excitation in the structure.

Parametric analysis of ESIW was performed in HFSS by adjusting the width  $a$  of ESIW (since this is the only parameter that can be adjusted) and the optimum dimension  $a=20\text{mm}$  is selected where the return loss is greater than 50 dB and the insertion loss is better than 0.03 dB practically throughout the whole X-band. The optimum values were chosen based on trade off between stability of plots within X band and higher and spurious order modes excitation in the structure.

Transitions between various SIW and other technologies like waveguide, microstrip and ESIW are studied. Simulation based design of these structures are presented. The popular taper transition between microstrip and SIW has been studied and is further modified to get a broader bandwidth by deploying stepped taper transition technique. The simulation results show a much broader response than single taper microstrip to SIW transitions in the literature.

## SIW THEORETICAL CONCEPTS AND TRANSITIONS

---

Transitions between the SIW and waveguide using dual slots were also studied with the help of two designs simulated in ANSYS HFSS. The slots are arranged in such a fashion that they results in a broader band, as opposed to a single slot by resonating them at closer frequencies, and, if they are resonated at distant frequencies, they yields dual band transition response.

A transition operating within the C-Band frequency range, connecting two widely utilized SIC technologies, SIW and ESIW, has been meticulously designed and subjected to simulation. The transfer of power is facilitated by an etched complementary split ring resonator (CSRR), which additionally plays a pivotal role in achieving optimal impedance matching. This compact transition solution, owing to its simplicity and realization on the same substrate, emerges as an effective means of integrating SIW and ESIW components in a multilayered configuration. Consequently, it serves to advance the broader concept of Substrate Integrated Circuits (SIC) by facilitating seamless integration and enhancing overall system functionality.

Some more recent works on different forms of transitions were also studied in [39]-[42] and these can form part of future work.

### References:

- [1] J. Hirokawa and M. Ando, "Single-Layer Feed Waveguide Consisting of Posts for Plane TEM Wave Excitation in Parallel Plates," *IEEE Trans. Ant. Propag.*, vol.46, no.5, pp.625-630, May 1998.
- [2] H. Uchimura, T. Takenoshita, M. Fujii, "Development of a Laminated Waveguide," *IEEE Trans. Microw. Theory Tech.*, vol. 46, no. 12, pp.2438-2443, Dec. 1998

- [3] J. Hirokawa and M. Ando, "Efficiency of 76 GHz Post-Wall Waveguide-Fed Parallel Plate Slot Arrays," in *Proc. 29<sup>th</sup> Eur. Microw. Conf. (EuMC)*, Munich, pp. 271-274, Oct. 1999.
- [4] K. Wu, D. Deslandes, and Y. Cassivi, "The Substrate Integrated Circuits—A New Concept for High-Frequency Electronics and Optoelectronics," *Telecommun. Modern Satellite, Cable, Broadcast. Service*, vol. 1, pp. P-III–P-X, Oct. 2003.
- [5] W. Che, K. Deng and Y. L. Chow, "Equivalence between Waveguides with Side Walls of Cylinders (SIRW) and of Regular Solid Sheets," *Asia Pacific Microwave Conference APMC 2005*, Dec. 2005.
- [6] W. Che, K. Deng, D. Wang, and Y. L. Chow, "Analytical Equivalence between Substrate-Integrated Waveguide and Rectangular Waveguide," *IET Microwaves, Antennas and Propag.*, vol. 2, no. 1, pp. 35–41, 2008.
- [7] A. A. Khan, M. K. Mandal, S. Sanyal, "Unloaded Quality Factor of a Substrate Integrated Waveguide Resonator and its Variation with the Substrate Parameters," in *Proc. Int. Conf. Microw. Photo. Dhanbad*, pp. 1-4, Dec. 2013.
- [8] M. Bozzi, A. Georgiadis, and K. Wu, "Review of Substrate-Integrated Waveguide Circuits and Antennas," *IET Microw. Antennas Propag.*, vol. 5, no. 8, pp. 909–920, Jun. 2011.
- [9] M. Bozzi, L. Perregrini, K. Wu and P. Arcioni "Current and Future Research Trends in Substrate Integrated Waveguide Technology," *RadioEngineering*, vol. 18, no. 2, pp. 201–209, Jun. 2009.
- [10] R.Q. Li, X.H. Tang and F. Xiao, "Substrate Integrated Waveguide Dual-Mode Filter Using Slot Lines Perturbation," *Electron. Lett.*, vol. 46, no. 12, pp. 845-846, Jun. 2010.
- [11] A. J. M. Ros, J.L. G. Tornero, and G. Goussetis, "Multifunctional Angular Bandpass Filter SIW Leaky-Wave Antenna," *IEEE Ant. Wave Propag. Lett.*, vol. 16, pp. 936-939, Oct. 2016.
- [12] D. Deslandes and K. Wu, "Single-Substrate Integration Technique of Planar Circuits and Waveguide Filters," *IEEE Trans. Microw. Theory Tech.*, vol. 51, no. 2, pp. 593–596, Apr. 2003.
- [13] Y. Cassivi, L. Perregrini, K. Wu, and G. Conciauro, "Low-Cost and High-Q Millimeter-Wave Resonator Using Substrate Integrated Waveguide Technique," in *Proc. 32nd Eur. Microwave Conf.*, vol. 2, Milan, Italy, Sep. 23–27, 2002, pp. 737–740, 2002.
- [14] W. D'Orazio and K. Wu, "Substrate-Integrated-Waveguide Circulators Suitable for Millimeter-Wave Integration," *IEEE Trans. Microw. Theory Tech.*, vol. 54, no. 10, pp. 3675–3680, Oct. 2006.



- [15] J. X. Chen, W. Hong, Z. C. Hao, H. Li, and K. Wu, "Development of a Low Cost Microwave Mixer Using a Broad-Band Substrate Integrated Waveguide (SIW) Coupler," *IEEE Microw. Wireless Compon. Lett.*, vol. 16, no. 2, pp. 84–86, Feb. 2006.
- [16] Y. Cassivi and K. Wu, "Low Cost Microwave Oscillator Using Substrate Integrated Waveguide Cavity," *IEEE Microw. Wireless Compon. Lett.*, vol. 13, no. 2, pp. 48–50, Feb. 2003.
- [17] M. Abdolhamidi and M. Shahabadi, "X-band Substrate Integrated Waveguide Amplifier," *IEEE Microw. Wireless Compon. Lett.*, vol. 18, no. 12, pp. 815–817, Dec. 2008.
- [18] Y. Li, W. Hong, G. Hua, J. X. Chen, K. Wu and T. J. Cui, "Simulation and Experiment on SIW Slot Array Antennas," *IEEE Microw. Wireless Compon. Lett.*, vol. 14, no. 9, pp. 446–448, Sep. 2004.
- [19] A. Suntives and R. Abhari, "Design and Characterization of the EBG Waveguide-Based Interconnects," *IEEE Trans. Adv. Packag.*, vol. 30, no. 2, pp. 163–170, May 2007.
- [20] Y. Wang, C. Zhou, K. Zhou, and, W. Wu, "Compact dual-band filtering power divider based on SIW triangular cavities," *Electronic Letters*, vol. 54, no. 18, pp. 1072-1074, Sept. 2018.
- [21] A. A. Khan and M. K. Mandal, "Miniaturized Substrate Integrated Waveguide (SIW) Power Dividers," *IEEE Microw. Wireless Compon. Lett.*, vol. 26, no. 11, pp. 888–890, Nov. 2016.
- [22] K. Song and Y. Fan, "Broadband travelling-wave power divider based on substrate integrated rectangular waveguide," *Electronic Letters*, vol. 45, no. 12, pp. 631–632, July 2009.
- [23] D. Deslandes and K. Wu, "Accurate Modelling, Wave Mechanisms, and Design Considerations of a Substrate Integrated Waveguide," *IEEE Trans. Microw. Theory Tech.*, vol. 54, no. 6, pp. 2516-2526, Jun. 2006.
- [24] F. Xu and K. Wu, "Guided-Wave and Leakage Characteristics of Substrate Integrated Waveguide," *IEEE Trans. Microw. Theory Techn.*, vol. 53, no. 1, pp. 66–73, Jan. 2005.
- [25] M. Bozzi, L. Perregrini, and K. Wu, "Modeling of Radiation, Conductor, and Dielectric Losses in SIW Components by the BI-RME Method," in *Proc. 3<sup>rd</sup> Eur. Microw. Int. Circuits Conf.*, Netherlands, pp. 230-233, Oct. 2008.
- [26] M. Bozzi, M. Pasian, L. Perregrini and K. Wu, "On the Losses in Substrate Integrated Waveguides," in *Proc. 37<sup>th</sup> Eur. Microw. Conf.*, pp. 384–387, Oct. 2007.
- [27] W. Hong, B.Liu, Y. Q. Wang, Y. Q. Wang, Q. H. Lai and K. Wu, "Half Mode Substrate Integrated

- Waveguide: A New Guided Wave Structure for Microwave and Millimeter Wave Application,” in *Proc. Joint 31st Int. Conf. Infr. Millim. Waves 14th Int. Conf. Terahertz Electron.*, China, Sep. 2006.
- [28] Y. J. Cheng, W. Hong, and K. Wu, “Half Mode Substrate Integrated Waveguide (HMSIW) Directional Filter,” *IEEE Microw. Wireless Compon. Lett.*, vol. 17, no. 7, pp. 504–506, Jul. 2007.
- [29] Z. Zhang, N. Yang, and K. Wu, “5-GHz Bandpass Filter Demonstration Using Quarter-Mode Substrate Integrated Waveguide Cavity for Wireless Systems,” in *Proc. IEEE Radio Wirel. Symp.*, pp. 95–98, Jan. 2009.
- [30] C. Jin, R. Li, A. Alphones, and X. Bao, “Quarter-Mode Substrate Integrated Waveguide and its Application to Antennas Design,” *IEEE Trans. Antennas Propag.*, vol. 61, no. 6, pp. 2921–2928, Jun. 2013.
- [31] N. Grigoropoulos, B. Sanz-Izquierdo and P. R. Young, “Substrate Integrated Folded Waveguides (SIFW) and Filters,” *IEEE Microw. Wireless Compon. Lett.*, vol. 15, no. 12, pp. 829–831, Dec. 2005.
- [32] C. Zhao, C. Fumeaux and C. –C.Lim, “Folded Substrate-Integrated Waveguide Band-Pass Filters,” *IEEE Microw. Wireless Compon. Lett.*, vol. 27, no. 1, pp. 22–24, Jan. 2017.
- [33] G. H. Zhai, W. Hong, K. Wuet *al.*, “Folded Half Mode Substrate Integrated Waveguide 3-dB Coupler,” *IEEE Microw. Wireless Compon. Lett.*, vol. 18, no. 8, pp. 512–514, Aug. 2008.
- [34] A. Belenguer, H. Esteban, and V. E. Boria, “Novel Empty Substrate Integrated Waveguide for High-Performance Microwave Integrated Circuits,” *IEEE Trans. Microw. Theory Techn.*, vol. 62, no. 4, pp. 832–839, Apr. 2014.
- [35] F. Parment, A. Ghiotto, T.P. Vuong, J.M. Duchamp, and K. Wu, “Air-Filled Substrate Integrated Waveguide for Low-Loss and High Power-Handling Millimeter-Wave Substrate Integrated Circuits,” *IEEE Trans. Microw. Theory Tech.*, vol.63, no.4, pp.1228-1238, Apr. 2015.
- [36] D. Deslandes and K. Wu, “Integrated microstrip and rectangular waveguide in planar form,” *IEEE Microw. Wireless Compon. Lett.*, vol. 11, no. 2, pp. 68–70, Feb. 2001.
- [37] L. Li, X. Chen, R. Khazaka, and K. Wu, “A transition from substrate integrated waveguide (SIW) to rectangular waveguide,” *Asia Pacific, Microwave Conf. 2009, (APMC 2009), Singapore*, pp. 2605–2608, Dec. 2009.

- [38] L. Li, X. Chen, R. Khazaka, and K. Wu, "Broadband Ka-band rectangular waveguide to substrate integrated waveguide transition," *Electronic Letters*, vol. 49, no. 9, pp. 602–604, Apr. 2013.
- [39] A. K. Nayak, I. M. Filanosky, K. Moez and A. Patnaik, "Broadband Conductor Backed-CPW to Substrate Integrated Slab Waveguide Transition for Ku-Band," *2022 IEEE Radio and Wireless Symposium (RWS), Las Vegas, NV, USA*, pp. 30-33, Jan. 2022.
- [40] A. K. Nayak, I. M. Filanovsky, K. Moez and A. Patnaik, "Broadband Conductor Backed-CPW with Substrate-Integrated Coaxial Line to SIW Transition for C-Band," *IEEE Transactions on Circuits and Systems II: Express Briefs*, vol. 69, no. 5, pp. 2488-2492, May 2022.
- [41] A. K. Nayak, I. M. Filanovsky, K. Moez and A. Patnaik, "A Broadband Coaxial Line-to-SIW Transition Using Aperture-Coupling Method," *IEEE Microwave and Wireless Components Letters*, vol. 32, no. 11, pp. 1271-1274, Nov. 2022.
- [42] A. K. Nayak, I. M. Filanovsky, K. Moez and A. Patnaik, "Broadband Conductor Backed-CPW with Tapered Microstrip Line to Corrugated Via Wall-SIW Transition for Different-Bands (2–40 GHz)," *2023 IEEE International Symposium on Circuits and Systems (ISCAS), Monterey*, pp. 1-5, May 2023.

# CHAPTER 4

## ***A COMPACT, BROADBAND THREE-WAY SIW RIBLET COUPLER***

---

### **4.1. Objective**

The objective in this chapter is to design compact three-way substrate integrated waveguide (SIW) power divider based on Riblet configuration at X-band. The power coupling among the three output ports is achieved due to short openings in the narrow walls of the central SIW channel. Matching posts are additionally placed to improve the performance in return loss and isolation among ports as well. The posts are placed at the input and output ends of the coupling region. This is the only SIW three-way power divider that shows non-adjacent port isolation among six-port couplers.

### **4.2. Introduction**

Multi-way power dividers and splitters are used in the design of phased array antennas, high power amplifiers, and beam forming networks and are also gaining popularity within the substrate integrated waveguide (SIW) technologies [1]. SIW based power dividers are proposed in various configurations such as Wilkinson power dividers [2], Gysel power dividers [3], Riblet couplers [4], crisscross directional couplers [5], multi-aperture couplers [6], and recombinant couplers [7]. Wilkinson power divider requires lumped resistors which makes it inapt at microwave and millimeterwave frequencies [2]. Though, Gysel power dividers [3] are compact,

## A COMPACT, BROADBAND THREE-WAY SIW RIBLET COUPLER

---

they suffer from higher insertion loss, narrow bandwidth and design complexities. Riblet couplers [4] are compact and provide moderate bandwidth, but they are mostly used for even ways of power division. Crisscross power dividers [5] are multi-way power dividers, but they are narrow band and are not compact. Though, multi-aperture [6] and recombinant power dividers [7] provide wide bandwidth and good power division characteristics, they are large. Conventional three-way power dividers in waveguide technology [8]-[9] provide low insertion loss and good isolation characteristics, but have narrow fractional bandwidth of 10 to 15% and are bulky. The demand within the researchers and the industry is to design less bulky multi-way splitters and power dividers which would be effective as a Substrate Integrated Circuit (SIC) [10]-[11]. Wideband six-port SIW power dividers/ combiners reported in [12] present a low cost and planar design. Researchers proposed a compact substrate integrated waveguide-based six-port coupler at X-band [13]. A multi-functional half mode SIW six-port power divider using the slot in the coupling region was proposed [14], however, due to the slot in the SIW, it suffers from radiation losses. In [15] and [16] a three-way power divider in SIW using narrow wall coupling was designed, they exhibit good insertion loss but the isolation and reflection coefficient are poor. Moreover, the power dividers are narrowband. Though, these designs are compact, provide good reflection coefficient and isolation between adjacent ports, but do not report about isolation between non-adjacent output ports. The isolation between non-adjacent output ports would also affect the performance of the power divider as reflected signal would interfere with the signals in other ports resulting in a reduction of fractional bandwidth and affecting the overall performance of the transmitters and receivers.

This chapter presents a study on compact planar three-way SIW power divider. The power divider utilizes Riblet configuration for power division. By enhancing the  $TE_{m0}$  modes in the

## A COMPACT, BROADBAND THREE-WAY SIW RIBLET COUPLER

---

coupling region using symmetrical posts at input and output ends the isolation and return loss for the power divider are achieved. It achieves good return loss and isolation characteristics over 27.3% fractional bandwidth. The coupling length of the power divider is  $1.55\lambda_g$  at a center frequency of 9.6 GHz. The power divider may find applications in transmitters as power combiner and in receivers as power divider to feed LO signals.

### 4.3. Riblet Coupler

Directional couplers are critical components for implementing power splitting and combining networks [8]-[18]. The four-port coupler is a fundamental component that can be implemented in a variety of electrical and geometrical configurations. Compact power splitting and combining networks can be created using multiport directional couplers with six or more ports.

The traditional two-ways division narrow-wall short slot coupler or the Riblet coupler is a four-port device composed of two parallel waveguides connected by a single aperture created by removing the common narrow wall [17], [18]. The phase difference between the  $TE_{10}$  and  $TE_{20}$  modes flowing through the coupling region determines the coupling. The efficient coupling to the coupled port of the two way directional coupler depends on the efficient interaction between the two modes  $TE_{10}$  and  $TE_{20}$  [18].  $TE_{10}$  and  $TE_{20}$  indicate one half cycle variation and two half cycle variations along the width of the guide structure respectively with maximum of the field at the center of the respective line. Hence for two way division,  $TE_{20}$  mode excitation plays a very important role which has two half cycle variations with each cycle coupled to each one of two output ports. The coupler's coupling zone functions as an enlarged waveguide, with dimensions

## A COMPACT, BROADBAND THREE-WAY SIW RIBLET COUPLER

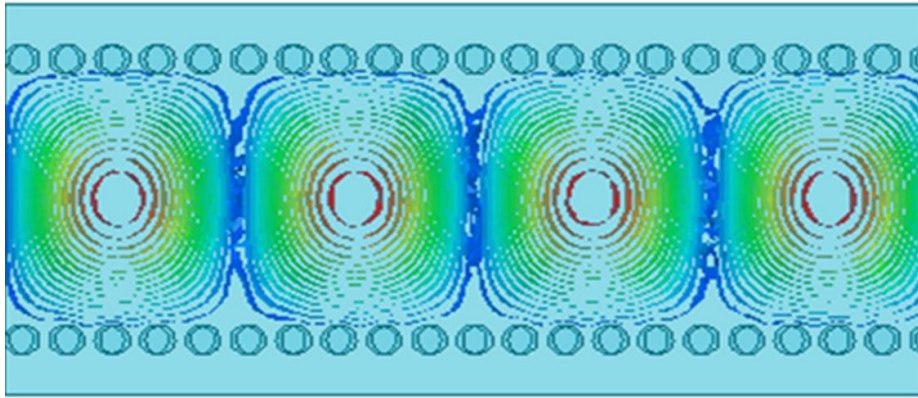
---

that allow the  $TE_{10}$  (even) and  $TE_{20}$  (odd) modes to exist while the  $TE_{30}$  mode is cutoff and non-propagative. The development of  $TE_{30}$  mode limits the bandwidth of a Riblet coupler [17]. As a result, the breadth of the contact region must be lowered in general to prevent the spread of the undesirable  $TE_{30}$  mode. For broad bandwidth coupling, the interaction zone and the two adjacent rectangular waveguides must be conjugate matched. To achieve the impedance match, H-plane tapers are used.

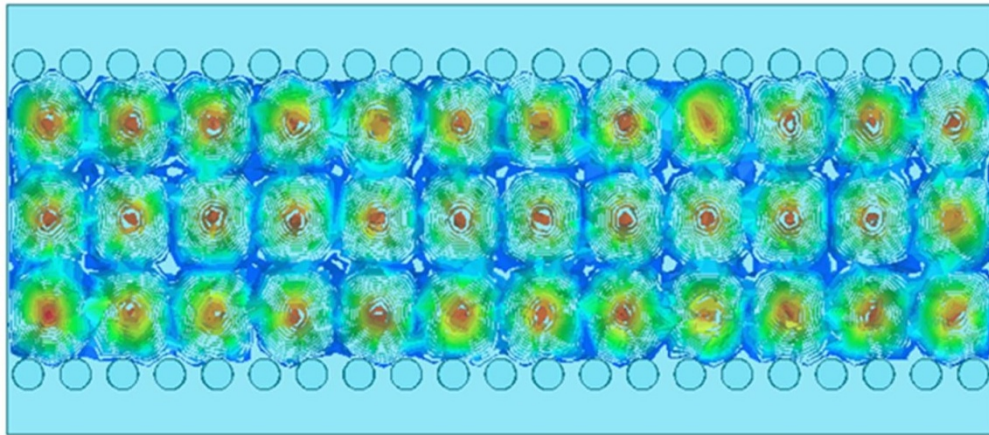
Three-ways division Riblet coupler [8] is made up of three waveguides separated by two metallic shims, with the coupling region constructed by inserting narrow slots along the smaller waveguide dimension. The efficient coupling to the coupled port of the three way directional coupler depends on the efficient interaction between the two modes  $TE_{10}$  and  $TE_{30}$  [17].  $TE_{10}$  and  $TE_{30}$  indicate one half cycle variation and three half cycle variations along the width of the guide structure respectively with maximum of the field at the center of the respective line. Hence for three way division,  $TE_{30}$  mode excitation plays a very important role which has three half cycle variations with each cycle coupled to each one of three output ports. The width of the coupling region is determined by the matching elements on each side of it. The matching components are configured in such a way that modes greater than  $TE_{30}$  do not propagate in the coupling region. In [8], in the coupling zone, two cylindrical posts are symmetrically positioned. To reduce reflections, a linear taper in the input waveguide is used near the coupling region. The waveguide matched terminations absorb the power in the isolated ports. EccosorbR MF-117 is used to create the waveguide pyramidal terminations. The two cylindrical posts have three functions: a) creation of the  $TE_{30}$  mode, which works in conjunction with the  $TE_{10}$  mode to give equal power division at the three output ports; b) reduction in reflections from the metallic shims, resulting in a broader bandwidth; and c) reduction in coupling length compared to conventional power

## A COMPACT, BROADBAND THREE-WAY SIW RIBLET COUPLER

divider. In the  $TE_{mn}$  mode, m denotes the number of half cycle variations of E field along the breadth of the guide structure and n along the height of the same. For example,  $TE_{30}$  mode indicates there is three half cycles variation of E field along the breadth, and no variations of E field along the height of the structure, which means that the magnitude and phase of the E field is constant. The E-field configurations for  $TE_{10}$  and  $TE_{30}$  modes in SIW are illustrated in Fig. 4.1, which is generated using Ansys HFSS.



(a)



(b)

Fig. 4.1. Ansys HFSS E-field plot in an SIW channel for (a)  $TE_{10}$  and (b)  $TE_{30}$  modes.



### 4.4. Three-way SIW Riblet Coupler

#### A. Layout

The coupler consists of three SIW channels, as shown in Fig. 4.2. The coupling region is optimized by using the coupling tapers, to achieve good power division. SIW to microstrip transition is used for the measurement of the power divider. Matching posts are used at the input and output of the coupling region for the improvement of the reflection coefficient and isolation of the power divider. The transition is designed using a microstrip taper and two transition-vias placed symmetrically about it [10]. Transition-vias are used to achieve good transmission and reflection coefficients for the transitions. As the power divider's ports are designed with the microstrip to SIW transition to feed the signals with standard SMA connectors, matching posts at input and output of the coupling region are used for the improvement of the reflection coefficient and isolation of the power divider.

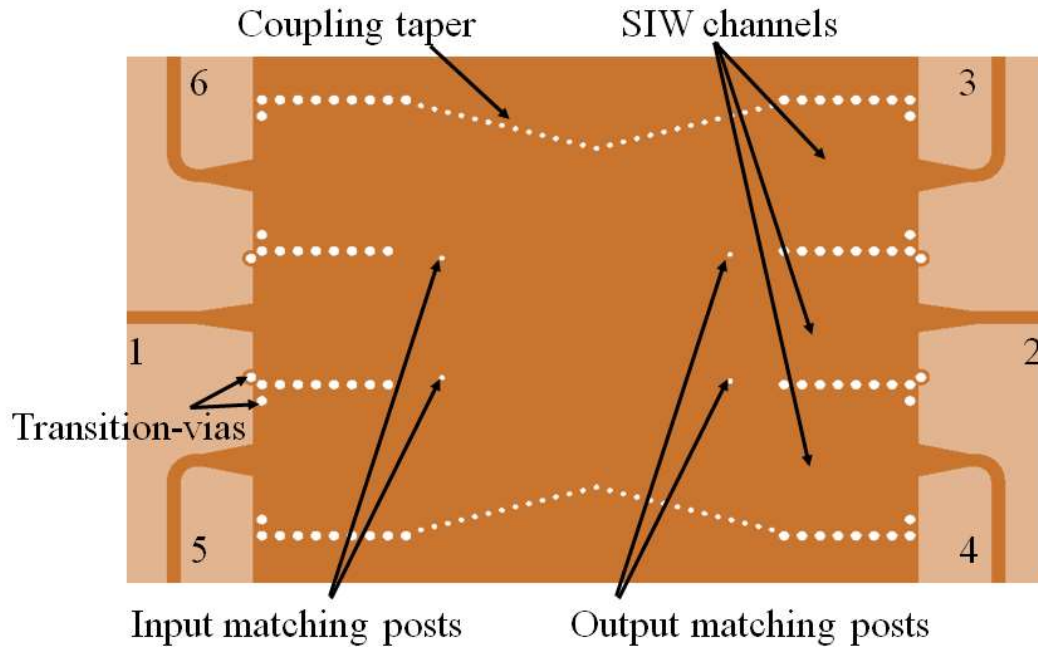


Fig. 4.2. The proposed structure of the three-way SIW Riblet Coupler

### *B. Design Principle*

The steps for designing the power divider are summarized below based on the Fig. 4.3:

1. The design process starts with the selection of SIW channel dimensions, to propagate dominant  $TE_{10}$  mode. The three-way coupler's SIW channels are designed with standard SIW waveguide dimensions  $a$ . The equivalent width of the channels  $W_{siw}$  is given below [11].

$$W_{siw} = a - \frac{(2R_4)^2}{0.95p} \quad (4.1)$$

2. The coupling area is designed as described by [9]. The coupling area is widened to enhance the bandwidth. This is achieved by increasing the outer SIW channel. The width of the coupling region  $W$  is governed by the relation given by  $3\lambda_g/2 < W < 5\lambda_g/2$ .
3. The length of the coupling region  $L$  is given as  $L = (2m+1)\pi/(\beta_1 - \beta_3)$ , where  $\beta_1$  and  $\beta_3$  are the propagation constants of  $TE_{10}$  and  $TE_{30}$  modes, respectively. Based on the above steps the initial design dimensions are calculated.
4. An increase in channel width results in the degradation of return loss and isolation at the mid-band frequencies due to reflections from SIW channel walls and also due to the interaction of reflected waves between the non-adjacent ports, respectively. Metallic posts are introduced at the input to reduce the reflections and introduce  $TE_{30}$  mode, which would interact with the  $TE_{10}$  mode to give equal power division at the three output ports. The vias are symmetrically placed at an initial distance of  $\lambda_g/3$  from the central SIW channel walls based on the electric field distribution.

## A COMPACT, BROADBAND THREE-WAY SIW RIBLET COUPLER

5. Electromagnetic optimization is carried out to obtain the required return loss over the bandwidth. Though, return loss improves, the isolation between the non-adjacent ports has a resonance in the required bandwidth.
6. The outer posts are also symmetrically placed at an initial distance of  $\lambda_g/3$  and optimized to obtain isolation better than 15 dB over the bandwidth. These posts impede the interaction of the non-adjacent port reflections and also the reflections from input posts resulting in enhanced return loss and isolation bandwidths.

The dimensions and optimized values of the coupler's structure are shown in Fig. 4.3 and Table 4.1, respectively.

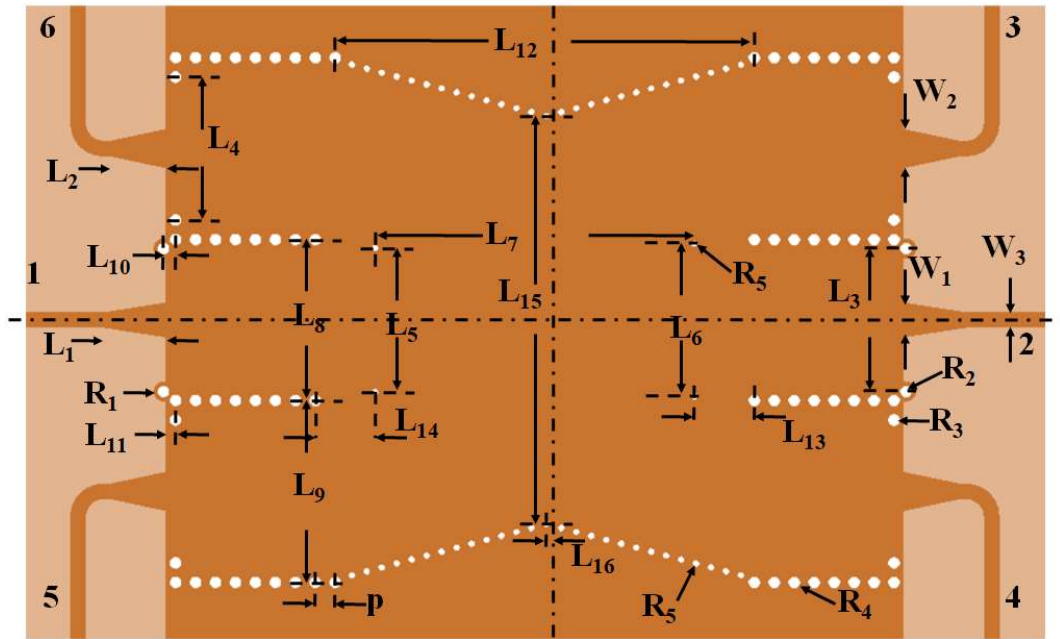


Fig. 4.3. Design parameters of the three-way SIW Riblet Coupler.

## A COMPACT, BROADBAND THREE-WAY SIW RIBLET COUPLER

TABLE 4.1  
Optimized Dimensions of the Three-Way SIW Riblet Coupler (Unit: Millimeters)

L1	L2	L3	L4	L5	L6	L7	L8	L9
5.8	5.2	13.6	13.6	13.7	14.5	30.4	15.3	17.3
L10	L11	L12	L13	L14	L15	L16	W1	W2
1.15	1	39.9	5.7	5.7	38.8	1.1	3.4	3.8
W3	R1	R2	R3	R4	R5	p	$\epsilon_r$	h
1.6	1	0.5	0.5	0.5	0.25	1.9	2.2	0.508

### *C. Working Principle based on the design*

It is known that the power division in couplers depends on the interaction of  $TE_{10}$  and  $TE_{30}$  modes in the coupling region [8]-[9]. The coupling tapers are optimized to achieve the required power division and eliminate higher-order modes. Since the coupling region is dependent on the guided wavelength, the bandwidth is limited to 10-15% as shown in Fig. 4.4 and 4.5. Based on the layout in Fig. 4.2 and the design steps mentioned in the previous section, Fig. 4.4 and 4.5 shows the variation of the simulated input return loss  $S_{11}$ , and, simulated isolation between non-adjacent output ports  $S_{43}$ , respectively, in the coupler, between equal waveguide channel (without posts), unequal waveguide channels (without posts), unequal waveguide channels (with two input posts), unequal waveguide channels (with two input and two output posts).

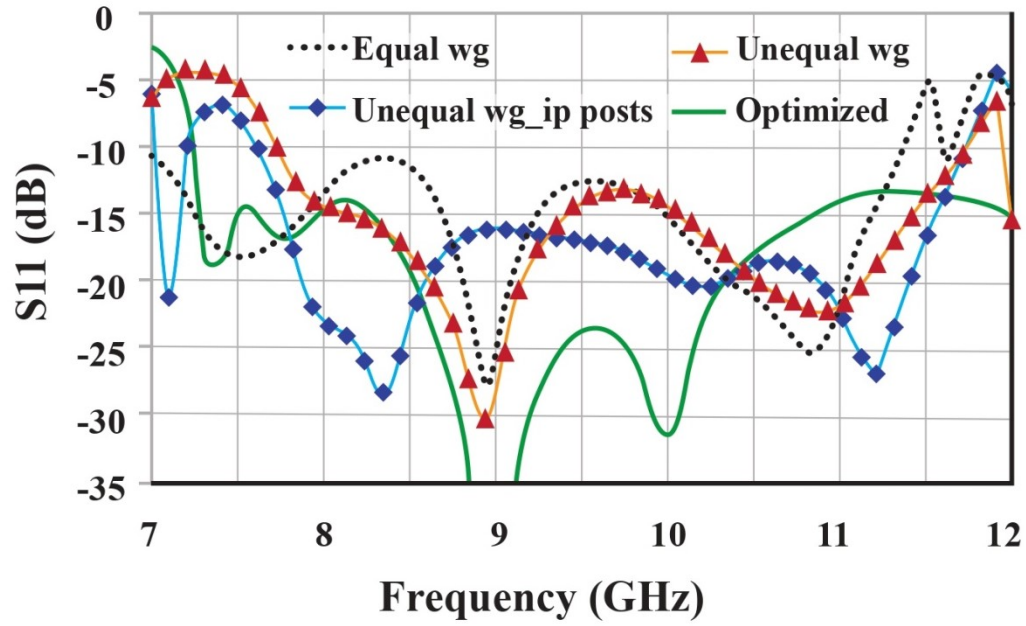


Fig. 4.4. Simulated reflection coefficient with variations in the coupler structure. The optimized structure consists of unequal SIW channels, input, and output posts.

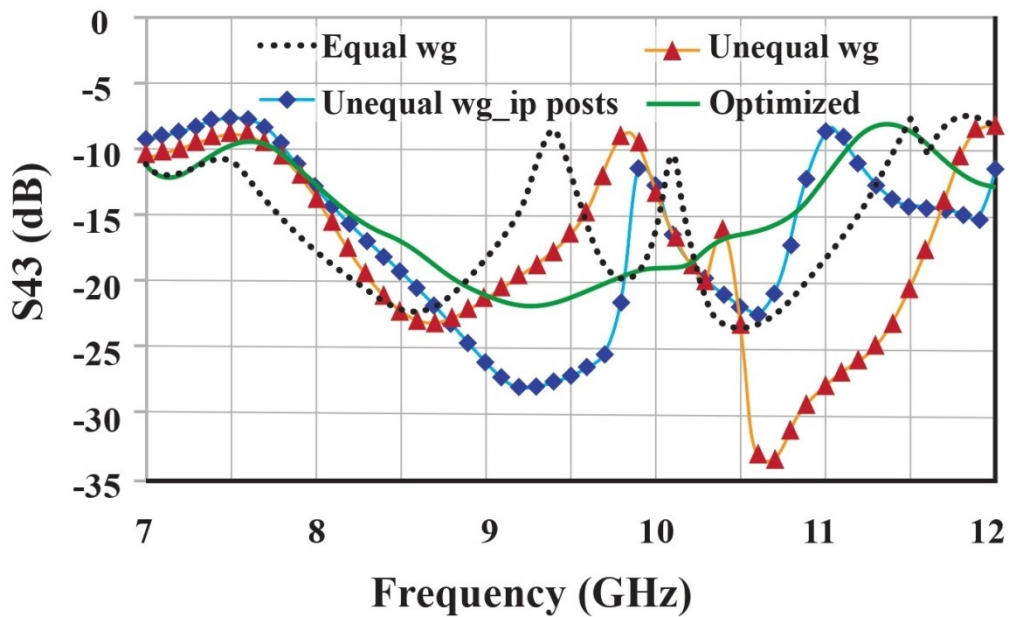


Fig. 4.5. Simulated isolation coefficient with variations in the coupler structure. The optimized structure consists of unequal SIW channels, input, and output posts.

## A COMPACT, BROADBAND THREE-WAY SIW RIBLET COUPLER

---

It shows that the three SIW channels are symmetrical provides 10% fractional bandwidth for equal power division, and better than 15 dB reflection coefficient and isolation among ports. To increase the bandwidth without affecting the isolation characteristics, unequal channel widths are proposed. The outer channels of SIW are extended to enhance the coupling areas for broader power division bandwidth. The power division bandwidth increases to 29.7%, however, there is no significant improvement in reflection coefficient and isolation at mid-band frequencies as shown in Fig. 4.4 and 4.5. The signal from port 3 entering the coupling area is leaked towards port 4 and vice versa due to the wider coupling region. As the coupling region is increased, higher-order  $TE_{m0}$  modes are excited causing degradation of isolation and reflection coefficient between the outer channels. In order to restrict this, matching posts are introduced at the input side in the coupling region based on electric field distribution. The input posts improve the reflection coefficient but slightly over couple the energy into the outer SIW channels. Though the power division and reflection coefficient improvement is seen, the isolation bandwidth is only 17%. To improve the isolation, output side posts are introduced. The optimized output posts in conjunction with input posts improve the reflection coefficient as well as isolation by reducing the reflections from the SIW channel vias and suppressing the higher  $TE_{m0}$  modes, respectively. The only disadvantage is the over coupling of power to the outer SIW channels. The overall isolation bandwidth of the optimized power divider is 27.3%. The investigation of unequal SIW channels widths, matching posts at input and output sides of the coupling region are validated by examining the reflection and isolation coefficient characteristics of the power divider as shown in Fig. 4.4 and 4.5, respectively. The E-field and H-field distribution for the power divider at centre frequency are shown in Fig. 4.6.

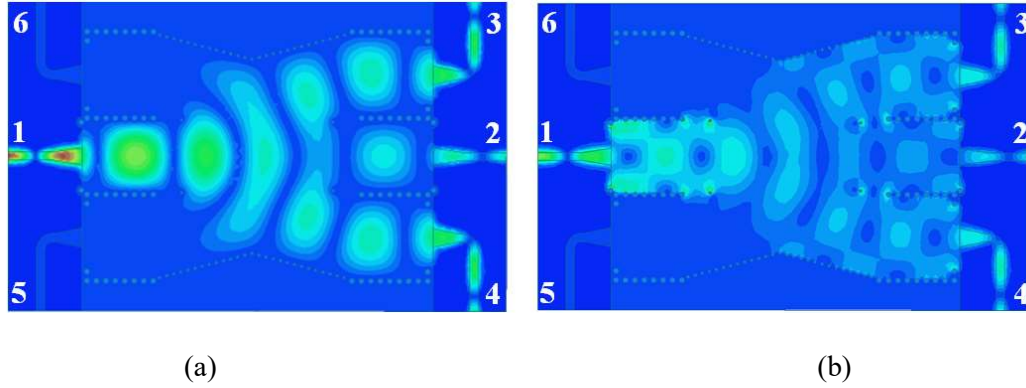


Fig. 4.6. Field distribution of the three-way SIW riblet coupler at the centre frequency with excitation at port 1. (a) Electric field distribution (b) Magnetic field distribution.

### ***D. Fabrication and Experimental results***

The power divider is simulated in 3D EM simulator Ansys HFSS. The analysis presented in Section 2 is based on the simulations accounting for the variations in SIW channels, input, and output posts. The power divider is optimized to achieve better reflection and isolation coefficients. The optimized power divider is fabricated on Rogers 5880 substrate with 20 mil thickness to demonstrate the feasibility of the power divider. The fabricated photograph of the power divider is shown in Fig. 4.7.

## A COMPACT, BROADBAND THREE-WAY SIW RIBLET COUPLER

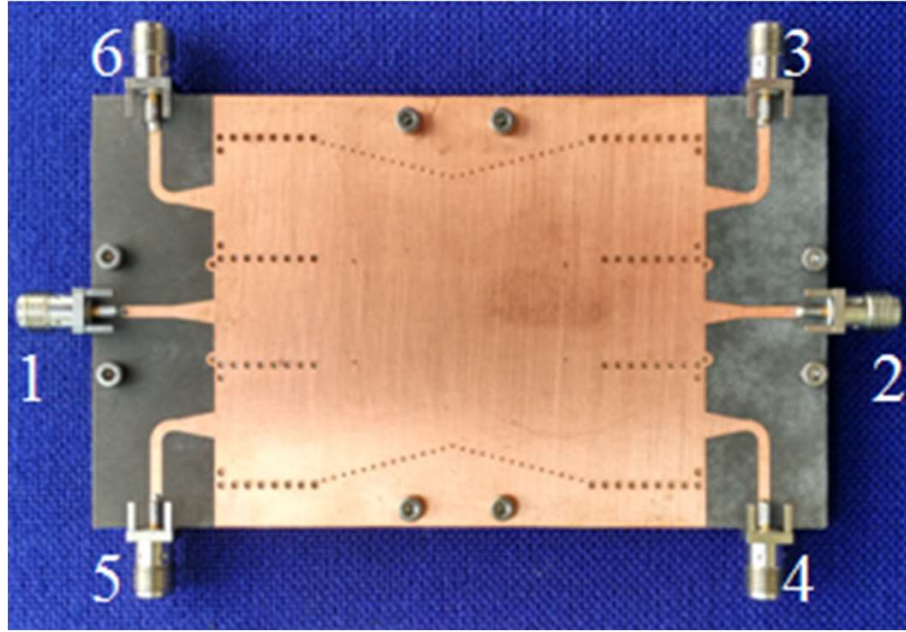


Fig. 4.7. The fabricated prototype of three-way SIW Riblet Coupler.

The measured data are obtained by Keysight E8364B vector network analyzer. During the measurement of the power divider, port 5 and port 6 are terminated with a matched load. Further reduction in the power divider size can be achieved by internally terminating ports 5 and 6. The simulated and measured power division characteristics of the power divider are shown in Fig. 4.8. The over coupling in the outer SIW channels as discussed in section 2 is due to input and output matching posts. SIW to microstrip and microstrip to SMA connector transition losses contribute to the insertion loss.



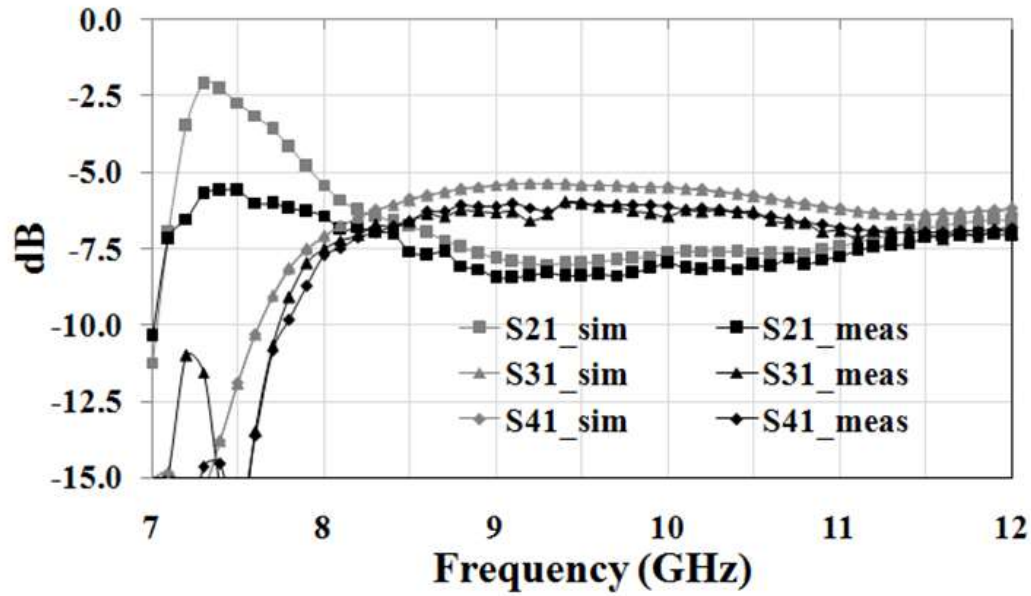


Fig. 4.8. Simulated and measured power division at three output ports of the three-way SIW riblet coupler.

The power divider reflection coefficient and isolation characteristics are shown in Fig. 4.9. The measured isolation and reflection coefficient is better than 15 dB over a fractional bandwidth of 27.3%. There is a close agreement between the simulated and measurement results validating the proposed power divider design. The fabrication tolerances may cause a slight mismatch in the simulated and measured results.

## A COMPACT, BROADBAND THREE-WAY SIW RIBLET COUPLER

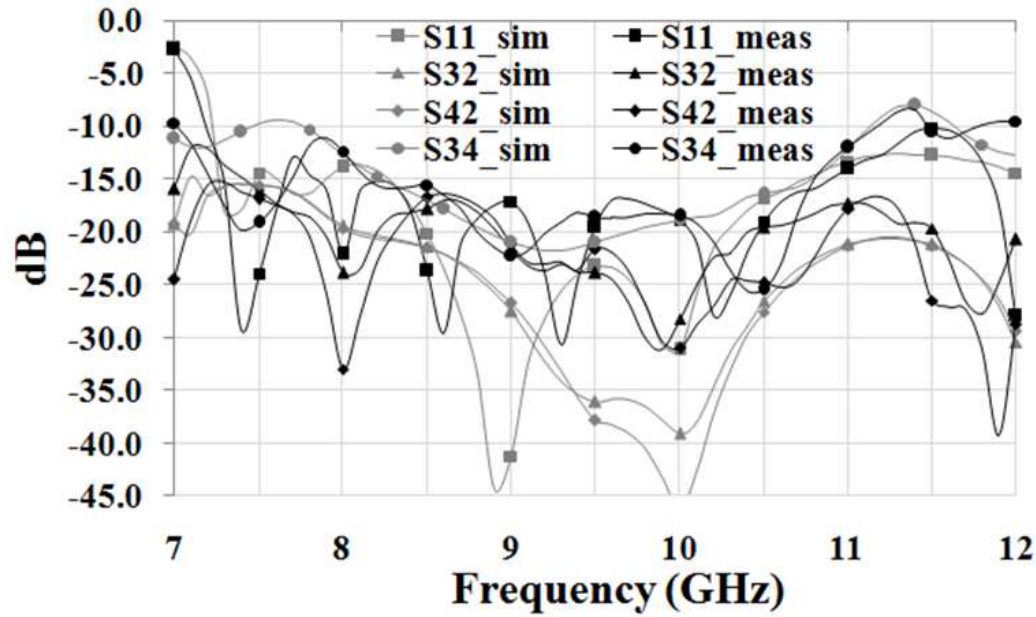


Fig. 4.9. Simulated and measured reflection and isolation coefficient between the ports of the three-way SIW riblet coupler.

The output transmission phase is shown in Fig. 4.10. The  $\angle S_{31}$  and  $\angle S_{41}$  plots are in-phase, and  $\angle S_{21}$  is slightly shifted due to different path lengths of port 3 (port 4). It is also evident from Fig. 4.5 that  $\angle S_{21}$  shifts with the insertion of posts in the coupling region.

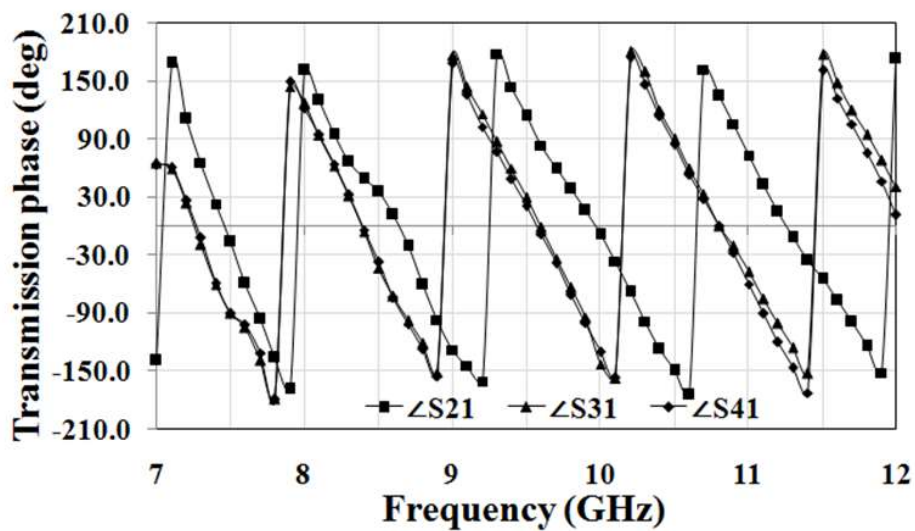


Fig. 4.10. Measured transmission phase of output ports of the three-way SIW riblet coupler.

## A COMPACT, BROADBAND THREE-WAY SIW RIBLET COUPLER

The measured fractional bandwidth of 27.3% is achieved with a coupling length of 41.8mm, which corresponds to  $1.55\lambda_g$  at the centre frequency. Table 4.2 shows the comparison of the proposed power divider with other reported power dividers. All the power dividers have an operating frequency in X-band. The implementation configurations for all the power dividers are six-port coupler. The coupling length of this work compared with ref [12], ref [13] and ref [6] are much smaller. However, the fractional bandwidth is higher than the above references. The isolation and return loss for the power dividers is better than 15 dB; however, none of the references provide non-adjacent output port isolation, which is critical in designing power dividers for transmitters and receivers. From the comparison, it is evident that the power divider provides compact size, broad bandwidth, and good isolation characteristics between the adjacent and non-adjacent ports.

TABLE 4.2  
Comparison of performances with other reported structures

Reported papers	<i>Ref [6]</i>	<i>Ref [12]</i>	<i>Ref [13]</i>	<i>Ref [14]</i>	<i>Ref [15]</i>	This work
Technology	SIW	SIW	SIW	SIW	SIW	SIW
Configuration	Multi-aperture	Six-port	Six-port	Six-port	Six-port	Six-port
Frequency (GHz)	12.5-16.4	11.7-12.7	11-12.4	10.03-12.28	27.3-28.7	8.2-10.8
Size (Coupling length)	$2.77\lambda_g$	$2.00\lambda_g$	$2.32\lambda_g$	$1.63\lambda_g$	$1.69\lambda_g$	$1.55\lambda_g$
Fractional Bandwidth (%)	27	15	13	23.5	5	27.3
Isolation non-adjacent ports (dB)	-	-	-	-	-	>15
Isolation adjacent ports (dB)	>16.5	>15	>15	>15	>11	>15
Return loss (dB)	>16.5	>15	>15	>15	>11	>15

### 4.5. Conclusion

A compact, broadband X-band SIW three-way power divider based on a six-port coupler with enhanced isolation among the ports is presented. The power divider exhibits a reflection coefficient and isolation better than 15 dB over a fractional bandwidth of 27.3%. The coupling length is only 41.8mm which corresponds to  $1.55\lambda_g$  at the centre frequency. Compared with other reported three-way power dividers, the proposed design is considerably compact, broadband, and provides higher isolation among the output ports. Specifically, it is used in X-band transmitters for power combining to enhance the power handling capacity of the power amplifiers and in X-band three-channel receivers for LO power division which is used for pumping mixers. The power divider can also be used in sub-arrays for feeding the signal. The presented design exhibits good isolation characteristics between adjacent and non-adjacent ports.

### References:

- [1] K. Wu, "State-of-the-art and future perspective of substrate integrated circuits (SICs)," *IEEE Substrate Integr. Circuits*, in *Proc. MTT-S Int. Microwave Symp.*, Anaheim, CA, USA, May 2010.
- [2] T. Djerafi, D. Hammou, K. Wu, and S. O. Tatu, "Ring -shaped substrate integrated waveguide Wilkinson power dividers/combiners," *IEEE Trans. Compon..Packag. and Manufac. Techn.*, vol. 4, no.9, pp. 1461–1469, Sept.2014.
- [3] H. Chen, W. Che, X. Wang and W.Feng, "Size-reduced planar and non-planar SIW Gysel power divider based on low temperature co-fired ceramic technology," *IEEE Microw. Wireless Compon. Lett.*, vol. 27, no.12, pp. 1065-1067, Dec. 2017.
- [4] Q. L. Yang, Y. L. Ban, k. Kang, C. Y. D. Sim and G. Wu, "SIW multibeam array for 5G mobile devices," *IEEE Access*, vol. 4, no.12, pp. 2788-2796, 2016.

- [5] K. Takahashi, T. Kawai, M. Kishihara, I. Ohta and A. Enokihara, "Multiple-port SIW power divider utilizing cascade-connected crisscross directional couplers," in *Proc. German. Microw. Conf.*, Nurember, Germany, Mar. 2015.
- [6] Z. Liu, and G. Xiao, "Design of SIW-based multi-aperture couplers using ray tracing method," *IEEE Trans. Compon., Packag., Manuf. Techno.*, vol. 7, no.1, pp. 106–113, Jan. 2017.
- [7] T. Djerafi, A. Patrovsky, K. Wu, and S. O. Tatu, "Recombinant waveguide power divider," *IEEE Trans. Microw. Theory Tech.*, vol. 61, no.11, pp. 3884–3891, Nov. 2013.
- [8] G. A. Kumar, B. Biswas and D. R. Poddar, "A compact broadband Riblet-type three-way power divider in rectangular waveguide," *IEEE Microw. Wireless Compon. Lett.*, vol. 27, no.2, pp. 141–143, Feb. 2017.
- [9] F. Alessandri, M. Giordano, M. Guglielmi, G. Martirano and F. Vitulli, "A new multiple-tuned six-port Riblet-type directional coupler in rectangular waveguide," *IEEE Trans. Microw. Theory Tech.*, vol. 51, no.5, pp. 1441–1448, May 2003.
- [10] Z. Kordiboroujeni, and J. Bornemann, "New Wideband transition from microstrip line to substrate integrated waveguide," *IEEE Trans. Microw. Theory Tech.*, vol. 62, no.12, pp. 2983–2989, Dec. 2014.
- [11] M. Bozzi, A. Georgiadis and K. Wu, "Review of substrate-integrated waveguide circuits and antennas," *IET Microwaves, Antennas & Propagation*, vol.5, no.8, pp. 909–920, 2011.
- [12] M. Salehi, J. Bornemann, and E. Mehrshah, "Wideband substrate-integrated waveguide six-port power divider/combiner", *Microwave and Optical Technology Letters*, vol. 55, no. 12, pp. 2984–2986, Dec. 2013.
- [13] G. Venanzoni, D. Mencarelli, A. Morini, M. Farina, O. Losito, and F. Prudenzeno, "Compact substrate integrated waveguide six-port directional coupler for X-band applications", *Microwave and Optical Technology Letters*, vol. 57, no. 11, pp. 2589–2592, Nov. 2015.
- [14] S. Karamzadeh, V. Rafiei, and H. Saygin, "A new multi-functional half mode substrate integrated waveguide six-port microwave component", *Progress in Electromagnetics Research Letters*, vol. 69, pp. 71–78, July 2017.
- [15] T. Guo, B. You, and K. Wu, "A 2 X 3 hybrid substrate integrated waveguide coupler applied to beam forming network", *In Proceedings of 49<sup>th</sup> European Microwave Conference, Paris, France*, 2019.

- [16] J. W. Lian, Y. L. Ban, J. Q. Zhu, K. Kang, and Z. Nie, "Compact 2-D scanning multibeam array utilizing the SIW three-way couplers at 28 GHz", *IEEE Antennas and Wireless Propagation Letters*, vol. 17, no. 10, pp. 1915-1919, Oct. 2018.
- [17] T. Tanaka, "Ridge-Shaped Narrow Wall Directional Coupler Using TE<sub>10</sub>, TE<sub>20</sub>, and TE<sub>30</sub> Modes", *IEEE Transactions on Microwave Theory and Techniques*, vol. 28, no. 3, pp. 239-245, Mar. 1980.
- [18] K. Kuroiwa, A. Gonzalez, M. Koyano, T. Kojima, Y. Fujii, Y. Uzawa, and H. Ogawa "Short-slot Hybrid Coupler Using Linear Taper in W-band", *Journal of Infrared, Millimeter, and Terahertz Waves*, vol. 34, pp. 815-823, Oct. 2013.



# CHAPTER 5

## ***COMPACT, BROADBAND AND MULTIBAND SIW RADIAL POWER DIVIDER***

---

### **5.1. Objective**

The objective in this chapter is to design a compact eight-way substrate integrated waveguide (SIW) based radial power divider for broadband and dual band applications. This is achieved by introducing planar impedance transformer consisting of an annular slot and circular patch at the input and output feed positions. The equivalent circuit analysis helps in the optimization of the annular slot and circular patch on the substrate which results in a broadband operational bandwidth. Additionally, by employing complementary split ring resonator (CSRR) metamaterial, dual band results are achieved.

### **5.2. Introduction**

Multi-way planar power dividers are used in various microwave applications such as antenna array feed networks, multiplexers, and high power amplifiers, which are some of the integral components in sub 6-GHz 5G base stations and satellite communication systems at C-Band. Compact, low cost and ease of integration are the basic requirements of planar power dividers in modern dense packaged systems. Since, SIW has similar field distributions as



rectangular metallic waveguides and has a Quality factor higher than most of the planar transmission line technologies, and, can be integrated in the planar systems without any mechanical assembly [1], it has become quite popular to design planar power dividers,. Several planar multi-way power dividers designed in various transmission lines and technologies, are investigated [2]-[11], however, they have their own advantages and limitations.

An eight-way ridge SIW power divider is presented in [2], in which grounded coplanar waveguide to ridge SIW transitions, T-junctions and  $90^\circ$  bends are used. Although, it has a broadband response of 28.13% bandwidth, the design is complex and integration is difficult. Moreover, at certain frequencies within the band, it exhibits an insertion loss higher than 1dB. The five-way Wilkinson power divider designed in microstrip uses an additional layer for the interconnection of the isolation resistors in order to improve the insertion loss [3]. Broadband responses are achieved in two four-way microstrip power dividers, operating in the entire S-band and X-band, respectively [4],[5]. Though, the footprints of the circuit are slightly higher, they produce filtering responses during the power division outputs. Subsequently, in order to reduce the size, instead of using SIW-microstrip transitions, direct co-axial feed is appended at the input of various miniaturized  $1/32$ th mode SIW power dividers [6]. This technique is also used in the design of radial SIW power divider [7]. Though, the compact dividers reported in [6],[7] have lower insertion loss, they are narrow band. Various techniques have been proposed to enhance the bandwidth characteristics of direct co-axial fed multi-way power dividers [8]-[11]. A coaxial taper is designed in a waveguide to provide a smooth impedance match over a broad bandwidth between the SMA connectors and the microstrip power divider [8] and waveguide power divider [9], respectively. Stepped coaxial transformer is used, instead of coaxial taper impedance

transformers, along with a dual-disk probe in a broadband SIW four-way power divider [10] which has a 15dB return loss bandwidth over 35.29%. Suspended stripline eight-way power combiner in [11] utilizes a cylindrical waveguide cavity to realize a wide band response of 28.78%. However, the additional coaxial transformers mentioned in [8]-[11] require complicated mechanical fabrication, which makes the circuit bulky.

Passive devices and components such as power dividers, filters are essential in the present day's wireless communication systems. However, with the demand for effectiveness and high integration capabilities in planar system assemblies, along with the minimization of losses, intelligent multi-functional components are replacing multi-component systems, such as the microstrip filtering power dividers in [12]-[14]. The microstrip Wilkinson power divider reported in [12] have two-way power division with dual-band filtering in their response at S-band (at 2.3 and 3.5 GHz) by incorporating dual resonance resonators at the two outputs. It also exhibits a wide stop band with 20 dB rejection level. A dual band filtering power divider in microstrip configuration with wideband response is proposed in [13] at S-band. The tested fabricated power divider has a 3 dB bandwidth of 36.5% and 22.3%. It is achieved by introducing a coupling topology with the help of two open stub resonators. In [14], two multi mode resonators have been used to construct the dual band power divider at 1.58 and 2.89 GHz, with isolation better than 21 db in the entire pass bands. However, even though [12]-[14] show good filtering characteristics, the insertion losses are more than 0.8 dB. Multiway planar power dividers, which finds usages in various microwave applications and act as integral components in wireless communication systems have also been developed into filtering power dividers [15]-[17]. A dual-band three-way microstrip Wilkinson power divider is reported in [15], which operates in the L-band at 0.6 GHz and in the S-band at 2.45 GHz. However, the structure is not

compact and results in amplitude imbalances of more than 1 dB at the higher band. The Bagley Polygon designs [16] are realized in both three and five-ways of power division at L- and S-bands. They show good rejection of more than 10 dB between two passbands with 0.8 GHz in the three-way power divider and 1 GHz in the five-way power divider. Subsequently, high isolation and good matching are obtained in the four-way dual-band microstrip design [17]. Due to the high-quality factor of SIW ( $270 \pm 20$ ) [18], compact multi-functional components are also realized and integrated into the planar systems without any extra mechanical assembly like the dual-band power divider in [19]. Even though the power divider shows good rejection between two passbands in C- and X- bands, the insertion loss is 0.9 dB, and 1.5 dB respectively. At present, filtering power dividers in SIW are not developed for multiway power division and are hence limited to two ways of division.

This chapter presents a study on direct-coaxial fed  $N$ -way multiway radial power dividers in SIW configuration operating at C-band. Equivalent circuit analysis is carried out to understand the behavior of the power division from narrow band response to a broader bandwidth, for various  $N$ -way radial SIW power dividers. Planar impedance matching is the key for obtaining broader bandwidth. This is achieved through proper optimization of planar annular slot and circular patch at the input and output ports. A broadband eight-way radial SIW power divider is also fabricated and measured. The percentage bandwidth for the power divider is 53.5% with 15 dB input return loss. The advantage of this multi-way planar power divider is its broad bandwidth, compactness and ease of integration with other planar circuits. Further, an eight-way dual-band radial SIW power divider which operates at S-band and C-band is also designed. The combined design of complementary split-ring resonators (CSRR) and the radial power divider resulted in dual-band multiway power division. Proper etching of CSRRs at the common walls of

the sectorized power divider is the key to obtain a stopband in the otherwise broadband power divider response. The proposed power divider operates at 3.5 GHz and 7 GHz having a 10 dB return loss bandwidth of 17.14 % and 25.92 %, respectively. The planar configuration along with its filtering capabilities without any usage of discrete components for power division and filtering makes the multiway dual-band power divider advantageous. A good rejection between the two desired passbands is achieved at 5.5 GHz with a return loss of 28.35 dB. The rejection bandwidth of more than 10 dB is measured at 2.25 GHz. This power divider can find usages in beamforming arrays for 5G communications (n78 band) and satellite communications. Moreover, the stopband helps in blocking the WiMAX frequencies in order to avoid interferences in the communication system.

### 5.3. Multiway SIW radial power dividers

#### 5.3.1. Layout

The basic layout of an  $N$ -way SIW radial power divider is composed of one central input port and  $N$  radially spaced identical output ports on the opposite side of the substrate. Input and output power is fed through SMA connectors. At each of the feed points, a circular patch and an annular slot is present. Initially, the output ports are symmetrically placed at half wavelength distance from the input port and quarter wavelength from the outer circumference of the radial waveguide. The dimensions of the central port may be different from those of the peripheral output ports. The central input port and peripheral output ports can either be on the same or the opposite sides of the SIW radial cavity. The boundary wall is realized using a series of equally spaced radial metalized vias, which act as an electric wall that suppresses the parallel plate leaky modes. The layout of an 8-way SIW radial power divider is shown in Fig. 5.1.

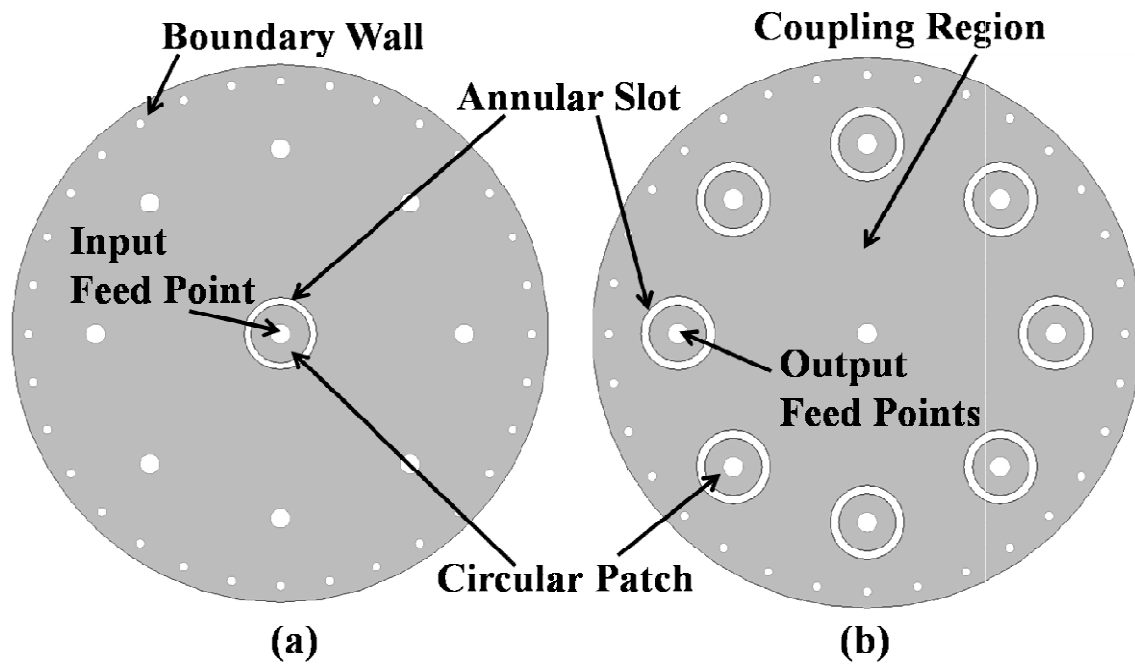


Fig. 5.1. Layout of an eight way substrate integrated waveguide radial power divider. (a) Top view. b) Bottom view.

### 5.3.2. Equivalent Circuit

For power transfer over a significant bandwidth, it is important to properly match the input and output port impedances. The impedance transformer circuitry is mainly composed of two parts. One is a circular patch around the feed points and the other is an annular slot etched around the circular patch. If the  $N$ -way radial SIW power divider structure is radially divided into  $N$  sectors, then each sector shall form a branch of the power divider, which consists of an input and output impedance transformation network connected in series with a line having a characteristic impedance of  $Z_1$ . The impedance matching is described in the equivalent circuit of the radial power divider as shown in Fig. 5.2 and Fig. 5.3. Fig. 5.2 displays the equivalent circuit

## COMPACT, BROADBAND AND MULTIBAND SIW RADIAL POWER DIVIDER

of a single sector of the power divider and Fig. 5.3 shows how  $N$  sectors together are connected to form the  $N$ -way radial SIW power divider.

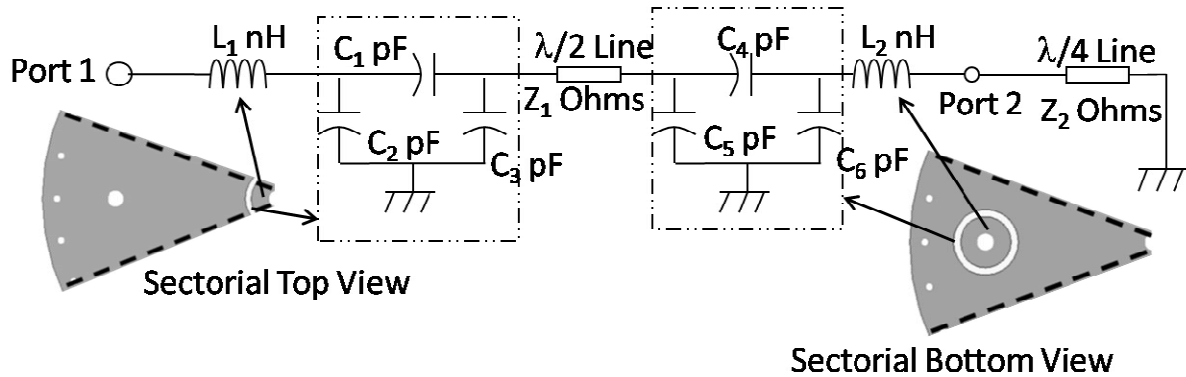


Fig. 5.2. Extraction of the equivalent circuit from the  $N$ -way radial SIW power divider of a single sector.

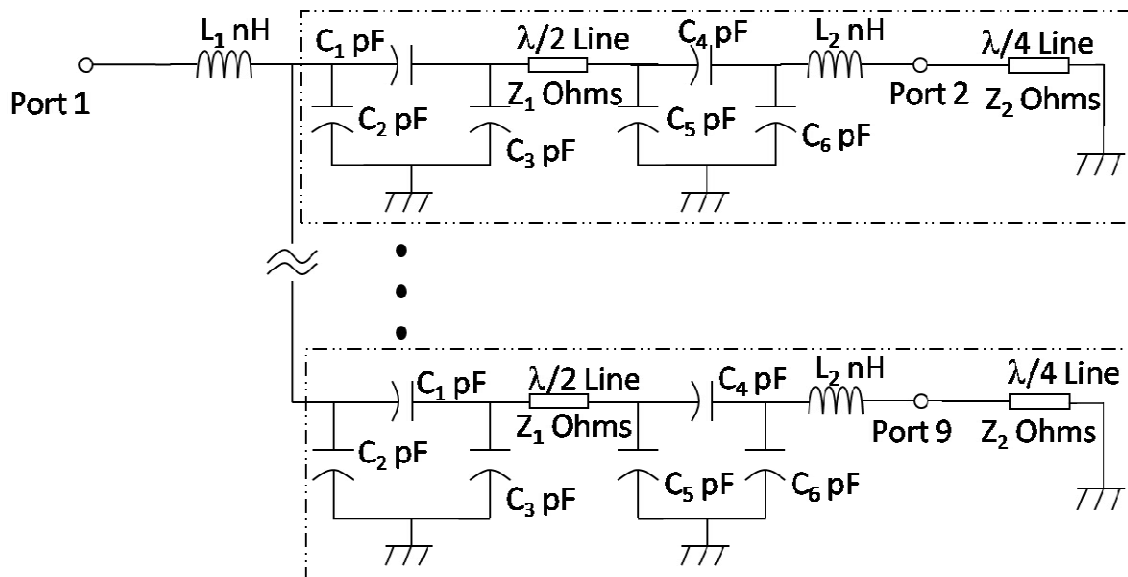


Fig. 5.3. Equivalent circuit from the 8-way radial SIW power divider.

In the equivalent circuit, power from the input and output coaxial lines are coupled to the SIW by the circular patches, which can be modeled by inductances  $L_1$  and  $L_2$ , respectively. The slot capacitances are formed by gap capacitances ( $C_1$  and  $C_4$ ) and fringing capacitances ( $C_2$ ,  $C_3$  at the input, and  $C_5$ ,  $C_6$  at the output side). The output port terminates to a line with a characteristic impedance of  $Z_2$ . Since the circuit elements of each branch of the power divider are identical, the branches can be considered to be connected in parallel with each other. Thus, if the input port impedance is  $Z_0$ , the line impedance of each branch would be  $NZ_0$  for an  $N$ -way power divider. This results in equal power division in each branch of the structure. Using standard formulas [22] initial value of the circuit parameters are calculated from the dimensions of the power divider for two ways of power division and four ways of power division. These circuit parameters are further optimized using Keysight Technologies' ADS in order to achieve broadband power division for a two-way power divider and a four-way power divider. It is observed that increasing the inductance,  $L_1$  and capacitance,  $C_1$  at the input leads to a broadband response. However, in addition to these, the inductance and capacitances at the output side are also increased, as they contribute in the improvement of the overall input return loss. The S-parameters of the equivalent circuit from the ADS simulation are shown in Fig. 5.4 and Fig. 5.5, respectively.

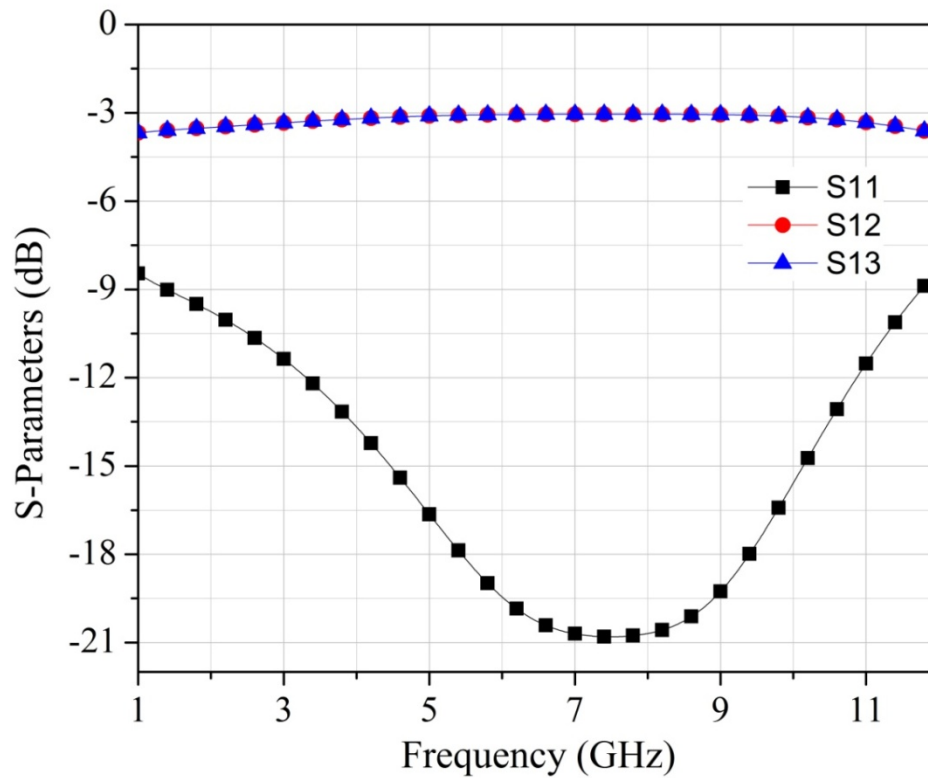


Fig. 5.4. Simulated input return loss (S11) and insertion loss (S12, S13) of ADS equivalent circuit model of 2-way SIW radial power divider.



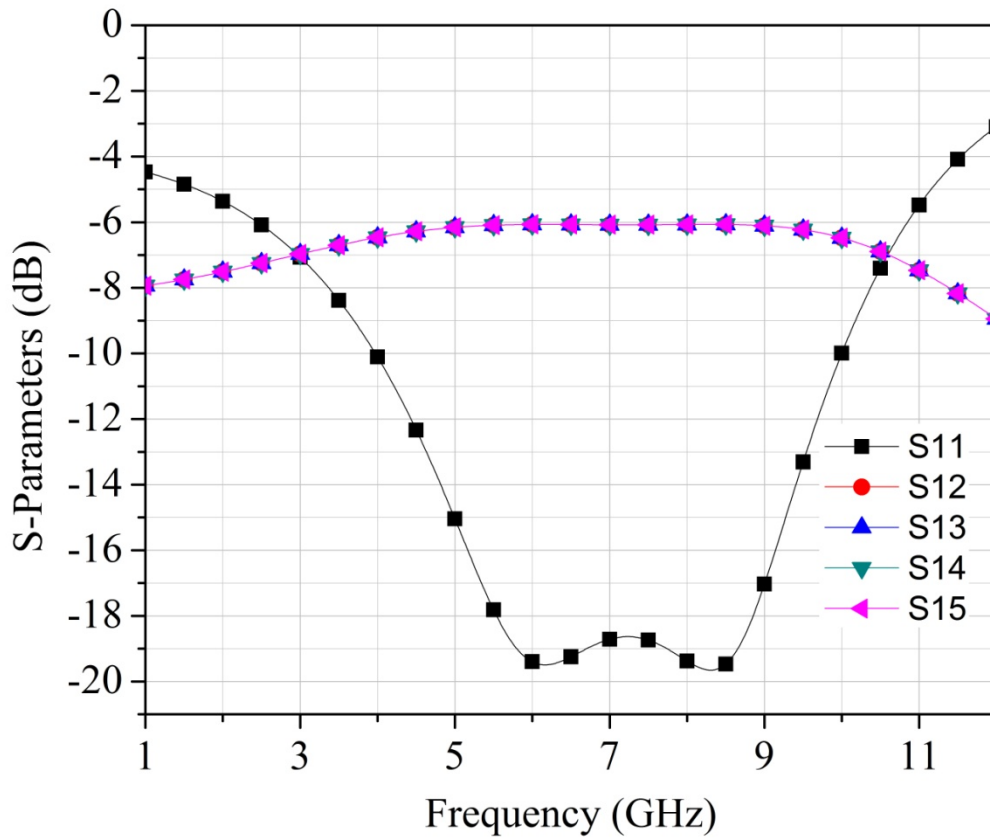
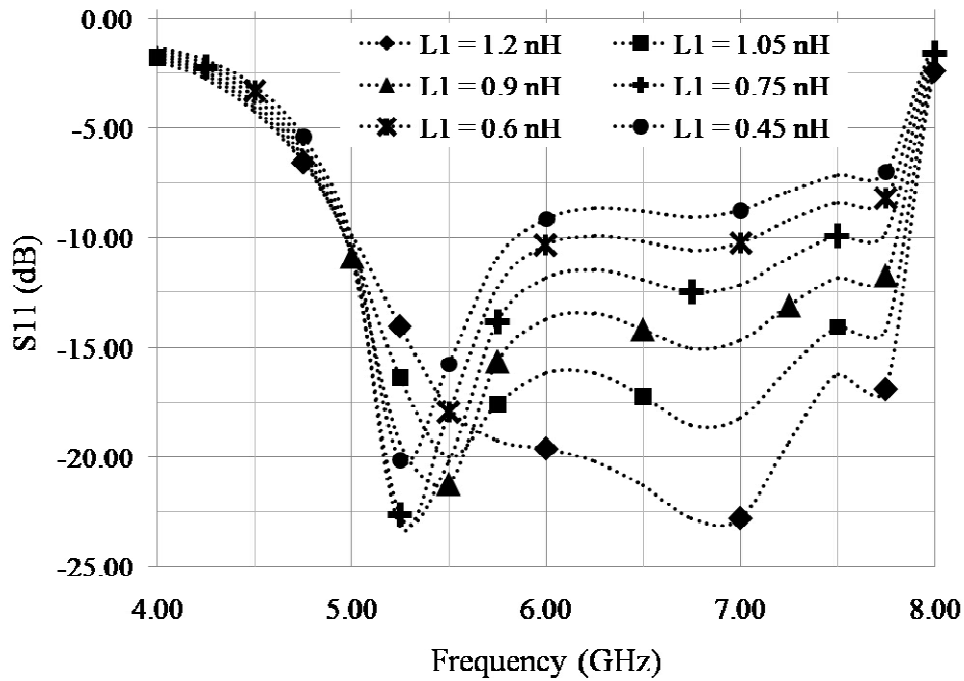


Fig. 5.5. Simulated input return loss (S11) and insertion loss (S12, S13, S14, S15) of ADS equivalent circuit model of 4-way radial SIW power divider.

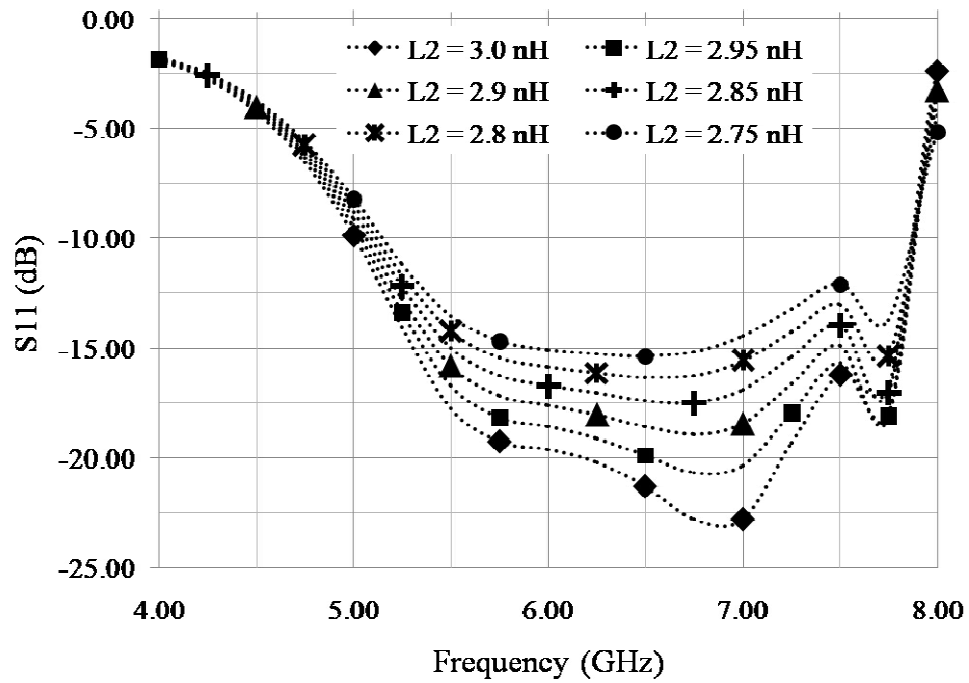
The experimental results show a 15 dB return loss bandwidth of 5.67 GHz and 4.27 GHz for the 2-way and 4-way radial SIW power divider respectively. At a centre frequency of 7.49 GHz, the insertion loss for the 2-way power divider is 3.04 dB and at a centre frequency of 7.27 GHz, the insertion loss for the 4-way power divider is 6.17 dB.

## 5.3.3. Eight Way Radial SIW Power Dividers (Single Band)

Using the equivalent circuit analysis for  $N$ -way power dividers and the standard formulas [22] initial value of the circuit elements are calculated from the dimensions of an eight-way radial SIW power divider. Keysight Technologies' ADS is used to further optimize these circuit parameters in order to achieve the power division over a broader bandwidth. As discussed, that a broadband power division in the  $N$ -way radial SIW power dividers can be achieved by increasing the inductance,  $L_1$  and capacitance,  $C_1$  at the input, and, the inductance and capacitances at the output side are additionally increased, as they contribute in the improvement of the overall input return loss. The dependence of the input return loss on the circuit elements, namely the inductances  $L_1$ ,  $L_2$  and gap capacitances  $C_1$ ,  $C_4$ , obtained from ADS simulations, are shown in Fig. 5.6 and Fig. 5.7, respectively.

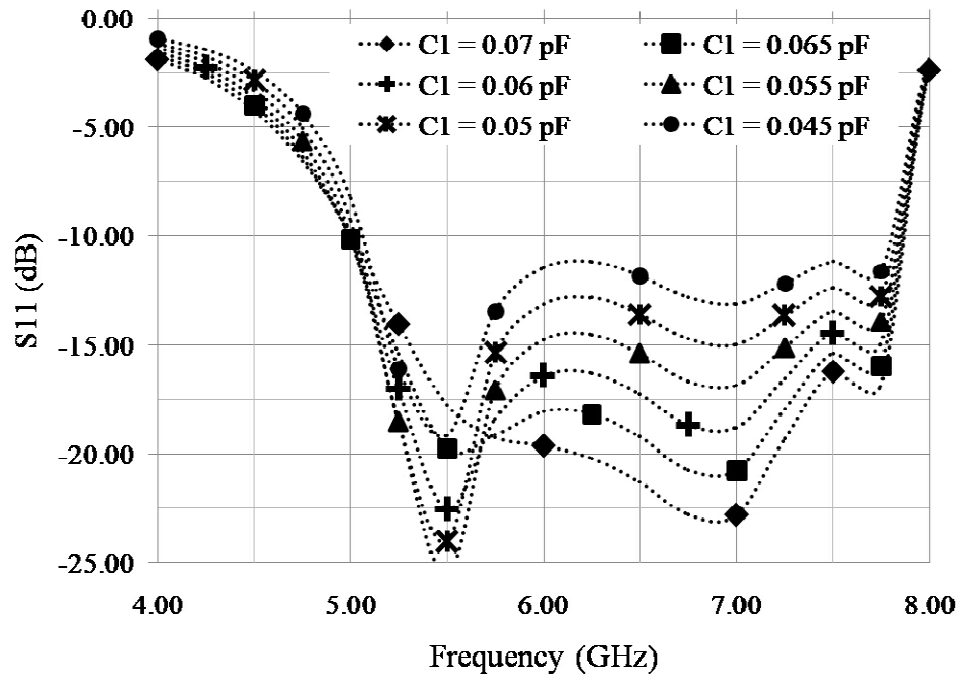


(a)



(b)

Fig. 5.6. Dependence of the input return loss on (a)  $L_1$  and (b)  $L_2$  for an 8-way radial SIW power divider.



(a)

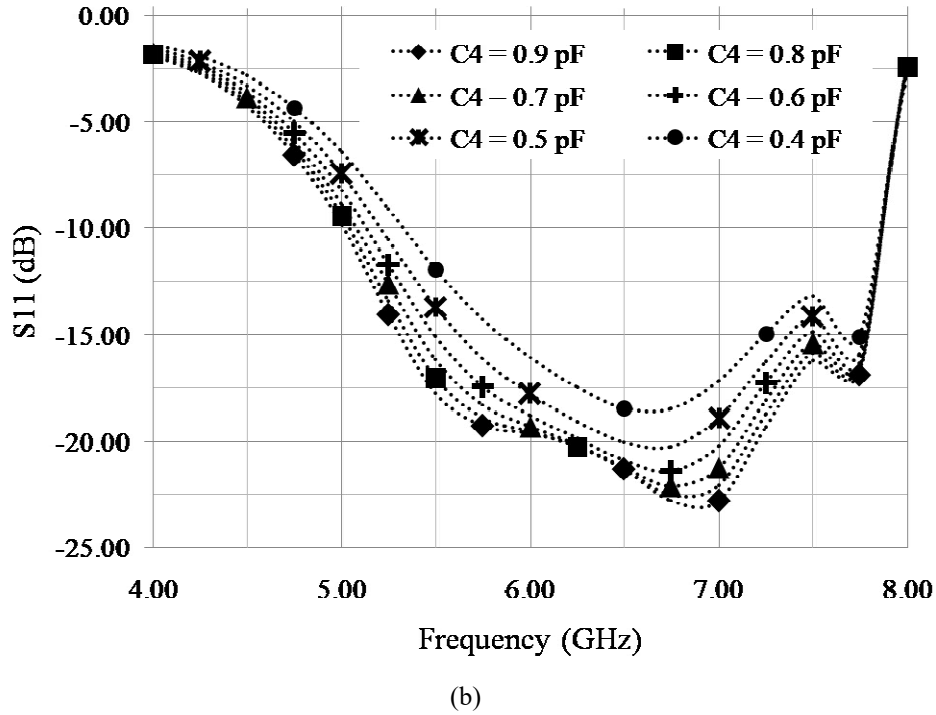


Fig. 5.7. Dependence of the input return loss on (a) C1 and (b) C4 for an 8-way SIW power divider

Hence, from Fig. 5.6 and Fig. 5.7 we see that if the circular patch radius is increased and the annular slot width is decreased it is possible to achieve a broadband response. Accordingly, the structure is simulated in Ansys HFSS (Fig. 5.8).

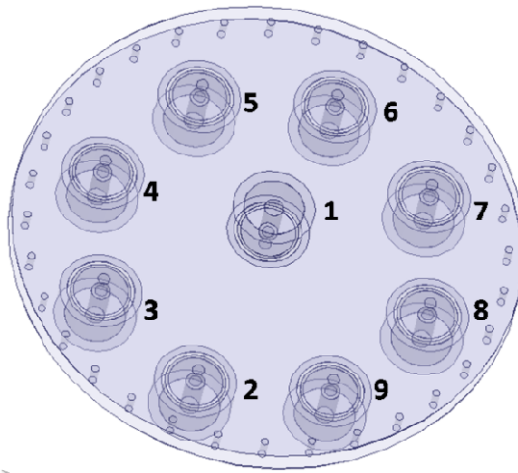


Fig. 5.8. Simulation structure of the proposed eight way radial SIW power divider;

Port 1: Input, Port 2-9: Output.

## COMPACT, BROADBAND AND MULTIBAND SIW RADIAL POWER DIVIDER

The structure in Fig. 5.8 is modeled along with the SMA connectors, and optimized to get the required performance. The design parameters of the structure are shown in Fig. 5.9.

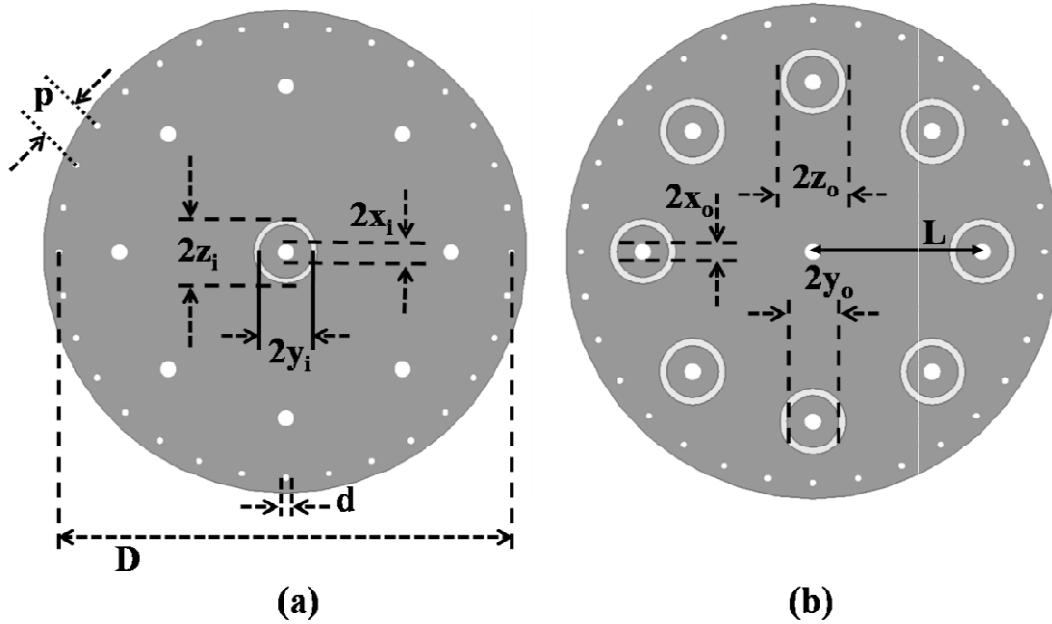


Fig. 5.9. Design parameters of the proposed eight-way radial SIW power divider

(a) Top view, (b) Bottom view.

The optimized dimensions for the initial narrow band design are listed in Table 5.1 and the S-parameters of the 3D EM model on a 62mil Rogers RT/Duroid 5880 substrate having a dielectric constant of 2.2 and loss tangent of 0.0009 from the Ansys HFSS simulation are shown in Fig. 5.10.

TABLE 5.1  
Optimized Dimensions of Narrow Band Eight-Way Radial SIW Power Divider (Unit: Millimeters)

Dimensions	$x_i$	$y_i$	$z_i$	$x_o$	$y_o$	$z_o$	$d$	$p$	$D$	$L$
Optimized Values	0.7	1.2	1.7	0.7	1.2	1.7	0.5	3.16	32.2	11.8

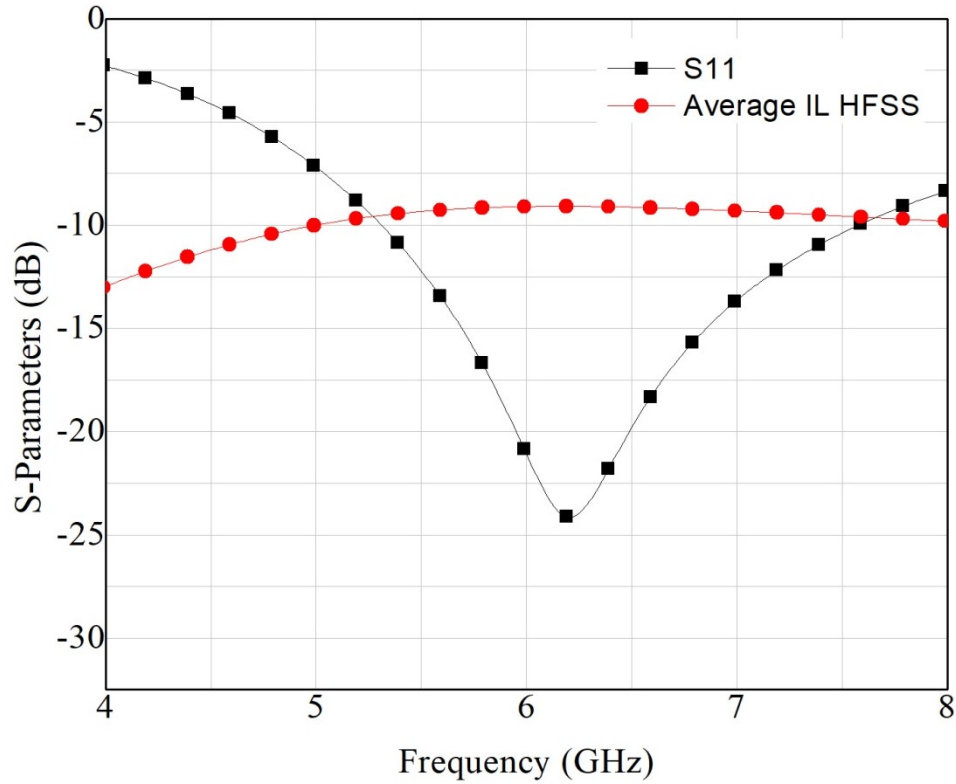


Fig. 5.10. Simulated input return loss (S11) and average insertion loss (IL) of HFSS 3D model of 8-way radial SIW power divider.

The experimental results obtained from Fig. 5.10 shows a 15 dB return loss bandwidth of 1.1 GHz and at a centre frequency of 6.2 GHz, the insertion loss for the 8-way power divider is 9.07 dB and the S11 is -24.4 dB. The optimized dimensions for the broadband design are listed in Table 5.2 and the S-parameters of the equivalent circuit from the ADS simulation and 3D EM model from the HFSS simulation are shown in Fig. 5.11 and they are in good agreement.

TABLE 5.2  
Optimized Dimensions of Broadband Eight-Way Radial SIW Power Divider (Unit: Millimeters)

Dimensions	$x_i$	$y_i$	$z_i$	$x_o$	$y_o$	$z_o$	d	p	D	L
Optimized Values	0.4	1.85	2.27	0.4	1.75	2.27	0.5	3.16	32.2	11.8

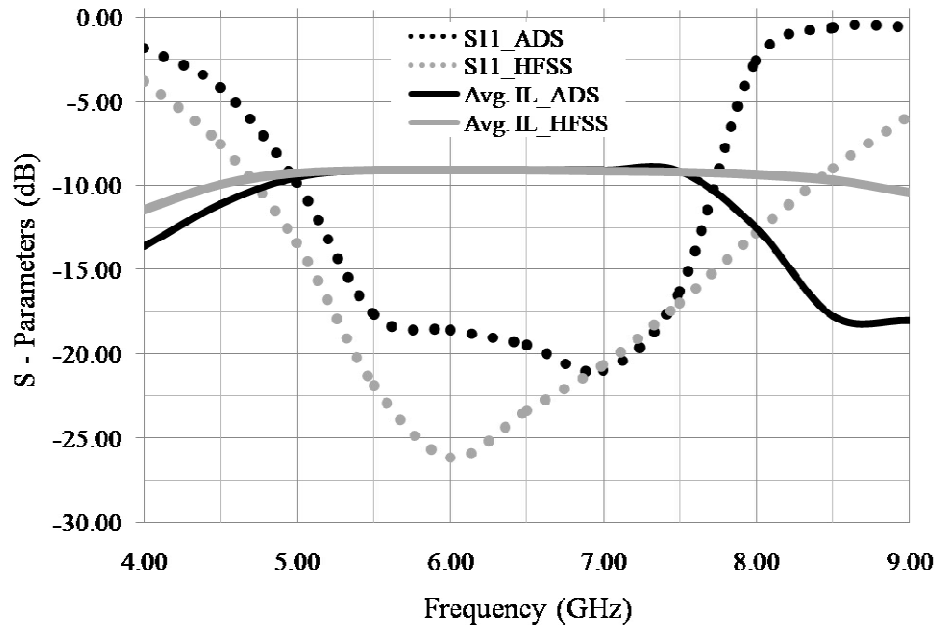


Fig. 5.11. Simulated input return loss (S11) and average insertion loss (IL) of ADS equivalent circuit and HFSS 3D model of the eight-way radial SIW power divider.

The optimized broadband eight-way radial SIW power divider, with dimensions mentioned in Table 5.2, is fabricated on a 62mil Rogers RT/Duroid 5880 substrate with a dielectric constant of 2.2 and loss tangent of 0.0009. The photograph of the fabricated power divider is shown in Fig. 5.12. The power divider is measured using Keysight E8364B vector network analyzer. The simulated and measured results of the power divider are shown in Fig. 5.13, Fig. 5.14, Fig. 5.15.

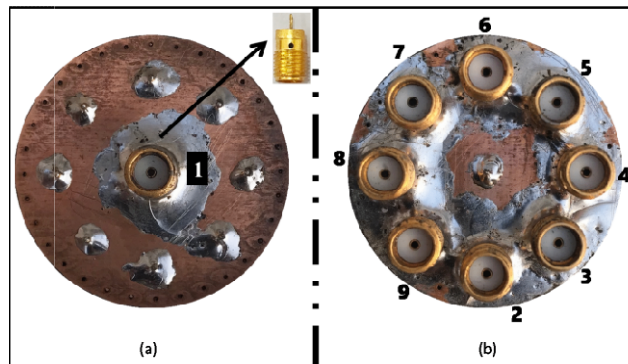


Fig. 5.12. Fabricated power divider (a) Top view and machined SMA connector (inset), (b) Bottom view

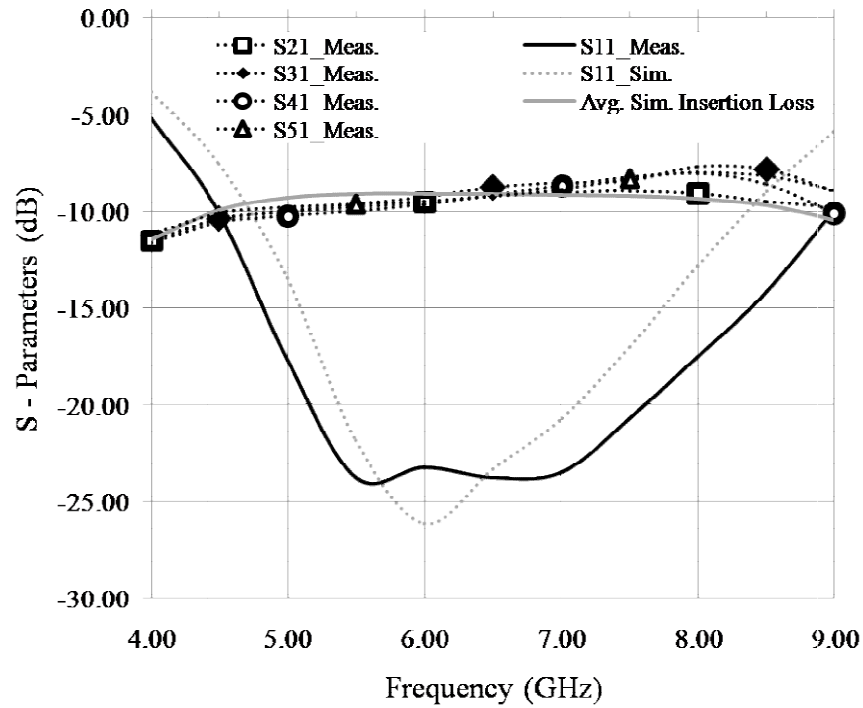


Fig. 5.13. Simulated & measured transmission and reflection parameters of the power divider for port 2-5

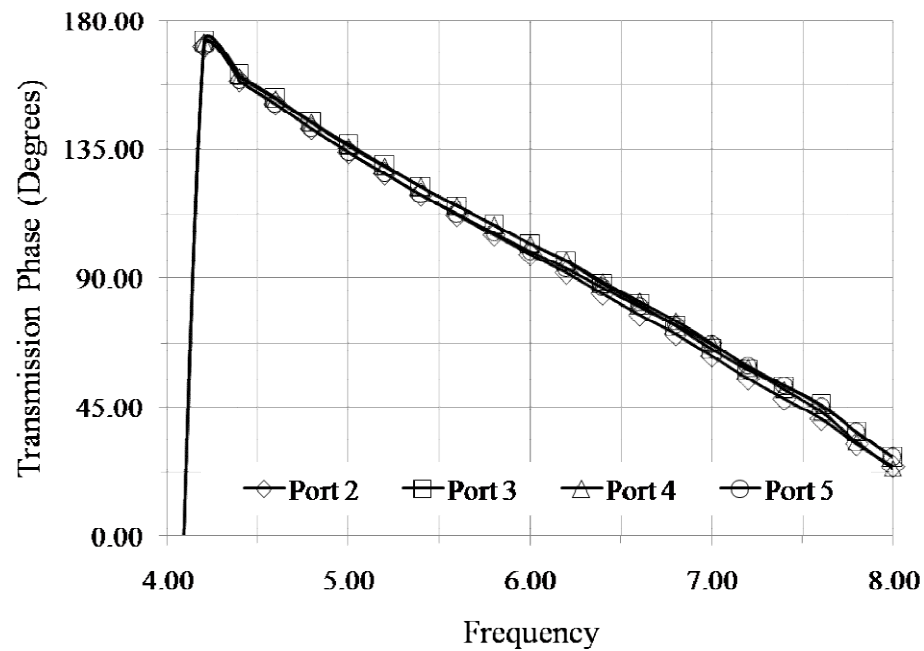


Fig. 5.14. Measured transmission phase of the power divider from port 2 to port 5.



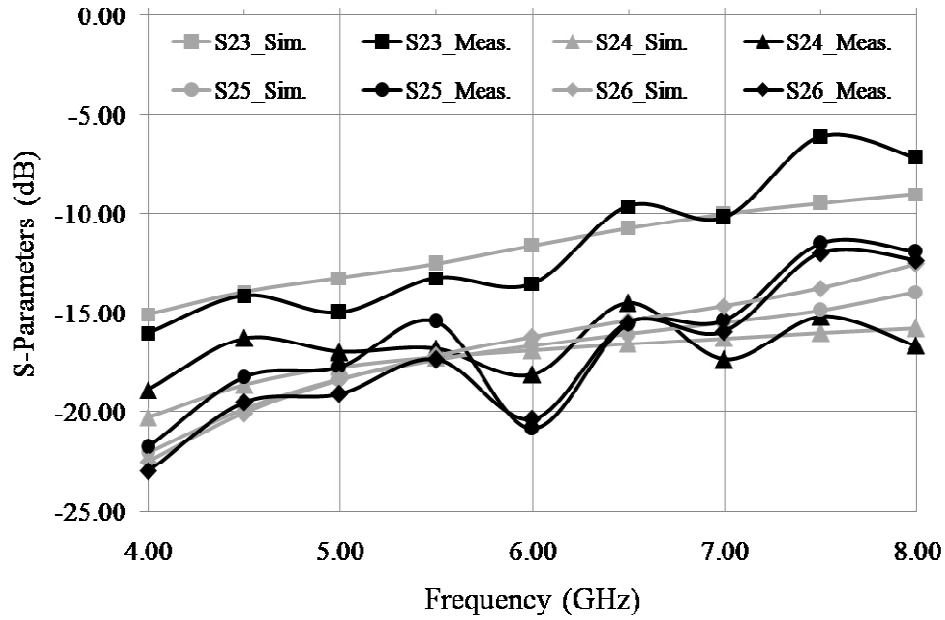


Fig. 5.15. Simulated and measured isolation of the power divider between output port 2 and output ports 3, 4, 5, 6.

The simulated and measured input return loss and insertion loss for four adjacent output ports (port 2 to port 5) of the power divider are shown in Fig. 5.13. At a centre frequency of 6.6 GHz, the measured return loss is 23.9 dB and the minimum average insertion loss is better than 0.5 dB. 15dB return loss fractional bandwidth of 53.5% is achieved. The measured transmission phase at the output ports is shown in Fig. 5.14. Fig. 5.15 shows the plot for isolation between the output port 2 and the output ports 3, 4, 5, 6, where port 3 is the adjacent port and port 6 is the farthest from port 2. It is observed that as the distance between the output ports increases, the isolation between them improves. The symmetry of the structure results in similar frequency response for all the output ports. The power divider is compact in size with a radius of 16.1mm and an area of  $0.72 \lambda_g^2$ . The minute deviations of the measured results with the simulated results may be attributed to SIW losses, SMA to SIW transition losses, improper placement of SMA connectors, and fabrication errors.

## COMPACT, BROADBAND AND MULTIBAND SIW RADIAL POWER DIVIDER

A comparative study of the proposed eight-way SIW power divider with other reported multi-way planar power divider structures is shown in Table 5.3. Although, [6],[7] shows a direct planar matching between the coaxial feed and the PCB, the bandwidth is narrow. The planar multi-way dividers in [10] and [11], presents broadband characteristics at the cost of bulky transformers between the SMA connector and the planar circuit. The planar power divider in [23] achieves a broader bandwidth than [6],[7], through planar matching but, at the cost of stacked multiple substrate layers. The proposed planar structure achieves a bandwidth broader than [6], [7], [10], [11] and [23] through planar matching between the SMA connectors and the PCB. Therefore, broadband power division is achieved using planar and compact design.

TABLE 5.3  
Comparison of Fabricated Planar Multi-Way Power Dividers

	Ref. [6] 8-way	Ref. [7] 8-way	Ref. [10] 4-way	Ref. [11] 8-way	Ref. [23] 7-way	This work 8-way
<b>Technology</b>	1/32 <sup>th</sup> mode SIW	SIW	SIW	Suspended stripline	SIW	SIW
<b>Frequency Band</b>	S	C	C	Ku	K	C
<b>15 dB FBW (%)</b>	5.42	9.53	35.29	28.78	19.2	53.56
<b>Size (mm<sup>2</sup>)</b>	1366.04	813.92	1148.89	417.07	2025	813.92
<b>Centre Frequency (GHz)</b>	2.44	5.25	6.8	13.9	18.25	6.61
<b>Size (<math>\lambda_g^2</math>)</b>	0.49	0.91	-	1.35	-	0.72
<b>Matching Technique used for feed connector</b>	Direct coaxial feed and planar narrowband matching	Direct coaxial feed and planar narrowband matching	Stepped coaxial transformer	Cylindrical cavity transformer	Planar matching through substrates stacked in multiple layers	Planar broadband matching by optimizing circular patch and annular slot

### 5.3.4. Eight Way Radial SIW Power Dividers (Multi Band)

#### A. Basic Layout and Design

The design of the power divider is an extended version to the broadband eight-way power divider. With the configurations mentioned above in the previous sections, power is equally

## COMPACT, BROADBAND AND MULTIBAND SIW RADIAL POWER DIVIDER

divided amongst the eight ports and transferred over a broader bandwidth. However, a broadband SIW radial power divider can also be transformed to act as multi-band power dividers with the placement of etched-out complementary split-ring resonators (CSRRs) in the structure. The layout of a dual-band SIW radial power divider is shown in **Fig. 5.16**. Eight CSRR structures are etched in the power divider and placed on every sector of a radial power divider, such that one CSRR is etched in between two adjacent output ports.

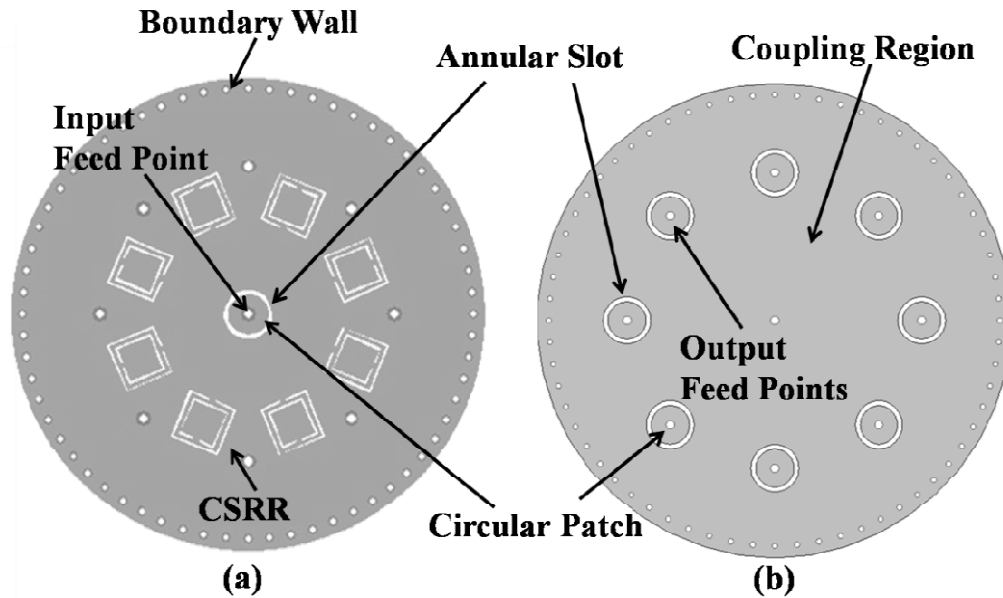


Fig. 5.16. Layout of a dual-band eight-way radial SIW power divider. (a) Top view. b) Bottom view.

The design process of the eight-way dual-band power divider is mentioned below:

- In the substrate, a series of equispaced metallic via holes are drilled radially at a distance of  $\frac{D}{2}$  from the center. This forms the electric wall of the radial waveguide.

$$\frac{D}{2} = 3 \frac{\lambda_g}{4} \quad (5.1)$$

- A metallic via of radius  $x_i$  is drilled at the center of the substrate to design the input port.

- c. Around the input port, at a distance of  $y_i$  from the center, a circular slot (having a width of:  $z_i - y_i$ ) is etched out on the top side of the conductor.
- d. At a distance of  $L$  from the center, eight equispaced metallic via holes of radius  $x_o$  are drilled radially. This forms the eight output probes.

$$L = \frac{\lambda_g}{2} \quad (5.2)$$

- e. Around the input port, at a distance of  $y_o$  from the center, a circular slot (having a width of:  $z_o - y_o$ ) is etched out on the top side of the conductor.
- f. Between the output ports, on every sectorized line of the radial power divider, CSRR structures are etched out on the substrate at a distance of  $L_s$  from the centre.

$$L_s = \frac{\lambda_g}{2} \quad (5.3)$$

- g. The CSRR structures are designed based on the standard formulas ( $l_1, l_2, w_1, w_2, g_1, g_2, g_{12}$ ) [20].
- h. SMA connectors are appended to the structure at the input and output ports through soldering.

Accordingly, the structure, along with the model of the SMA connector, is simulated in Ansys HFSS (Fig. 5.17) and optimized to get the required performance.

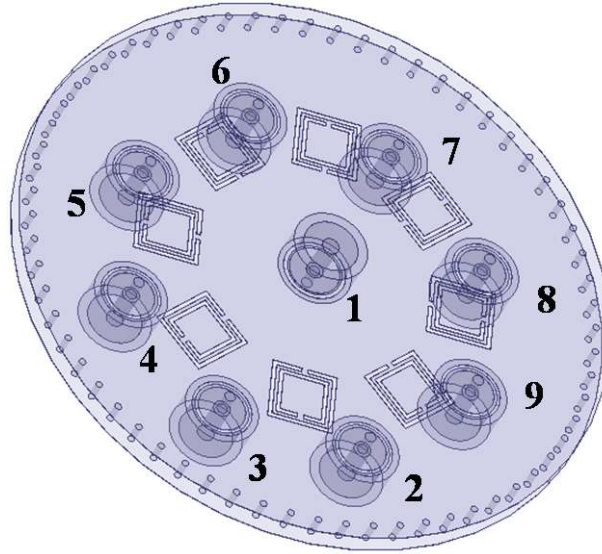


Fig. 5.17. Simulation structure of the dual-band eight-way radial SIW power divider;  
Port 1: Input, Port 2-9: Output.

The design parameters of the structure are shown in Fig. 5.18.

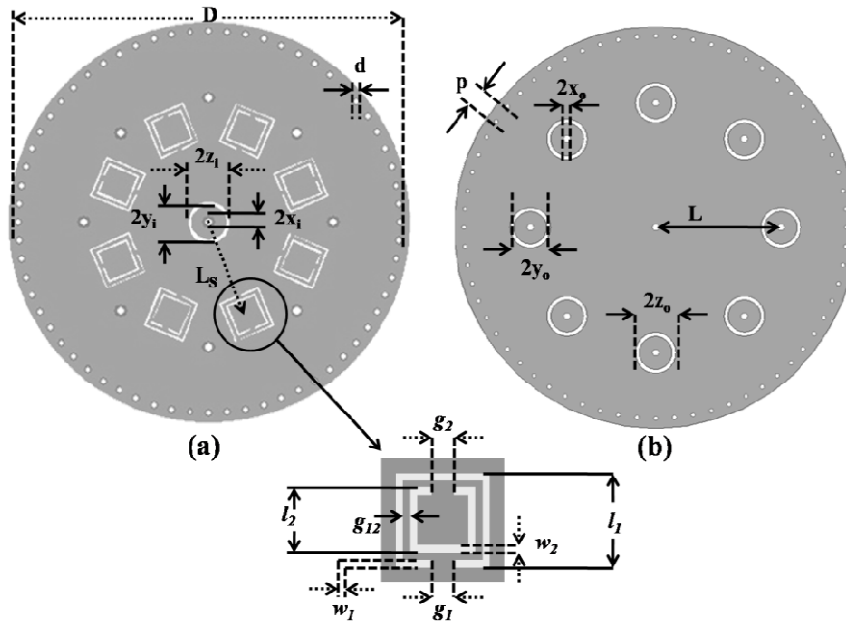


Fig. 5.18. Design parameters of the dual-band eight-way radial SIW power divider  
(a) Top view, (b) Bottom view.

### ***B. Basic Working Principle***

It can be noted from the previous sections that the isolation between the output ports of a broadband SIW radial power divider is poor. However, as the isolation between the output ports is improved, the insertion loss and the input return loss characteristic of the power divider degrades. To improve the isolation performance and to achieve good stop band performs CSRRs have been employed. The designed CSRRs, at their resonant frequency, provide negative permittivity resulting in evanescent wave propagation within the power divider. However, just a stopband will not improve the power division characteristics in the passband. The CSRRs, which are designed to achieve a stopband, contribute to the improvement of the passbands and discussed below.

In the natural course of propagation of power in a radial SIW, the fields, after entering the SIW from the input port, travel radially towards the boundary wall. In the proposed dual-band power divider, the fields, prior to the output ports, primarily interact with the individual CSRRs. At the stopband frequency, the time-varying electric fields which are parallel to the CSRR's axis, i.e. the fields which are perpendicular to the top and bottom walls of the radial structure through the dielectric substrate, results in a strong electric coupling with the CSRR as they constitute a single negative medium with negative permittivity. As a result, the propagating waves become evanescent waves, and hence the signal is inhibited and can't end up at the output ports. The Ansys HFSS simulated field propagation at the stopband centre frequency of 5.5 GHz is shown in Fig. 5.19. At the passband frequencies, since the field wavelengths are much larger than the CSRRs' electrical length, the CSRRs reflect the entire power to the adjacent output ports since the output, between which it is placed, and this helps in the enhancement of the power division at

the passband leading to a dual-band response. Furthermore, since CSRRs are known to exhibit very sharp transitions from passband to stopband at the lower frequencies of the stopband and from stopband to passband at the higher frequencies of the stopband [21], they will help in providing proper isolation between the dual-bands.

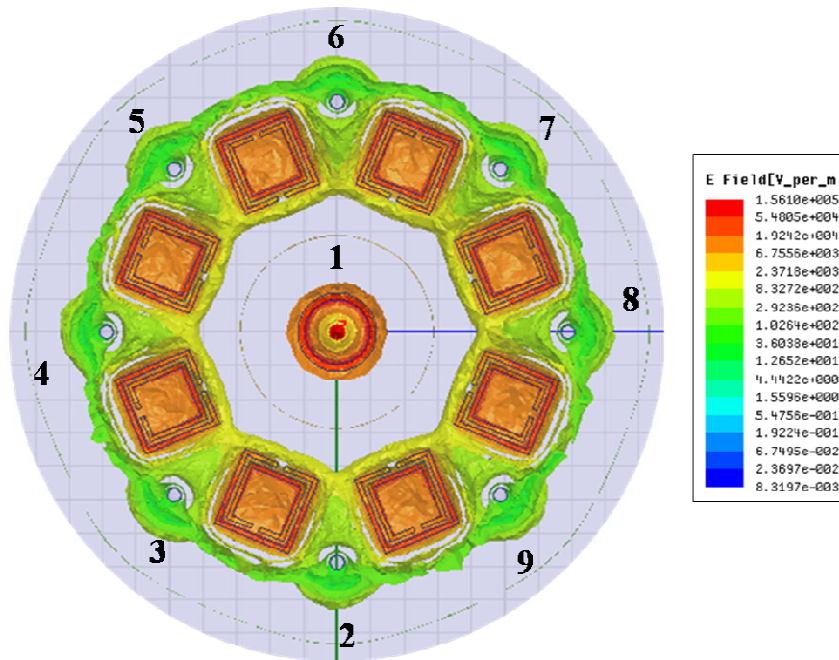


Fig. 5.19. Ansys HFSS simulated field propagation at the stopband centre frequency of 5.5 GHz.

Due to the symmetry of the structure, dual-band response could also have been achieved using four CSRRs instead of eight, and these four CSRRs were to be placed at alternate sector lines of the power divider, as shown in Fig. 5.20. However, CSRRs are known to improve the passband return loss characteristics and the rejection in the stopbands. Moreover, with four CSRRs at alternate sector lines resulted in additional lower isolation between the output ports where the CSRR was missing.

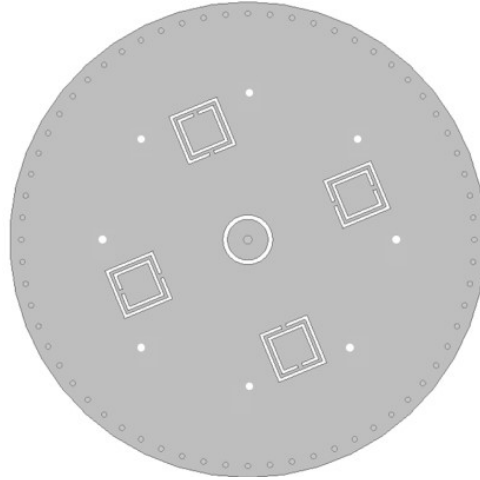


Fig. 5.20. Layout of the dual-band eight-way substrate integrated waveguide radial power divider with four CSRRs (Top view).

The Ansys HFSS simulation study between the usage of four CSRRs and eight CSRRs in a radial SIW power divider with eight-way division is shown in Fig. 5.21 and Fig. 5.22. The simulations shows that the usage of eight CSRRs over four is advantageous.

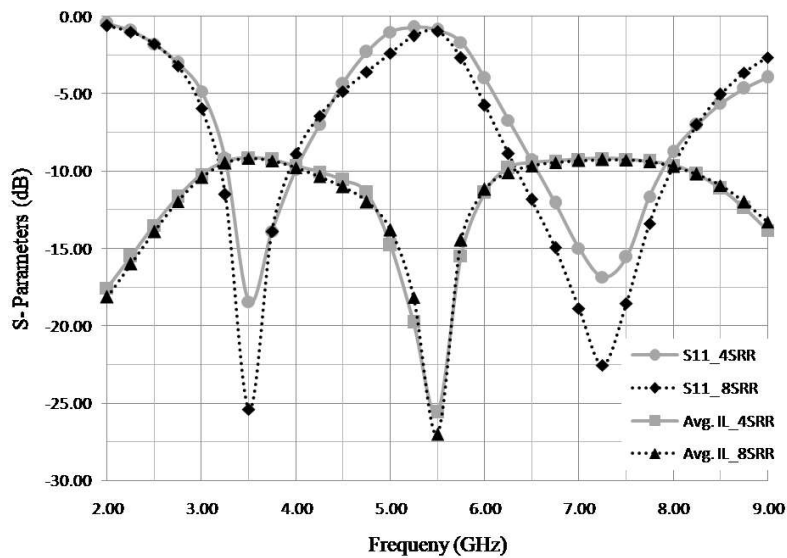


Fig. 5.21. Simulated input return loss (S11) and average insertion loss (IL) of Ansys HFSS 3D model of the proposed power divider using four and eight CSRRs.



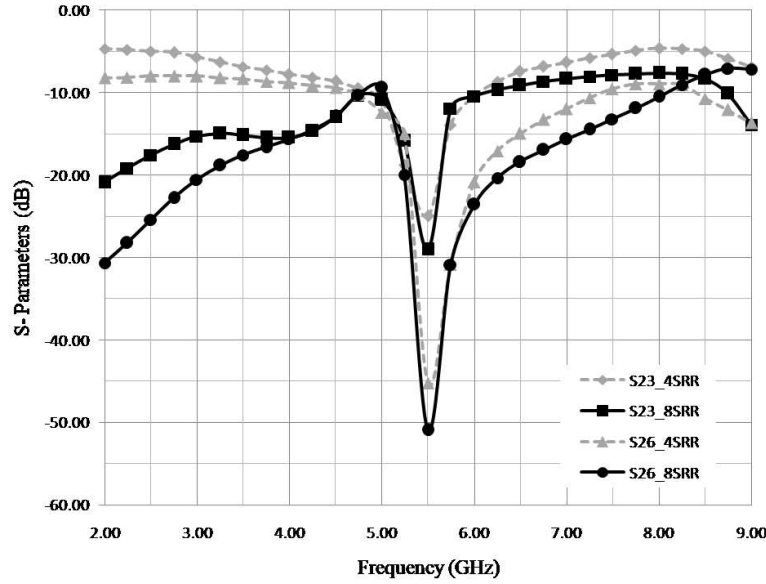


Fig. 5.22. Simulated isolation of Ansys HFSS 3D model of the proposed power divider between port 2 and port 3 (adjacent ports), and, between port 2 and port 6 (farthest ports), with four and eight SRRs.

## C. Fabrication and Measurement

The optimized dual band eight-way radial SIW power divider, with dimensions mentioned in Table 5.4 as per the design structure in Fig. 5.18, is fabricated on a 62mil Rogers RT/Duroid 5880 substrate with a dielectric constant of 2.2 and loss tangent of 0.0009.

TABLE 5.4

Optimized Dimensions of Dual-band Eight-Way radial SIW Power Divider (Unit: millimeters)

Dimensions	$x_i$	$y_i$	$z_i$	$x_o$	$y_o$	$z_o$	$d$	$p$	$D$
Optimized Values	0.4	1.89	2.34	0.4	1.78	2.25	0.5	2.07	42.2
Dimensions	$L$	$L_S$	$l_1$	$l_2$	$w_1$	$w_2$	$g_1$	$g_2$	$g_{12}$
Optimized Values	13.8	13.4	4.82	3.68	0.31	0.31	0.45	0.45	0.26

## COMPACT, BROADBAND AND MULTIBAND SIW RADIAL POWER DIVIDER

The photograph of the fabricated power divider is displayed in Fig. 5.23. It is measured using a Keysight E8364B vector network analyzer. The simulated and measured results of the power divider are shown in Fig. 5.24, Fig. 5.25, Fig. 5.26, Fig. 5.27 and Fig. 5.28.

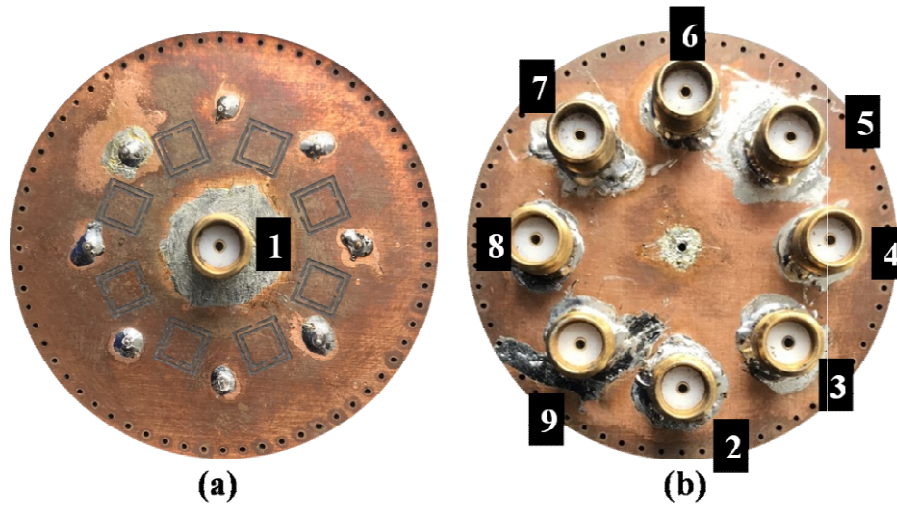


Fig. 5.23. Photograph of the fabricated dual band eight-way radial SIW power divider.

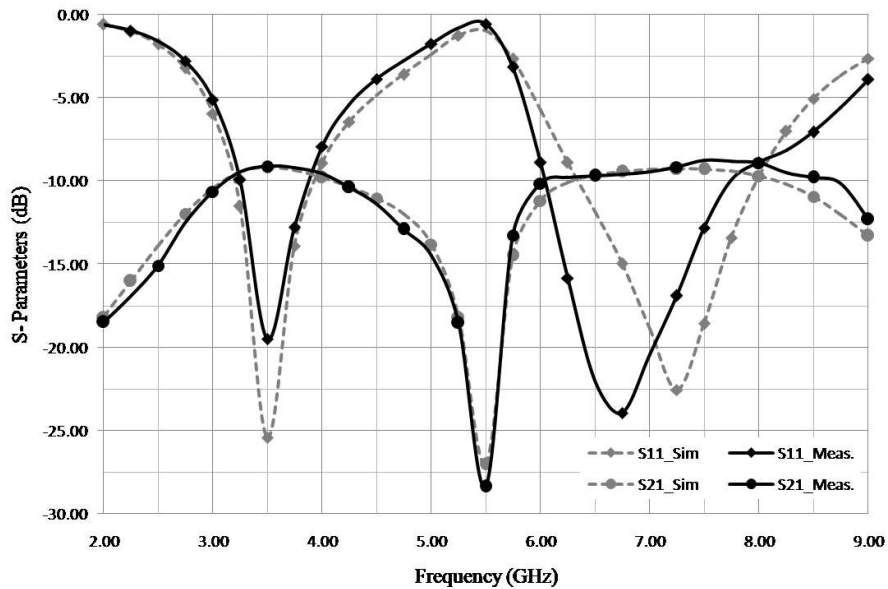


Fig. 5.24. Simulated and measured transmission and reflection parameters of the dual band eight-way radial SIW power divider.

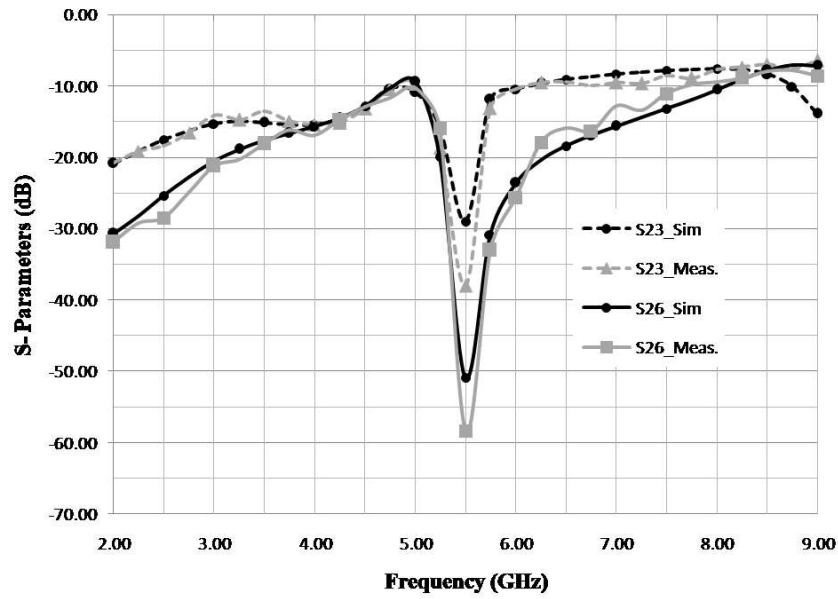


Fig. 5.25. Simulated and measured isolation of the dual band eight-way radial SIW power divider between port 2 and port 3 (adjacent ports), and, between port 2 and port 6 (farthest ports).

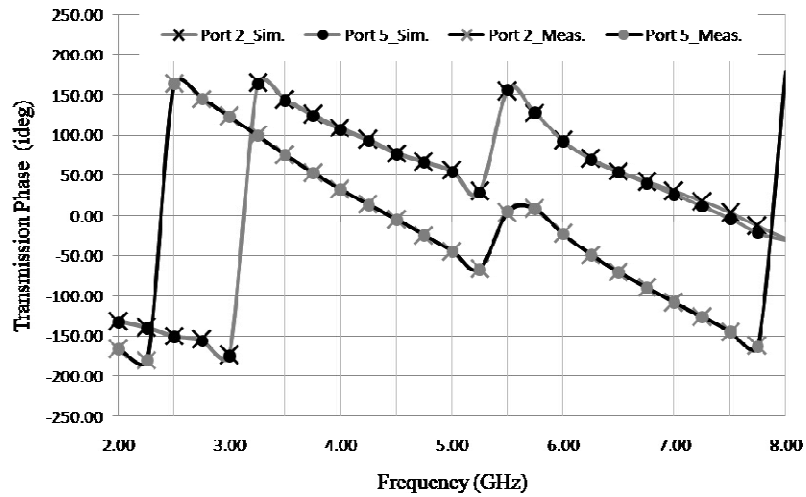


Fig. 5.26. Simulated and measured transmission phase of the dual band eight-way radial SIW power divider between port 2 and port 6 (farthest ports).

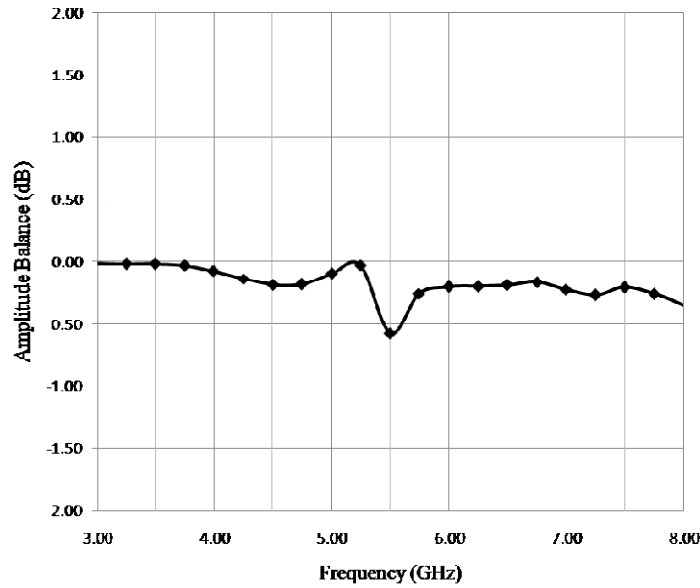


Fig. 5.27. Measured amplitude balance between output ports 2 and 6 of the dual band eight-way radial SIW power divider.

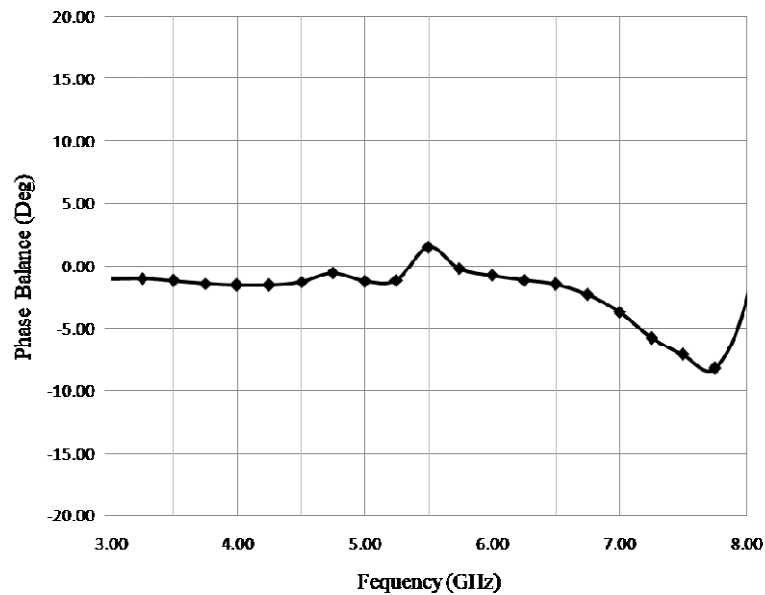


Fig. 5.28. Measured phase balance between output ports 2 and 6 of the dual band eight-way radial SIW power divider

The simulated and measured input return loss and insertion loss for the output port of the power divider are shown in Fig. 5.24. At a frequency of 5.5 GHz, the measured rejection is 28.35 dB. The 10dB rejection bandwidth of 2.25 GHz is achieved between the two passbands at S and

C band. The minimum average insertion loss is not more than 0.5 dB. The output ports present a similar frequency response due to the symmetry of the structure. The dual-band multiway power divider is compact in size with a radius of 21.1 mm and an area of  $1.24 \lambda_g^2$ . In Fig. 5.25, the simulated and measured isolation between two adjacent output ports and two output ports that are farthest are displayed. It substantiates that at the stopband, the isolation between the adjacent ports improves to such an extent that at the 5.5 GHz stopband centre frequency, the isolation is more than 55 dB, whereas, at the passbands, the isolation is similar to that of standard eight-way radial SIW power dividers. As the distance between the output ports increases, the isolation between them improves. Fig. 5.26 shows the simulated and measured transmission phase of the two farthest output ports. The deviations in the measured results from the simulated results may be attributed to SMA to SIW transition losses, improper placement of SMA connectors, SIW losses, and fabrication errors. Fig. 5.27 and Fig. 5.28 show the amplitude and phase balances, respectively, between the farthest output ports 2 and 6. The amplitude balance is within 0.6 dB, and, the phase balances between the ports are within  $\pm 8^\circ$ . The slight shift in the centre frequency of the higher passband may be attributed to the cause of the loading effect from the CSRRs. However, the 10 dB return loss bandwidth of the measured circuit nearly matches with the simulation results.

### 5.4. Conclusion

An innovative broadband and compact eight-way Substrate Integrated Waveguide (SIW) radial power divider is introduced and presented in this chapter. This power divider boasts a remarkable fractional bandwidth of 53.5%, offering coverage across almost the entire C-band at a central frequency of 6.6 GHz. Despite its broadband capability, the power divider maintains a

## COMPACT, BROADBAND AND MULTIBAND SIW RADIAL POWER DIVIDER

---

compact form factor, measuring just 0.72 times the guided wavelength ( $\lambda_g^2$ ) in size. The power divider's extensive bandwidth is achieved through the utilization of planar annular slot and circular patch impedance transformers integrated into the planar substrate itself. This innovative approach ensures broadband performance without adding bulkiness to the design. The impedance matching between the coaxial fed ports and the radial SIW power divider structure is carefully analyzed and validated through equivalent circuit simulations. This approach streamlines the 3D electromagnetic (EM) simulations, minimizing the need for iterations and improving design efficiency. The impressive combination of broad bandwidth and compactness makes this power divider well-suited for various applications. It holds significant potential for sub-6 GHz 5G base stations and satellite communication systems. The power divider's adaptability for use in antenna arrays, multiplexers, and high-power amplifiers further underscores its utility across diverse communication scenarios.

This technique of obtaining a dual-band response within the proposed power divider by incorporating CSRRs, which have smaller electrical size, promises easy fabrication of the structure using standard planar circuit fabrication methods for printed circuit boards. It requires no extra circuit area and can even be etched out on any of the conducting planes of the power divider. It is thus able to retain the compactness of the entire structure unlike other solutions which would either make the circuit bulky or complex in design. Since the dimensions of the CSRR, which includes the length, width, and gap of the CSRR rings, can influence the frequency of operation, they can be tuned and further designed to obtain dual-bands at desired frequencies by determining the nature of the stopband. However, this is possible only within the bandwidth of operation of the power divider in the absence of the CSRRs, which in its original form acts as a broadband SIW radial power divider. Dual-band performance is achieved using etched

complementary split-ring resonators in the planar substrate itself, which would otherwise require a separate filtering component to reject out the unwanted frequencies. The composite dual-bandwidth operation in this compact multiway power divider makes it useful in various wireless communication systems such as antenna arrays, multiplexers, and high power amplifiers, as it provides lower losses without being bulky. The design can be further extended for a triple band power divider as well by incorporating CSRR rings so as to produce two stop bands.

### References:

- [1] M. Bozzi, A. Georgiadis, and K. Wu, "Review of substrate-integrated waveguide circuits and antennas," *IET Microwaves, Antennas and Propagation*, vol. 5, no. 8, pp. 909–920, June 2011.
- [2] R. Kazemi and A. E. Fathy, "Design of a wideband eight-way single ridge substrate integrated waveguide power divider," *IET Microwaves, Antennas and Propagation*, vol. 9, no. 7, pp. 648–656, May 2015.
- [3] A. H. Ali, K. W. Hameed, N. T. Ali, M. S. Bakr, R. A. Abd-Alhameed, N. J. McEwan, "A general design for multi-output ports planar Wilkinson power divider," *Microw. Opt. Technol. Lett.*, vol. 61, no. 3, pp. 578–582, Dec. 2018.
- [4] K. Song, X. Li, M. Fan, Y. Mo, and, Y. Fan, "Multiple-mode-based four-way filtering-response power divider with wide stopband and high fabrication tolerance," *Microw. Opt. Technol. Lett.*, vol. 58, no. 12, pp. 2993–2996, Sept. 2016.
- [5] W. Wang, Y. Zheng, and, Q. Cao. "A four-way broadband filtering power divider with improved matching network for X-band application," *Microw. Opt. Technol. Lett.*, vol. 61, no. 9, pp. 2155–2160, Sept. 2019.
- [6] A. A. Khan and M. K. Mandal, "Miniaturized Substrate Integrated Waveguide (SIW) Power Dividers," *IEEE Microw. Wireless Compon. Lett.*, vol. 26, no. 11, pp. 888–890, Nov. 2016.
- [7] K. Song, Y. Fan, and Y. Zhang, "Eight-way substrate integrated waveguide power divider with low insertion loss," *IEEE Trans. Microw. Theory Techn.*, vol. 56, no. 6, pp. 1473–1477, June 2008.
- [8] K. Song and Q. Xue, "Planar Probe Coaxial-Waveguide Power Combiner/Divider," *IEEE Trans. Microw. Theory Techn.*, vol. 57, no. 11, pp. 2671–2767, Nov. 2009.

- [9] K. Song and Q. Xue, "Ultra-Wideband 12-Way Coaxial Waveguide Power Divider with rotated electric field mode," *IET Microwaves, Antennas and Propagation*, vol. 5, no. 5, pp. 512–518, May 2011.
- [10] K. Song and Y. Fan, "Broadband travelling-wave power divider based on substrate integrated rectangular waveguide," *Electronic Letters*, vol. 45, no. 12, pp. 631–632, July 2009.
- [11] X. Shan and Z. Shen, "A Suspended-Substrate Ku-Band Symmetric Radial Power Combiner" *IEEE Microw. Wireless Compon. Lett.*, vol. 21, no. 12, pp. 652–654, Dec. 2011.
- [12] P. Wen, Z. Ma, H. Liu, S. Zhu, B. Ren, Y. Song, X. Wang, and, M. Ohira, "Dual-Band Filtering Power Divider Using Dual-Resonance Resonators With Ultrawide Stopband and Good Isolation," *IEEE Microw. Wireless Compon. Lett.*, vol. 29, no. 2, pp. 101-103, Jan. 2019.
- [13] X. Wang , J. Wang, G. Zhang, J. S. Hong, and, W. Wu, "Dual-Wideband Filtering Power Divider With Good Isolation and High Selectivity," *IEEE Microw. Wireless Compon. Lett.*, vol. 27, no. 12, pp. 1071- 1073, Dec. 2017.
- [14] G. Zhang, J. Wang, L. Zhu, and, W. Wu, "Dual-Band Filtering Power Divider With High Selectivity and Good Isolation," *IEEE Microw. Wireless Compon. Lett.*, vol. 26, no. 10, pp. 774-776, Oct. 2016.
- [15] Y. Wu, Y. Liu, Q. Xue, S. Li, and C. Yu, "Analytical Design Method of Multiway Dual-Band Planar Power Dividers With Arbitrary Power Division," *IEEE Trans. Microw. Theory Techn.*, vol. 58, no. 12, pp. 3832-3841, Nov. 2010.
- [16] X. Liu, C. Yu, Y. Liu, S. Li, F. Wu, and, Y. Wu, "Design of Planar Dual-Band Multi-Way Power Dividers," *Proceedings of Asia-Pacific Microwave Conference 2010.*, pp. 722-725, Dec. 2010
- [17] T. Zhang, W. Che, H. Chen, and, W. Feng, "A Compact Four-way Dual-band Power Divider Using Lumped Elements," *IEEE Microw. Wireless Compon. Lett.*, vol. 25, no. 2, pp. 94-96, Feb. 2015.
- [18] A. Belenguier, H. Esteban, and, V. E. Boria, "Novel Empty Substrate Integrated Waveguide for High - Performance Microwave Integrated Circuits," *IEEE Trans. Microw. Theory Techn.*, vol. 62, no. 4, pp. 832-839, Apr. 2014.
- [19] Y. Wang, C. Zhou, K. Zhou, and, W. Wu, "Compact dual-band filtering power divider based on SIW triangular cavities," *Electronic Letters*, vol. 54, no. 18, pp. 1072-1074, Sept. 2018.
- [20] R. Marqués, F. Martin and M. Sorolla, "Metamaterials with Negative Parameters: Theory, Design, and Microwave Applications," *John Wiley & Sons, Inc*, pp. 119–185, 2007.



- [21] M. Danaeian, A. R. Moznebi, and, K. Afrooz, “Super compact dual-band substrate integrated waveguide filters and filtering power dividers based on evanescent-mode technique,” *AEU - International Journal of Electronics and Communications*, vol. 125, no. 6, July 2020.
- [22] T. -C. Edwards, *Foundations for Microstrip Design*. John Wiley, New York, pp. 225–268, 1981
- [23] C. Rave and A. F. Jacob, “A wideband radial substrate integrated power divider at K-band,” *Proc. German Microw. Conf.* Nuremberg, Germany, pp. 84–87, May 2015.

## ***CONCLUSION AND FUTURE SCOPE OF WORK***

---

### **6.1 Conclusion**

The fundamental theory underlying a Substrate Integrated Waveguide (SIW) is explored in the thesis, alongside a comprehensive understanding of its operational principles. SIW is a technology that employs a planar structure to mimic the behavior of traditional rectangular waveguides while integrating seamlessly with planar circuits. Its operation is rooted in the confinement and guiding of electromagnetic waves within a substrate with  $TE_{10}$  mode as the fundamental mode of propagation. This allows SIW to exhibit waveguide-like behavior while being compatible with standard printed circuit board (PCB) fabrication processes and hence is a light, low cost technology. The losses within a SIW are primarily conductor losses, dielectric losses, and radiation losses. These losses can be mitigated by making prudent choices in terms of utilizing appropriately sized vias and arranging them in close proximity. From the literature review in Chapter 2 on the characteristics of SIW and how it has proved to be a better solution to various applications, it shows huge potential to cater to the needs of multiple-input multiple-output (MIMO) techniques in an Substrate Integrated Circuits (SIC) system through multiway capabilities in power dividers and couplers. Multi-band operations in various components and sub-systems are of immense demand in satellite communication and 5G applications and SIW can be used to develop designing such components as well which are not only compact but presents multi-band outputs.

## CONCLUSION AND FUTURE SCOPE OF WORK

---

A comprehensive parametric study of a SIW was conducted using ANSYS HFSS at X-band in Chapter 3. This study involved varying the width, pitch, and diameter of the SIW structure to assess their impact on its performance. Through this study, specific values for these parameters were identified as optimal. The chosen parameter values were determined to ensure that the SIW's characteristics remained stable and consistent across the X-band. This stability is vital for reliable operation and consistent performance. Another crucial consideration was to avoid the unintentional excitation of higher-order modes or spurious modes within the SIW structure. This trade-off between maintaining stability within the desired frequency range and preventing unwanted mode excitation guided the determination of optimal parameter values for the SIW, ensuring its effective performance within the X-band. One of the effective and evolved form of SIW is the Empty Substrate Integrated Waveguide (ESIW) where the dielectric substrate is replaced by air. Parametric analysis of ESIW was also studied in the X-band by designing and simulating it in ANSYS HFSS. The width of ESIW was varied. Like SIW, designers should choose the optimum values based on the trade off between the stability of ESIW characteristics and higher and spurious order modes excitation in the structure.

Chapter 3 also delves into an in-depth study of transitions between SIW and other various technologies like waveguides, microstrips, and empty substrate integrated waveguides (ESIW). The chapter employs simulation-based design approaches to investigate and present these transition structures. The investigation begins with the exploration of a widely used taper transition between microstrip and SIW. This transition is modified to achieve a broader bandwidth using a stepped taper transition technique. The simulation outcomes reveal a significantly broader frequency response compared to single taper microstrip to SIW transitions

## CONCLUSION AND FUTURE SCOPE OF WORK

---

found in existing literature. Further, transitions between SIW and waveguides are explored through the use of dual slots. The arrangement of these slots leads to a broader band response by causing resonance at closer frequencies. Alternatively, resonating them at distant frequencies results in a dual-band transition response. Another significant contribution lies in the design of a transition between two widely utilized SIC technologies, SIW, and ESIW operating in the C-Band frequency range. Power transfer is enabled through an etched complementary split ring resonator (CSRR), which additionally aids in achieving optimal impedance matching. The compactness and simplicity of this transition, which is realized on the same substrate, allow for the effective integration of SIW and ESIW components within a multilayered configuration. This advancement aligns with the broader concept of SIC by enabling seamless integration and enhancing overall system functionality.

In Chapter 4, a compact and broadband X-band Substrate Integrated Waveguide (SIW) three-way power divider based on a six-port riblet coupler is introduced. This power divider showcases improved isolation among its ports, presenting significant advantages over other designs. The coupler demonstrates exceptional performance over a broad frequency range in the X-band. Its reflection coefficient and isolation are maintained at levels exceeding 15 dB across a fractional bandwidth of 27.3%. It achieves the desired performance within a compact size. This is advantageous in space-constrained applications. The coupling length for this power divider is impressively short. The design boasts robust isolation characteristics between both adjacent and non-adjacent ports, further enhancing its overall functionality. This power divider design is versatile and finds utility in various applications. It can be integrated into X-band transmitters for power combining, enhancing the power handling capacity of power amplifiers. Similarly, it can be employed in X-band three-channel receivers for local oscillator (LO) power

## CONCLUSION AND FUTURE SCOPE OF WORK

---

division, which is essential for pumping mixers. Additionally, the power divider can be used within sub-arrays for signal feeding. This work represents a significant advancement in the riblet coupler based power divider technology with multi-ways of power division, offering enhanced performance, compactness, and versatility for a range of applications.

In chapter 5, a noteworthy achievement is the introduction of a broadband and compact eight-way SIW radial power divider. The power divider boasts an exceptional 15 dB fractional bandwidth of 53.5%, effectively covering a substantial portion of the C-band. Despite its broad bandwidth, the power divider maintains a compact form factor. This compactness is highly advantageous for practical implementations with space constraints. The impedance matching between the coaxial fed ports and the SIW is rigorously examined. An equivalent circuit simulation approach is used, optimizing the 3D electromagnetic simulation with minimal iterations. This methodology aids in achieving efficient and accurate simulations. The power divider's broadband performance is achieved by incorporating planar annular slot and circular patch impedance transformers directly into the planar substrate. This approach avoids the bulkiness that would otherwise be associated with external components. The combined attributes of broadband coverage and compact size make this power divider design valuable for a range of applications. It holds potential in sub-6 GHz 5G base stations and satellite communication systems. It can be effectively utilized in various scenarios, including antenna arrays, multiplexers, and high-power amplifiers. This design can be further developed into a dual band eight way radial SIW power divider as well. The technique employed to achieve a dual-band response within the proposed power divider, using compact Complementary Split-Ring Resonators (CSRRs), holds several advantages. These CSRRs have smaller electrical sizes, enabling easy fabrication through standard planar circuit methods for printed circuit

## CONCLUSION AND FUTURE SCOPE OF WORK

---

boards. This technique ensures the power divider retains its compactness while delivering enhanced functionality, which is not the case with alternative approaches that might result in bulkier or more complex designs. The incorporation of CSRRs, which involves tailoring parameters such as length, width, and gap of the CSRR rings, allows for fine-tuning the dual-band frequencies based on the nature of the stopband. It enables the achievement of dual-band performance without requiring additional filtering components to reject unwanted frequencies. This dual-band operation holds significant potential for various wireless communication systems, including antenna arrays, multiplexers, and high-power amplifiers. The power divider design offers reduced losses without sacrificing compactness, making it a valuable solution for practical implementations. Moreover, this design approach could be extended to create a triple-band power divider by incorporating CSRR rings that introduce two stop bands, further expanding the capabilities of the system. Overall, the utilization of CSRRs within the compact multiway power divider design presents an innovative and practical solution to address dual-band requirements in applications, offering enhanced performance without compromising on space or complexity like satellite communication and 5G technologies.

### 6.2 Future Scope of Work

There is a huge potential of SIW technology at higher frequency ranges, such as millimeter-wave and terahertz frequencies. These frequency ranges are gaining importance in various applications, including high-speed communication and imaging. Unique SIW properties could make it a valuable tool in these domains. Some possibilities are listed below.

- One significant area of future scope for SIW is in the miniaturization and integration of RF systems. SIW's compact and planar structure makes it suitable for integration with other

## CONCLUSION AND FUTURE SCOPE OF WORK

---

components on a single substrate. This could lead to the development of smaller and more efficient communication devices.

- SIW can also be used for developing amplifiers, mixers, multipliers, voltage controlled oscillators. Compact design for these can be explored in SIW.
- Advancements in manufacturing techniques, such as 3D printing, nanofabrication and textile fabrication, could impact SIW technology. The potential for creating more intricate and customized SIW structures, could lead to improved performance and novel applications.
- There is potential for the integration of SIW with metamaterials and electromagnetic bandgap structures. These combinations could result in enhanced control over electromagnetic waves, enabling new functionalities like filtering, beam steering, and cloaking. Transitions from SIW to NRD guide transition can also be explored.
- There is also potential for the role of SIW in the evolution of wireless communication systems, particularly in the context of 5G and future generations of wireless networks. SIW can contribute to achieving higher data rates, lower latency, and improved spectrum efficiency.
- Nonlinear effects in SIW, active components integration, novel materials, and advanced signal processing techniques tailored for SIW-based systems could be the potential areas of research in near future.

# Appendix I

---

## List of Journal Publications:

- [1] **Souma Guha Mallick**, Arun Kumar Gande, Bijit Biswas, Sayan Chatterjee, D. R. Poddar, “A planar eight-way compact substrate integrated waveguide based radial power divider with broadband performance”, *Microwave and Optical Technology Letters*, vol. 62, no. 3, pp. No. 1169-1175, 2020
- [2] Arun Kumar Gande, **Souma Guha Mallick**, Bijit Biswas, Sayan Chatterjee, D. R. Poddar, “A compact, broadband three-way substrate integrated waveguide power divider with improved isolation”, *Circuit World*, vol. 48, no. 4, pp. No. 580-585, 2022

## List of Conference Publications:

- [1] **S. G. Mallick**, G. A. Kumar, S. Chatterjee, B. Biswas and D. R. Poddar, “Transitions from SIW to Various Transmission Lines for Substrate Integrated Circuits,” *2019 URSI Asia-Pacific Radio Science Conference (AP-RASC)*, New Delhi, India, 2019, pp. 1-4.
- [2] **S. G. Mallick**, B. Biswas, S. Chatterjee, G. A. Kumar and D. R. Poddar, “A Multilayered Transition between SIW and ESIW,” *2020 IEEE Calcutta Conference (CALCON)*, Kolkata, India, 2020, pp. 181-183.

